

UNIVERSITY OF OKLAHOMA

GRADUATE COLLEGE

SURVEY OF CATALYST AND REDUCTANT EFFECTS ON OXORHENIUM  
CATALYZED DEOXYDEHYDRATION OF GLYCOLS

A DISSERTATION

SUBMITTED TO THE GRADUATE FACULTY

in partial fulfillment of the requirements for the

Degree of

DOCTOR OF PHILOSOPHY

By

JAMES MICHAEL MCCLAIN II

Norman, Oklahoma

2015

SURVEY OF CATALYST AND REDUCTANT EFFECTS ON OXORHENIUM  
CATALYZED DEOXYDEHYDRATION OF GLYCOLS

A DISSERTATION APPROVED FOR THE  
DEPARTMENT OF CHEMISTRY AND BIOCHEMISTRY

BY

---

Dr. Kenneth M. Nicholas, Chair

---

Dr. Robert P. Houser

---

Dr. George Richter-Addo

---

Dr. Robert K. Thomson

---

Dr. Ronald L. Halterman

---

Dr. Lee R. Krumholz

© Copyright by JAMES MICHAEL MCCLAIN II 2015  
All Rights Reserved.

To my parents & sisters for a lifetime of love, support, and faith in my shenanigans,  
thank you.

## **Acknowledgements**

I would not have made it to where I am today without the friendship, mentorship, encouragement, and support of countless people. I know I cannot adequately thank everyone responsible for influencing me to develop into the person I am today and I will inevitably leave out many who deserve recognition, to those individuals I apologize and greatly thank you.

As a child, while working in my grandpa's workshop he would always tell me "can't ain't a word" anytime I said I couldn't do one thing or another. At the time I thought, ironically, he was giving me a grammatical lesson, it wasn't till after his passing and I was older that I truly understood what he was telling me. This has become my general philosophy in life when challenges present themselves; I concede that it occasionally leads me to pursue endeavors off the main track but I owe most of my accomplishments to this stubbornness. Of course, my parents and sisters are responsible for much of whom I am and have been a part of all that I have done. My friends have been a second family and have grown too numerous to thank them all for the good times and support but I am greatly appreciative. I have to mention some of my closest friends, Robert, Anna, Katie, and Camille for years of fun, listening to me complain about trivial things, and the motivation to keep moving forward. Thank you to my teachers and mentors all through my life. Particularly my grade school advanced program instructor Ms. Schaflein for encouraging me to think independently and abstractly. I am grateful to all my research mentors, Dr. Tim Hubin, Dr. Bob Houser, and Dr. Ken Nicholas for all that I learned from them, their inspiration, and individual perspectives.

## Table of Contents

Acknowledgements .....	iv
Table of Contents .....	v
List of Tables .....	ix
List of Figures .....	xi
Abstract.....	xvii
Chapter 1     Biomass, a Renewable Carbon Source.....	1
1.1     Dependence on Fossil-Based Resources .....	2
1.2     Sustainable Energy and Chemical Feedstocks .....	4
1.3     Utilization of Cellulosic Biomass .....	5
1.4     Conversions of Biomass Derived Sugars and Polyols .....	8
1.5     Deoxydehydration (DODH) .....	10
Chapter 2     Elemental Reductants in the Deoxydehydration of Polyols .....	25
2.1     Background and Introduction .....	26
2.2     Exploratory Reactions with the Activated Substrate DET.....	28
2.3     Aliphatic Glycols .....	29
2.4     Reflux Reactions.....	31
2.5     Electronically Different Substrates .....	32
2.6     Mass Balance for High Conversion/Moderate Yield Reactions.....	34
2.7     Discussion .....	41
2.8     Conclusion.....	42
2.9     Experimental.....	43
2.9.1     Reagents .....	43

2.9.2	Typical Reaction Conditions .....	43
2.9.3	Notes on Elemental Metals.....	44
2.9.4	Instrumentation .....	45
2.9.5	Quantification Procedures .....	45
2.9.6	Standard Reaction .....	47
2.9.7	Procedure testing for CO and CO <sub>2</sub> .....	48
Chapter 3	Oxorhenium(V) Catalyzed DODH .....	50
3.1	Background and Introduction .....	51
3.2	Synthesis of <i>Trans</i> -[ReO <sub>2</sub> py <sub>4</sub> ]Cl (1a) .....	53
3.3	Establishing Catalytic Activity of [ReO <sub>2</sub> py <sub>4</sub> ]Cl (1a) for DODH with Glycols and Sodium Sulfite.....	54
3.4	Benzyl Alcohol as Reductant .....	61
3.5	Nature of Oxorhenium Catalyst in Reaction/Post-Reaction.....	64
3.6	Investigating the Activity of <i>trans</i> -[ReO <sub>2</sub> py <sub>4</sub> ] <sup>+</sup> in Additional DODH Reactions .....	65
3.7	Elemental Reductants for <i>trans</i> -[ReO <sub>2</sub> py <sub>4</sub> ] <sup>+</sup> catalyzed DODH. ....	69
3.8	ReO <sub>2</sub> (TPP) <sub>2</sub> I (2) as a DODH Catalyst .....	70
3.9	Conclusions .....	72
3.10	Experimental.....	73
3.10.1	Reagents .....	73
3.10.2	Instrumentation and Analytical Methods .....	74
3.10.3	Typical DODH Reaction Conditions .....	74
3.10.4	Quantification .....	75

3.10.5	Standard Reaction .....	75
3.10.6	Mass Spectrometric Experiment Described in <b>Section 3.5</b> .....	76
Chapter 4	Mechanistic Studies of Oxorhenium-Catalyzed DODH .....	77
4.1	Background and introduction .....	78
4.2	Initial reaction time course experiments .....	82
4.3	Establishing standard reaction conditions and stoichiometry effects .....	84
4.4	Substituted pyridine analogs of the type $[\text{ReO}_2(4\text{-X-py})_4]\text{PF}_6$ .....	90
4.5	Observed effect of added pyridine or triphenylphosphine oxide to the $[\text{ReO}_2\text{py}_4]\text{PF}_6/\text{BnOH}/1,2\text{-decanediol}$ DODH reaction .....	92
4.6	Kinetic isotope effect with singly and doubly benzylic deuterium labeled BnOH .....	93
4.7	Stoichiometric reactions .....	97
4.8	Conclusions .....	105
4.9	Experimental.....	107
4.9.1	Reagents .....	107
4.9.2	Instrumentation .....	110
4.9.3	Typical Catalytic DODH Reaction Conditions .....	111
4.9.4	Quantification .....	111
4.9.5	ESI-MS of ethylene glycol/ $[\text{ReO}_2\text{py}_4]^+$ .....	112
4.9.6	Rhenium calculations .....	113
Chapter 5	Project Summary and Future Directions .....	117
5.1	Project summary .....	118
5.2	Future directions .....	119

References.....	120
Appendix 1.....	130
Abbreviations.....	130

## List of Tables

Table 2.3.1 1,2-Decanediol/APR/elemental reductant reactions in benzene.....	30
Table 2.4.1 DODH of 1,2-decanediol to 1-decene using APR catalyst and elemental reductants in anisole. ....	32
Table 2.5.1 DODH of non-aliphatic glycols with APR. ....	34
Table 2.7.1 Comparison of APR/EI DODH to other APR/Red DODH systems.....	41
Table 2.9.1 Compounds and approximate identifiers. ....	47
Table 3.3.1 Comparison of 1a with other published oxorhenium compounds for DODH of styrene glycol using sulfite in benzene [54, 55]. ....	56
Table 3.3.2 Comparison of 1a with reported oxorhenium compounds in the DODH of 1,2-octanediol with sulfite in chlorobenzene reactions[54, 55].....	59
Table 3.4.1 Comparison of LReO <sub>x</sub> compounds using benzyl alcohol as reductant.....	62
Table 3.6.1 Temperature effects on diol conversion and alkene yield in 2.5 hours for [ReO <sub>2</sub> py <sub>4</sub> ]Cl/BnOH/1,2-octanediol reactions in chlorobenzene. ....	66
Table 3.6.2 Comparison of the reaction in benzene of the reported APR/BnOH/DET with that of [ReO <sub>2</sub> py <sub>4</sub> ]Cl/BnOH/DET in 24 hours. ....	67
Table 3.6.3 Counter ion comparison, Cl <sup>-</sup> versus PF <sub>6</sub> <sup>-</sup> , for the 30 minute DODH reaction catalyzed by [ReO <sub>2</sub> py <sub>4</sub> ] <sup>+</sup> on 1,2-decanediol with BnOH.....	69
Table 3.7.1 Reaction of elemental zinc as reductant for the DODH of 1,2-decanediol using [ReO <sub>2</sub> py <sub>4</sub> ] <sup>+</sup> both the chloride salt (1a) and hexafluorophosphate salt (1b). ....	70
Table 3.8.1 ReO <sub>2</sub> (TPP) <sub>2</sub> I (2) as catalyst for the DODH of 1,2-decanediol with benzyl alcohol in benzene at 150 °C. ....	72

Table 4.3.1 Variations from standard reaction conditions with corresponding effect on observed rate of decene production.....	88
Table 4.5.1 Effect of additive <i>L</i> on observed rate of the DODH for [ReO <sub>2</sub> py <sub>4</sub> ]PF <sub>6</sub> /BnOH/1,2-decanediol.....	93
Table 4.6.1 KIE of PhCD <sub>2</sub> OH and PhCH <sub>2</sub> OH.....	94
Table 4.6.2 Analysis of PhCDHOH DODH experiment.....	95
Table 4.6.3 Analysis of 50:50 BnOH/PhCD <sub>2</sub> OH DODH experiment.....	97
Table 4.7.1 Rhenium-glycolate NMR signals.....	101
Table 4.7.2 Rhenium-ethylene glycolates NMR signals.....	104

## List of Figures

Figure 1.1.1 The carbon cycle, illustrating the flow of carbon/carbon dioxide through nature. Image provided by NOAA ESRL Global Monitoring Division, Boulder, Colorado, USA [7] .....	3
Figure 1.2.1 Schematic depiction of the constituents of lignocellulose: lignin, hemicellulose, and cellulose. Image from Dusselier and coworkers [17]......	5
Figure 1.4.1 Transformations of biomass derived HMF and FUR into further chemicals. Image from Chatterjee et al. [29]......	9
Figure 1.4.2 Schematic representation of DODH of a glycol with an oxometal catalyst ( $\text{LMO}_x$ ) and a reductant (Red) producing an alkene along with the oxidized reductant (Red-O) and water.....	10
Figure 1.5.1 Schematic representation of uncatalyzed DODH of glycols to the corresponding alkene via the two step, dioxolane containing pathway, A [44-46] or by the one step, distillative pathway, B [47, 48].....	11
Figure 1.5.2 Schematic representation of the proposed pathway for $\text{Cp}^*\text{ReO}_3$ catalyzed DODH of styrene glycol with phosphine reductant. Image from Cook et al. [31]......	12
Figure 1.5.3 Schematic representation of the proposed pathway for DODH of glycols by $\text{Tp}^*\text{ReO}_3$ (bottom left) with TPP as reductant. Image from Gable et al. [49]......	13
Figure 1.5.4 Mechanistic analyses of alkene extrusion from $\text{LRe}^{\text{V}}\text{O}(\text{glycolate})$ . Adapted from Boucher-Jacobs & Nicholas [42]......	14
Figure 1.5.5 Structural representation of $\text{Cp}'\text{ReO}_3$ ......	15
Figure 1.5.6 Lowest calculated energy profile for MTO catalyzed DODH of ethylene glycol with sodium sulfite. Adapted from Boucher-Jacobs & Nicholas [42]......	17

Figure 1.5.7 Schematic representation of the MTO/glycerol distillative set up. Image from Boucher-Jacobs & Nicholas [42].	18
Figure 1.5.8 Alcohol driven DODH and tandem reactions as reported by Toste and Shiramizu [57].	20
Figure 1.5.9 Benzyl alcohol driven DODH with APR/DET recovery and reuse schematic. Image from Boucher-Jacobs & Nicholas [42].	21
Figure 1.5.10 Computationally evaluated potential alcohol driven MTO DODH of glycols pathways. Image from Wang et. al [60].	22
Figure 1.5.11 Highly efficient DODH with $\text{Bu}_4\text{N}(\text{dipic})\text{VO}_2$ employing $\text{Na}_2\text{SO}_3$ or TPP [37].	23
Figure 2.2.1 Schematic depiction of pilot reaction with elemental zinc: A. Benchmark reaction using APR/DET with benzyl alcohol as reductant, 24 hours[71]; B. Exploratory reaction using APR/DET with elemental zinc, 16 hours; C. Control reaction with DET and elemental zinc with no APR added, 16 hours.	28
Figure 2.5.1 Side product in styrene glycol reactions.	32
Figure 2.6.1 GC-FID of reaction mixture for Entry 2.3-1 from Table 2.3.1(APR/Zn/1,2-decanediol).	35
Figure 2.6.2 $^1\text{H-NMR}$ of reaction mixture for Entry 2.3-1 from Table 2.3.1(APR/Zn/1,2-decanediol).	36
Figure 2.6.3 GC-FID of reaction mixture for Entry 2.5-3, Table 2.5.1 APR/Fe/DET (top), GC-FID of control reaction Fe/DET (bottom).	37
Figure 2.6.4 GC-FID (top) and GC-MS (bottom) of reaction mixture Entry 2.4-2 from Table 2.4.1.	39

Figure 2.6.5 Fragmentation patterns for the long retention product at ca. 16.5 min and that of the remaining 1,2-decanediol in the reaction of Entry 2.4-2 from Table 2.4.1. ...	40
Figure 2.6.6 Peak ca. 17.5 min in GC-MS for Entry 2.4-2 of Table 2.4.1, likely plasticizer contamination. ....	40
Figure 2.7.1 Potential pathway for APR/EI/glycol DODH. ....	42
Figure 2.9.1 Typical reaction setup for reactions carried out in pressure tubes. ....	43
Figure 3.1.1 Examples of oxorhenium(VII) compounds used for the DODH of polyols. A – Cp*ReO <sub>3</sub> [31], B – MTO [35, 55, 68], C – Tp*ReO <sub>3</sub> [49], D – ZReO <sub>4</sub> (Z <sup>+</sup> = H <sup>+</sup> , NH <sub>4</sub> <sup>+</sup> , TBA <sup>+</sup> ) [54, 57, 71], E – Cp'ReO <sub>3</sub> [33].....	52
Figure 3.2.1 Structural representation of <i>trans</i> -dioxotetrapyridinerhenium chloride ([ReO <sub>2</sub> py <sub>4</sub> ]Cl, 1a).....	53
Figure 3.2.2 Synthesis of <i>trans</i> -[ReO <sub>2</sub> py <sub>4</sub> ]Cl (1a) by various intermediates with aqueous pyridine all starting from ZReO <sub>4</sub> (Z = H <sup>+</sup> , NH <sub>4</sub> <sup>+</sup> , K <sup>+</sup> , Na <sup>+</sup> ). Route A. K <sub>2</sub> [ReOCl <sub>5</sub> ] [107], B. K <sub>2</sub> [ReCl <sub>6</sub> ] [103], C. <i>trans</i> -[ReOCl <sub>3</sub> (TPP) <sub>2</sub> ] [108, 109].....	54
Figure 3.3.1 GC-FID of reaction of styrene glycol with sodium sulfite catalyzed by 1a in benzene with naphthalene internal standard. ....	57
Figure 3.3.2 GC-FID of the DODH reaction of 1,2-octanediol with sodium sulfite catalyzed by 1a in chlorobenzene with naphthalene internal standard. ....	60
Figure 3.4.1 <sup>1</sup> H-NMR of the 1a/BnOH/1,2-octanediol reaction in chlorobenzene.....	63
Figure 3.4.2 <sup>1</sup> H-NMR time course reaction of 1,2-octanediol with BnOH in chlorobenzene showing formation of additional peaks in the 6 ppm region. ....	63
Figure 3.4.3 Acid catalyzed acetal formation from benzaldehyde and 1,2-octanediol. ...	64

Figure 3.6.1 Structure of the octahedral $[\text{ReO}_2\text{py}_4]\text{Cl}$ compared to that of tetrahedral ammonium perrhenate. ....	66
Figure 3.6.2 Structural comparison of reductants tested in DODH. ....	68
Figure 3.8.1 Structural representation of the <i>cis</i> -dioxobis(triphenylphosphine)iodorhenium ( $\text{ReO}_2(\text{TPP})_2\text{I}$ , 2). ....	70
Figure 4.1.1 Generic summary of potential pathways for oxorhenium DODH. Adapted from Nicholas [54]. ....	79
Figure 4.2.1 General reaction using $[\text{ReO}_2\text{py}_4]^+$ and benzyl alcohol in the DODH of diols as demonstrated in Chapter 3. ....	82
Figure 4.2.2 Typical NMR-scale DODH reaction (top left) conducted in pressure tolerant NMR tube (bottom left) with representative reaction spectra with characteristic peaks accentuated (bottom right). ....	83
Figure 4.2.3 Representative data set from NMR-scale DODH reaction. ....	84
Figure 4.3.1 Standard reaction conditions for DODH reactions for the $[\text{ReO}_2\text{py}_4]\text{PF}_6/\text{BnOH}/1,2\text{-decanediol}$ system. ....	84
Figure 4.3.2 Modified pressure reactor with dip tube and regulating valve for sampling. ....	85
Figure 4.3.3 Idealized “simple” pathway for $[\text{ReO}_2\text{py}_4]^+/1,2\text{-decanediol}/\text{BnOH}$ DODH. ....	86
Figure 4.3.4 Generalization for interpreting plots for an empirical power law [120]. ....	87
Figure 4.3.5 Approximation of pseudo-orders graphically for the power rate law estimation for the DODH system $[\text{ReO}_2\text{py}_4]\text{PF}_6/\text{BnOH}/1,2\text{-decanediol}$ . ....	90

Figure 4.4.1 Observed effect of varying electronic properties of 4-X-py in [ReO <sub>2</sub> (4-X-py) <sub>4</sub> ]PF <sub>6</sub> (X= NMe <sub>2</sub> , Me, H, Cl) DODH of 1,2-decanediol/BnOH and consequent Hammett plot. (Values for $\sigma_p$ from Hansch & Leo [133]).....	92
Figure 4.7.1 Stoichiometric reaction of [ReO <sub>2</sub> py <sub>4</sub> ]Cl (1a) with 1,2-decanediol.....	98
Figure 4.7.2 <sup>1</sup> H-NMR of [ReO <sub>2</sub> py <sub>4</sub> ]PF <sub>6</sub> /1,2-decanediol reaction mixture in benzene after mild heating. Characteristic diol peaks are indicated with an arrow, new area of interest circled. ....	99
Figure 4.7.3 <sup>1</sup> H-NMR spectra in DMF of 1,2-propanediol (top), [ReO <sub>2</sub> py <sub>4</sub> ]PF <sub>6</sub> /diol before heating (middle), [ReO <sub>2</sub> py <sub>4</sub> ]PF <sub>6</sub> /diol after heating at 90 °C overnight (bottom). ....	100
Figure 4.7.4 Two proposed different binding modes for 1,2-propanediol Re-glycolate. Protons removed for clarity except glycolate protons.....	100
Figure 4.7.5 <sup>1</sup> H-NMR spectra in CD <sub>2</sub> Cl <sub>2</sub> of ethylene glycol (top), [ReO <sub>2</sub> py <sub>4</sub> ]PF <sub>6</sub> /diol before heating (middle), [ReO <sub>2</sub> py <sub>4</sub> ]PF <sub>6</sub> /diol after heating at 90 °C overnight (bottom). ....	103
Figure 4.7.6 Computed structure of [Re <sup>v</sup> O(glycolate)py <sub>2</sub> ] <sup>+</sup> (B3LYP/LANL2DZ). Protons removed for clarity except for those on ethylene glycolate.....	104
Figure 4.8.1 Proposed pathway of BnOH driven, [ReO <sub>2</sub> py <sub>4</sub> ] <sup>+</sup> catalyzed DODH.....	105
Figure 4.9.1 KBr FT-IR of [ReO <sub>2</sub> (4-Clpy) <sub>4</sub> ]PF <sub>6</sub> also showing presence of triphenylphosphine oxide. ....	109
Figure 4.9.2 High resolution ESI-MS of [ReO <sub>2</sub> (4-Clpy) <sub>4</sub> ]PF <sub>6</sub> also showing the presence of triphenylphosphine oxide. ....	110
Figure 4.9.3 ESI-MS [ReO <sub>3</sub> py] <sup>+</sup> and simulation.....	112

Figure 4.9.4 ESI-MS  $[\text{ReO}(\text{glycolate})\text{py}_2]^+$  and simulation. .... 113

## Abstract

Sustainable and renewable carbon sources are of great interest for long term succession of humankind. The sugars and polyols derived from cellulosic biomass offer such a sustainable feedstock considering cellulosic biomass is the largest carbon commodity on Earth. Selective deoxygenation of these sugars and polyols may well provide a feedstock for the synthesis of fine chemicals and fuels.

Deoxydehydration (DODH) is one of the selective deoxygenation methods for upgrading sugars and polyols to higher energy alkenes using an oxometal catalyst and a stoichiometric reductant. In this report several aspects for the oxorhenium catalyzed DODH of polyols are examined. An alternate realm of reductants are introduced for the oxorhenium catalyzed DODH of glycols. The commercially available ammonium perrhenate (APR) is employed along with zero-valent elements zinc, iron, manganese, or carbon as reductant for the effective DODH of various glycols. These elemental reductants and their oxidized products remain heterogeneous in the reaction mixture allowing for their simple separation.

Stable, ligated, cationic dioxorhenium(V) compounds of the form  $\text{Re}^{\text{V}}\text{O}_2\text{L}_n^+$  are demonstrated to be proficient pre-catalysts for the DODH of glycols with assorted reductants. The tetrapyridine dioxorhenium(V) complexes  $[\text{ReO}_2\text{py}_4]\text{Cl}$  and  $[\text{ReO}_2\text{py}_4]\text{PF}_6$  (py = pyridine) are demonstrated to be proficient pre-catalysts for the DODH of glycols with sodium sulfite, zinc, and benzyl alcohol (BnOH). In addition, the commercially available bis-triphenylphosphine(TPP) iodo dioxorhenium(V) complex  $(\text{ReO}_2(\text{TPP})_2\text{I})$  is established to be capable of BnOH driven DODH of glycols. Mechanistic aspects of  $[\text{ReO}_2\text{py}_4]^+$  DODH of glycols with BnOH are probed. There is

an apparent second order dependence on the oxorhenium complex. This second order dependence on rhenium is attributed to a bimolecular turn over limiting step involving one rhenium coordinating and activating BnOH for reduction of the second rhenium which has been oxidized through alkene extrusion from a rhenium-glycolate. The DODH reaction is also found to have a negative pseudo-order in the glycol and is attributed to inactive polyglycol rhenium species. The addition of catalytic concentrations of additional ligands such as pyridine or triphenylphosphine oxide accelerate the reaction and are likely involved in shifting the equilibrium towards the rhenium monoglycol and away from the polyglycol.

## **Chapter 1**

### **Biomass, a Renewable Carbon Source**

## **1.1 Dependence on Fossil-Based Resources**

Currently the world energy consumption is about 524 quadrillion Btu and is predicted to grow 1.5% annually to 820 quadrillion Btu by 2040. Fossil fuels (coal, petroleum and other liquid fuels, and natural gas) are projected to continue to account for three fourths of the energy through 2040[1]. Approximately 70-80% of extracted petroleum is consumed by the transportation sector. About another 10 percent is used for the production of chemicals; the remainder is accounted for as industrial fuels and buildings [2-6]. These fossil fuels were produced over a timespan of about a billion years and therefor are not renewable on the human timescale.

Fossil fuel resources are not evenly distributed between countries and regions. Areas such as Europe annually consume over five times the amount of petroleum that they produce and is projected to remain that way through 2040[1]. The many nations that this net dependence on imported petroleum affects, makes it a concern of national security. Therefore, alternative and sustainable sources of energy and chemical feedstocks are of foremost importance to many nations.

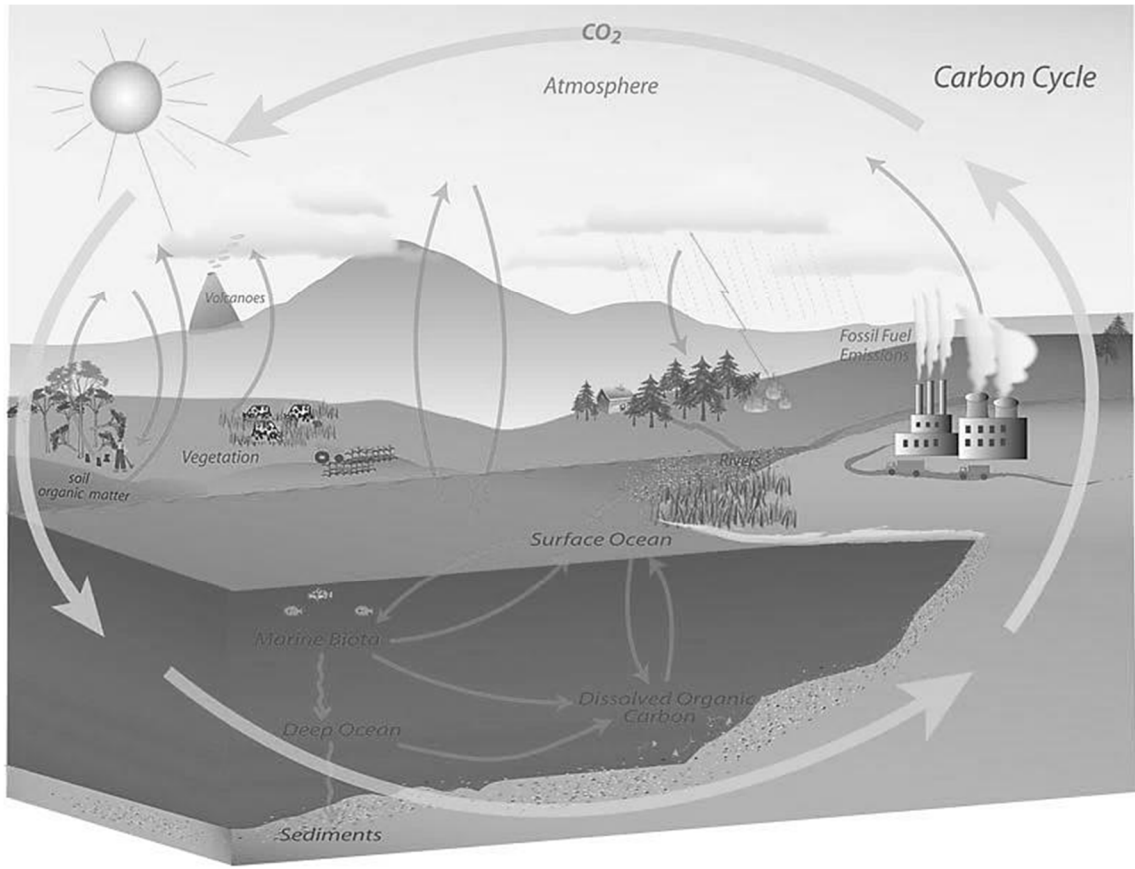


**Figure 1.1.1** The carbon cycle, illustrating the flow of carbon/carbon dioxide through nature. Image provided by NOAA ESRL Global Monitoring Division, Boulder, Colorado, USA [7]

Environmental motivations for alternative and sustainable sources of energy and chemicals have been extensively discussed in virtually all forms of mass communication and are commonly recognized to be topics of heated debate, such as carbon dioxide/greenhouse gases and the global climate. Consequently, these will not be a focus of this introduction past the simple point that we have a society that is profoundly reliant on carbon. Biomass presents a renewable source of carbon through the carbon cycle (see **Figure 1.1.1**) which depends on carbon dioxide.

## 1.2 Sustainable Energy and Chemical Feedstocks

There will not be a single solution to replace fossil fuel derived energy and chemicals but multiple contributors such as wind, water, nuclear, solar, and biomass, to name a few. A comprehensive review of all these alternative sources is beyond the scope of this introduction, thus focus will be placed on biomass, or more precisely lignocellulose biomass. Biomass is of particular interest to many researchers worldwide for its renewability and abundance. The most abundant form of biomass on the planet is cellulose (**Figure 1.2.1**, bottom right). Cellulose is an extraordinarily copious form of biomass worldwide consisting of polysaccharides of glucose. The cellulose is primarily part of a natural composite with lignin and hemicellulose (**Figure 1.2.1**, top left and top right respectively) designated lignocellulose. The lignin protects the polysaccharides of cellulose from degradation; ergo separation of the cellulose from the lignin is generally necessary to get to the sugars/polyols. Sugars and polyols derived from cellulosic biomass are particularly attractive as a renewable source of hydrocarbons[3, 8] and of refunctionalized chemicals[4, 9-15]. As of 2011, the U.S. was estimated to be able to potentially displace 30% of the current petroleum consumption through biomass feedstocks[16]. Biomass also has the advantage of naturally occurring stereocenters, making it very attractive for chemical production. The high value chemical coproduction could potentially offset and maintain the lower value fuel production. Ideally and ethically, non-edible biomass would be the major source of energy and chemicals and be adaptable for growth and harvesting proficiently in vastly different environments/climates.

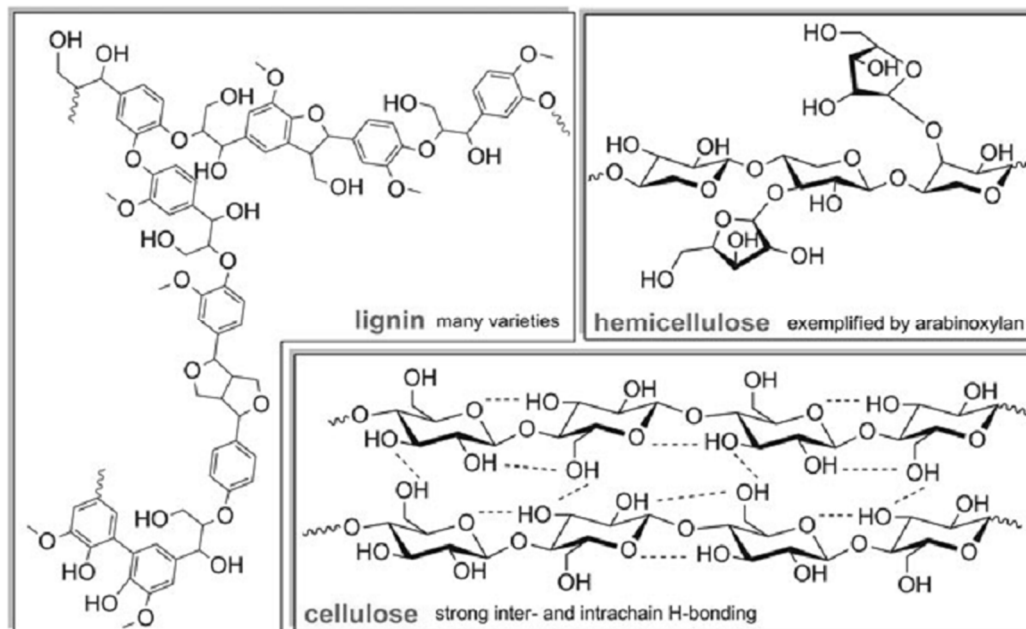


**Figure 1.2.1 Schematic depiction of the constituents of lignocellulose: lignin, hemicellulose, and cellulose. Image from Dusselier and coworkers [17].**

### 1.3 Utilization of Cellulosic Biomass

Numerous and diverse researcher groups are working on ways to efficiently utilize biomass feedstocks for energy and chemicals. These research efforts fall mainly in two categories: direct thermochemical conversion and upgrading; or biomass deconstruction to yield chemicals such as sugars followed by chemical or biological upgrading[18]. These two routes have been used by mankind for millennia. Thermochemically, humans have transformed biomass by fire for energy such as heat and for chemicals like charcoal. Humans have also used fermentation of different biomass sources for the deconstruction yielding sugars which can undergo further biochemical processing, like fermentation. Thus the valorization of biomass for energy and chemicals is not a recent concept in the history of humankind.

Modern thermochemical biomass application research is focused largely in pyrolysis and gasification. Pyrolysis is done by depolymerization of the biomass in the absence of oxygen at 400-600 °C and produces condensable vapors which can be recovered at room temperature as a liquid mixture of oxygenates. This recovered condensed product is known as bio-oil and is rich in energy; there are also small amounts of syngas and charcoal (biochar) produced. Electricity can be generated from burning the bio-oil. Alternatively, bio-oil can be steam reformed to hydrogen or hydroprocessed in to hydrocarbon liquids. Pyrolysis typically is limited to feedstocks with 10 weight percent moisture or less. A major benefit is the feedstock for pyrolysis can encompass the entire plant/biomass source, taking only several seconds for conversion [19, 20]. Gasification, which has been in use for nearly 200 years, involves the generation of thermal energy at 700-1000 °C and syngas. Early gasification was done on coal and can be used to produce fuels for transportation as was done by Germany during World War II and South Africa during apartheid. Early biomass gasification was employed in areas with excess wood such as waste shipping crates at Henry Ford's early automotive plant or when fossil fuels are not abundant like portable wood gasifiers used to power automobiles in Europe during World War II. The adaptability of the produced syngas can be applied to the generation of thermal power, hydrogen production, and synthesis of fuels and chemicals [20]. The loss of the naturally occurring stereochemistry of the biomass feedstocks is a shortcoming, particularly if the produced syngas is then used to manufacture stereochemically pure fine chemicals. Additionally the recovery of usable carbon from pyrolysis/gasification is relatively poor.

The production of chemicals like sugars by deconstructing/depolymerizing biomass opens up further chemical and biological conversion opportunities, but separation to the monomer units is not a simple process. Separation of cellulose biochemically frequently takes hours to days and is discussed elsewhere[21-25], alternatively expedited techniques such as chemical, physical, and thermal approaches are used. The first step is typically pretreatment of the recalcitrant lignocellulose material to increase the surface area of the biomass through decreasing the crystallinity of the cellulose, separating the hemicellulose and breaking the protective lignin seal. Compression and ball milling are physical methods that physically reduce the particle size of the biomass. Certain solvents (such as glycerol, ethylene glycol, dioxane, or hydrogen peroxide as examples) have been shown to break apart cellulose structures and promote hydrolysis, but are not practical given the expense involved. Some of the most promising pretreatments are those employing dilute acids, base treatment, hot water, and steam explosion [22]. The pretreatment processing is one of the most expensive steps to obtain the sugar monomers[4]. A comprehensive discussion about the pretreatment processes cannot be adequately addressed in this introduction and the reader is referred to recent literature [22, 26]. The strategic objective of this research effort is obtaining the sugars and polyols which have the potential for selective chemical and biological upgrading [27]. The removal of oxygen from biomass polyols is crucial to increase the energy content and allow their use as “drop-in” biofuels.[28] The production of commodity and specialty chemicals through controlled deoxygenation of biomass feedstocks is likely to be achieved more practically in the near term.

## 1.4 Conversions of Biomass Derived Sugars and Polyols

Microbial conversion through fermentation of the biomass derived sugars and polyols is one of the most common and well known methods. Fermentation has been used throughout history and therefore a wealth of knowledge is available for this strategy. The C<sub>2</sub>-C<sub>4</sub> primary alcohols that are produced through fermentation can be utilized for such uses as fuel additives. The time involved in biochemically converting the sugars/polyols is relatively slow, often requiring days. A large amount of waste water is produced which needs to be purified for reuse. Additionally, fermentation is not a carbon conservative pathway as CO<sub>2</sub> is produced along with the alcohols (e.g.  $C_6H_{12}O_6 \rightarrow 2C_2H_5OH + 2CO_2$ ). The same lack of carbon conservation from the starting sugars/polyols is also characteristic for other biological transformations like methanogenesis. Our primary interests lay in selective, catalytic oxygen removal transformations that conserve the carbon skeleton; therefore, processes which do not meet this criterion will not be discussed further. Catalytic carbon conservative pathways for selective deoxygenation of biomass-derived sugars/polyols are attractive for their atom efficiency and can be grouped prominently in three categories: (I) dehydration, (II) reduction (e.g. hydrogenolysis), and (III) deoxydehydration (DODH). These are especially important for the production of chemicals from biomass.

The catalytic dehydration of sugars/polyols is predominantly directed at the production of furans from C<sub>6</sub> sugars (hexoses, cellulose-derived) and C<sub>5</sub> sugars (pentoses, hemicellulose-derived) by acid catalysis. Hexoses are dehydrated to give 5-hydroxymethylfurfural (HMF) and pentoses to furfural (FUR) which can be transformed by further reactions or utilized as is (**Figure 1.4.1**). Both HMF and FUR

are becoming platform chemicals each branching off in to its own areas of research as illustrated in **Figure 1.4.1**. Product selectivity is a major area of concern for dehydration. It is also possible to completely dehydrate the sugar forming char. Dehydration is further discussed in recent reviews [29, 30].

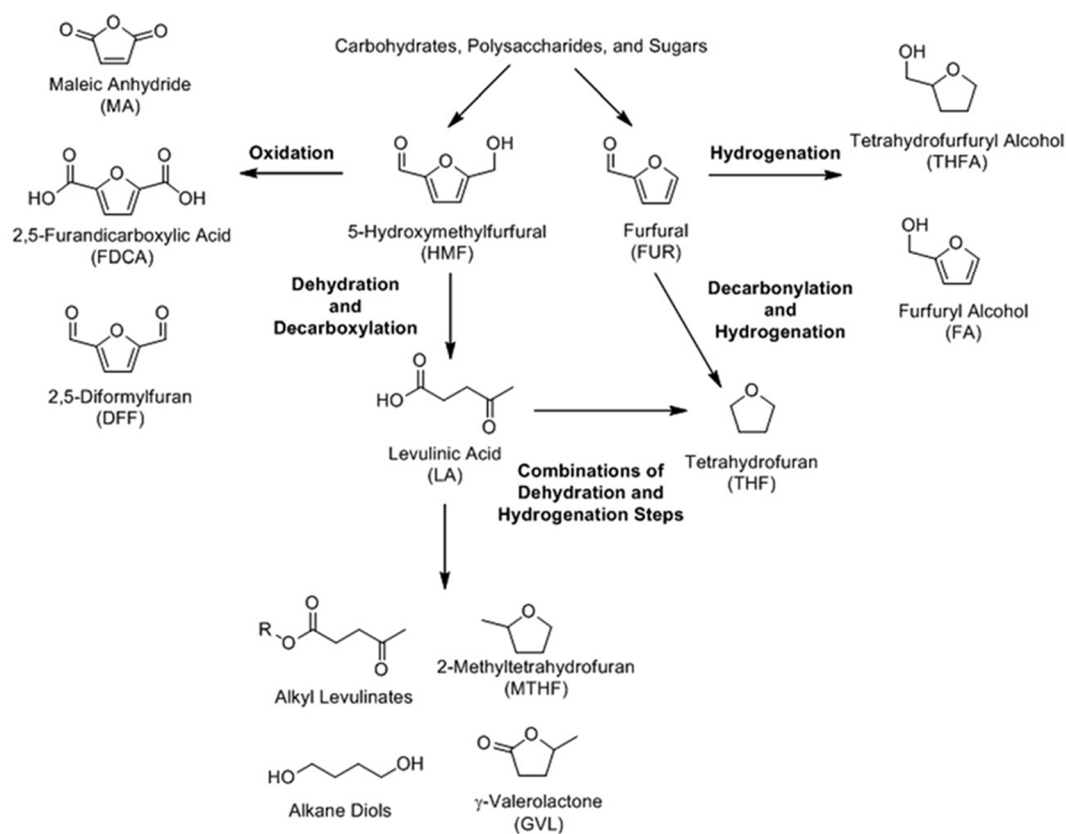


**Figure 1.4.1 Transformations of biomass derived HMF and FUR into further chemicals. Image from Chatterjee et al. [29].**

Selective deoxygenation via reductive methods such as hydrogenolysis represents another catalytic carbon conservative pathway to value-added chemicals. Typically hydrogenolysis occurs under several atmospheres of hydrogen gas, elevated temperatures in the presence of a metal catalyst and involves C-C or C-O bond breaking. Unlike fermentation, when C-O bond breakage occurs the carbon is not lost

as CO<sub>2</sub> but remains as a less oxidized species like methanol or methane for example. Sugars that undergo hydrogenolysis with C-O bond breakage form saturated alcohols while those with C-C cleavage can produce C<sub>2</sub> and C<sub>3</sub> polyols such as ethylene glycol, glycerol, 1,2-propanediol, ethanol and propanol.

The primary interest of our work is the final category of catalytic selective deoxygenation of sugars/polyols, the deoxydehydration (DODH) reaction, which involves the transformation of a glycol to an alkene with a reductant and an oxometal catalyst (**Figure 1.4.2**). Recent investigations of the DODH reaction have focused on establishing the substrate scope of the reaction with various oxo-metal catalysts and reductants and on its catalytic mechanism. The reports of DODH catalyzed by oxorhenium species have thus far predominated [31-35]. Recently, more Earth-abundant vanadium- and molybdenum-oxo complexes have been reported with DODH activity [36-39]. Deoxydehydration is discussed further in the following section, *vide infra*.

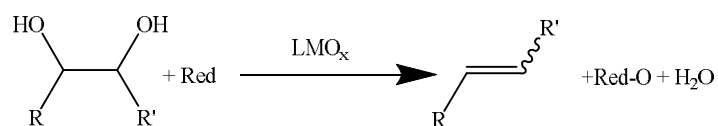


**Figure 1.4.2 Schematic representation of DODH of a glycol with an oxometal catalyst (LMO<sub>x</sub>) and a reductant (Red) producing an alkene along with the oxidized reductant (Red-O) and water.**

### 1.5 Deoxydehydration (DODH)

Deoxydehydration, schematically represented in **Figure 1.4.2**, involves net deoxygenation and dehydration of a glycol, to produce an alkene or unsaturated alcohol [40-43]. The unsaturated DODH products are proven precursors to saturated and aromatic hydrocarbons (fuels) and to other useful chemicals and materials via addition reactions (e.g. hydroformylation) or oligomerization/polymerization.

The uncatalyzed formation of alkenes from vicinal diols has been reported in the absence of an oxometal catalyst by several researchers such as two-step processes with a dioxolane intermediate stereospecifically yielding 40-95% of the alkene from a syn-elimination for a wide range of vicinal diols [44-46] (pathway **A. Figure 1.5.1**). A single step reaction using formic acid with glycols and polyols and an elevated temperature (240 °C), which distills off the alkene, yielded 80-90% of the alkenes of several vicinal diols/polyols [47, 48] (pathway **B. Figure 1.5.1**).

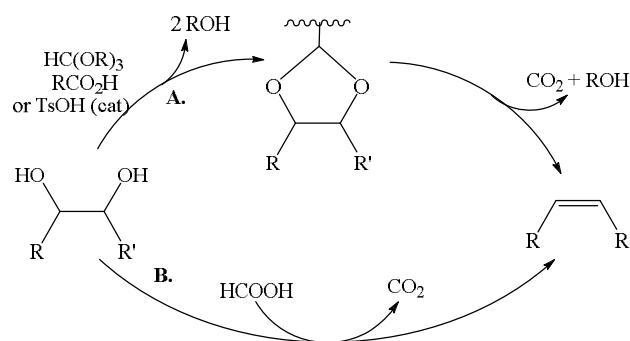


**Figure 1.5.1 Schematic representation of uncatalyzed DODH of glycols to the corresponding alkene via the two step, dioxolane containing pathway, A [44-46] or by the one step, distillative pathway, B [47, 48].**

The first reported oxometal catalyzed DODH of vicinal diols was that of Cook and Andrews [31] using (pentamethylcyclopentadienyl)trioxorhenium (Cp\*Re<sup>vii</sup>O<sub>3</sub>) as catalyst and triphenylphosphine (TPP) as the stoichiometric reductant. These reactions were performed in chlorobenzene over a 1-2 day period at 90-100 °C. This procedure was successful for 1-phenyl-1,2-ethanediol (styrene glycol) and several polyols yielding the corresponding alkenes in 80-95%. The use of coordinating solvents inhibited this reaction while *para*-toluenesulfonic acid (TsOH) enhanced the reaction by promoting glycol condensation. The authors proposed a catalytic cycle, **Figure 1.5.2**, involving Re<sup>vii</sup>/Re<sup>v</sup> intermediates, with deactivation being suggested to occur via over reduction to

$\text{Re}^{\text{iii}}$ . The first step of the proposed pathway involves reduction of the  $\text{Re}^{\text{vii}}$  to  $\text{Re}^{\text{v}}$  by a phosphine reductant, diol condensation followed by rate-limiting alkene extrusion with reoxidation of the  $\text{Re}^{\text{v}}$  to  $\text{Re}^{\text{vii}}$  (clockwise starting from the top, **Figure 1.5.2**). It is noteworthy that the rate with  $\text{Cp}^*\text{ReO}_3/\text{TsOH}$  was independent of reactant concentration but similar to the isolated rhenium-glycolate species, supporting retrocyclization (alkene extrusion) as rate limiting.

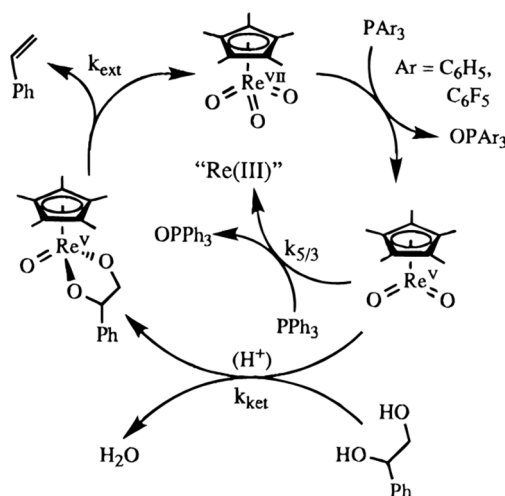


**Figure 1.5.2** Schematic representation of the proposed pathway for  $\text{Cp}^*\text{ReO}_3$  catalyzed DODH of styrene glycol with phosphine reductant. Image from Cook et al. [31].

Another catalytic DODH of glycols was reported several years later by Gable using (tris-dimethylpyrazolylborate)trioxorhenium ( $\text{Tp}^*\text{ReO}_3$ ) (bottom left **Figure 1.5.3**) catalyst and TPP as reductant [49]. The  $\text{Tp}^*$  ligand is a stronger donor compared with  $\text{Cp}^*$ , and the complex  $\text{Tp}^*\text{ReO}_3$  was found to be more robust than  $\text{Cp}^*\text{ReO}_3$  but also less active. These reactions were conducted in toluene at  $120\text{ }^\circ\text{C}$  for 1-5 days on styrene glycol and several other polyols. Again the rate-limiting step was found to be the alkene extrusion (**Figure 1.5.3**) with a proposed pathway involving  $\text{Re}^{\text{vii}} \leftrightarrow \text{Re}^{\text{v}}$  cycle similar to that of  $\text{Cp}^*\text{ReO}_3$ , *vide supra*.

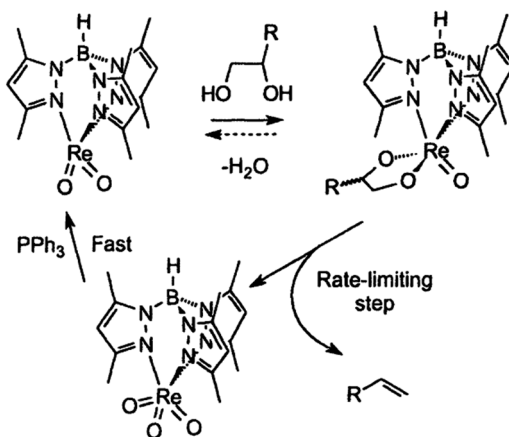


**Figure 1.5.3** Schematic representation of the proposed pathway for DODH of glycols by  $\text{Tp}^*\text{ReO}_3$  (bottom left) with TPP as reductant. Image from Gable et al. [49].

Mechanistic investigations of alkene extrusion from rhenium(V) glycolates were reported by Gable and coworkers, as seen in **Figure 1.5.4**, using both  $\text{Cp}^*\text{Re}^{\text{V}}\text{O}(\text{glycolate})$  [50-52] and  $\text{Tp}'\text{Re}^{\text{V}}\text{O}(\text{glycolate})$  ( $\text{Tp}' = \text{tris-pyrazolylborate}$ ) [32, 53]. From the valuable work of the Gable group it was determined that the addition/extrusion equilibrium is alkene ring strain dependent and the alkene extrusion rate dependence is first-order in the  $\text{LRe}^{\text{V}}\text{O}(\text{glycolate})$  complex. These studies attempted to elucidate the rhenium-glycolate alkene extrusion step as proceeding through either a concerted [3+2] transition state or stepwise via a metallaoxetane intermediate (**Figure 1.5.4**, top right and bottom right respectively).

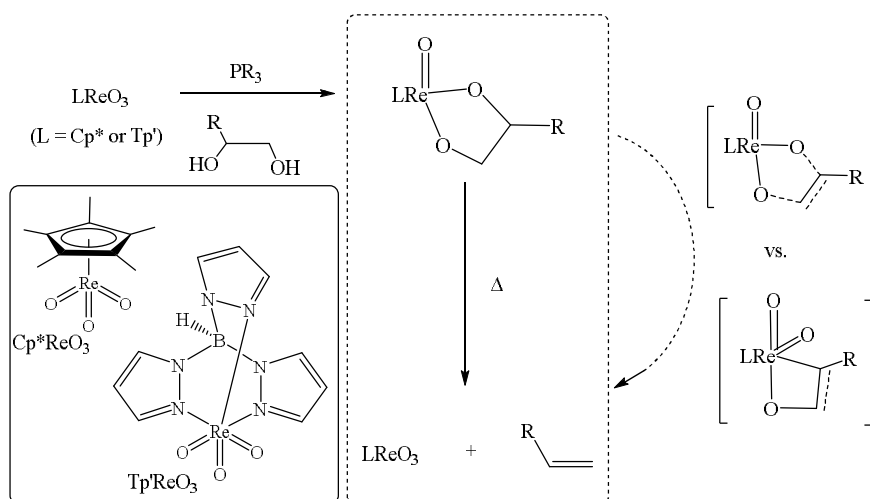


**Figure 1.5.4** Mechanistic analyses of alkene extrusion from  $L\text{Re}^{\text{V}}\text{O}(\text{glycolate})$ . Adapted from Boucher-Jacobs & Nicholas [42].

Recently, the group of Klein Gebbink reported another cyclopentadienyl-based trioxorhenium complex capable of DODH of glycols with TPP as reductant, (1,2,4-*tert*-butyl-cyclopentadienyl)trioxorhenium ( $\text{Cp}'\text{Re}^{\text{vii}}\text{O}_3$ )[33] as illustrated in **Figure 1.5.5**. This bulky oxorhenium(VII) compound was found to catalyze the DODH of polyols in chlorobenzene at 135-180 °C using primarily TPP as reductant yielding alkene at 80-95% and was found to be a more robust catalyst than  $\text{Cp}^*\text{ReO}_3$ . The authors examined more polar solvents and from this found the reaction of  $\text{Cp}'\text{ReO}_3$  with 1,2-octanediol and TPP in pyridine at 180 °C yielded 67% 1-octene and 83% conversion of the diol after 15 hours. This reactivity in pyridine is noteworthy given pyridine's potential to dissolve very polar polyol substrates and to coordinate to electrophilic metal centers.

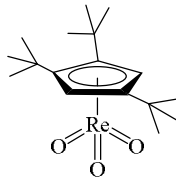


**Figure 1.5.5 Structural representation of Cp\*ReO<sub>3</sub>.**

Methyltrioxorhenium (MeRe<sup>viii</sup>O<sub>3</sub>, MTO) has been frequently used in catalytic DODH investigations [35, 54-61]. This popularity is not surprising given that MTO is relatively air and water stable, commercially available, and bountiful literature coverage exists of its properties and uses [62-67]. The DODH of many polyols have been shown with MTO as catalyst and a range of reductants including H<sub>2</sub> [35], sulfite [54, 55], and alcohols [57, 60, 61, 68].

The Abu-Omar group reported MTO catalyzed DODH using hydrogen gas, the first reported application of MTO for DODH and utilization of an economical, environmentally benign reductant [35]. The DODH reactions were typically carried out in THF at 150 °C with 5-20 atm H<sub>2</sub>, lower pressures and shorter reaction times favored olefin production while higher pressures and longer times favored over-reduction to the alkane. The authors proposed initial reduction of the MTO by H<sub>2</sub> to form MeReO<sub>2</sub>L (L = THF/solvent or H<sub>2</sub>O), followed by condensation of the glycol forming the Re<sup>v</sup>-glycolate and ensuing extrusion of the alkene.

Not long after the report of DODH by MTO with H<sub>2</sub> the Nicholas group reported DODH employing sodium sulfite as reductant [55]. In this report MTO was utilized as well as the first report of a perrhenate salt (NaRe<sup>vii</sup>O<sub>4</sub>) as catalysts for DODH on various glycols with inexpensive/environmentally benign sulfite reductants. The use of perrhenate salts is also significant given that they are typically a more economical

form of rhenium and quite thermodynamically stable. The reactions were typically conducted in chlorobenzene or benzene at 150 °C. This same group elaborated their initial report shortly thereafter by the examination of other catalysts in addition to the MTO and  $\text{NaReO}_4$  to include various perrhenate salts (tetrabutylammonium,  $\text{Bu}_4\text{NRe}^{\text{vii}}\text{O}_3^-$  and ammonium,  $\text{NH}_4\text{Re}^{\text{vii}}\text{O}_4/\text{APR}$ ) as well as rhenium oxide ( $\text{Re}^{\text{vii}}_2\text{O}_7$ ) [54]. They also expanded the scope of reductants including the sulfite salts ammonium sulfite ( $(\text{NH}_4)_2\text{SO}_3$ ) and sodium bisulfite ( $\text{NaHSO}_3$ ); secondary alcohols; phosphines; and a thioether ( $\text{PhSCH}_3$ ). Stoichiometric MTO/styrene glycol experiments suggest alkene extrusion was the likely turn over limiting step, which is in agreement with other DODH studies. Nicholas and coworker computationally evaluated the potential mechanism of MTO catalyzed DODH of ethylene glycol with sodium sulfite as reductant [56]. The lowest energy catalytic pathway that was calculated for this reaction is seen in **Figure 1.5.6**. This pathway starts with the reduction of MTO by  $\text{NaSO}_3^-$  to  $\text{MeRe}^{\text{v}}\text{O}_2(\text{OSO}_3\text{Na})^-$  which is followed by glycol coordination and several H-transfer steps leading to the glycolate species,  $\text{MeRe}^{\text{v}}\text{O}(\text{glycolate})(\text{OSO}_3\text{Na})(\text{H}_2\text{O})^-$ . This rhenium glycolate complex then concertedly extrudes alkene and dissociation of  $\text{NaSO}_4^-$  leads to the regeneration of MTO. These calculations also support glycolate fragmentation as turnover-limiting.

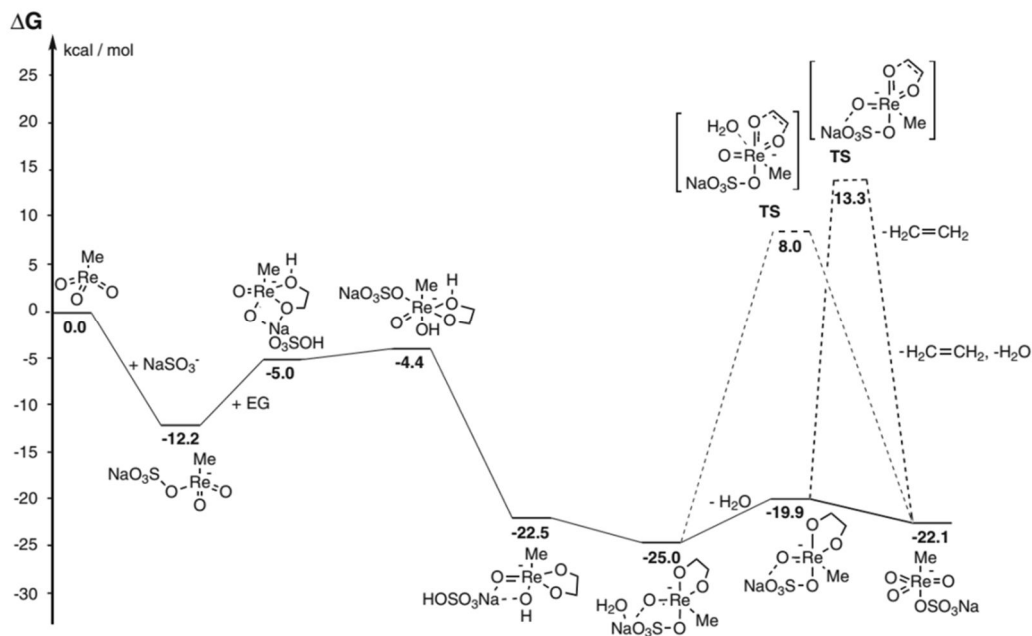


**Figure 1.5.6** Lowest calculated energy profile for MTO catalyzed DODH of ethylene glycol with sodium sulfite. Adapted from Boucher-Jacobs & Nicholas [42].

Secondary alcohols were first reported as effective reductants for DODH by Bergman, Ellman, and coworkers [34]. They used low-valent  $\text{Re}_2(\text{CO})_{10}$  as the precatalyst with the requirement of aerobic reaction conditions for the DODH of glycols. The secondary alcohol reductant (e.g. 3-octanol) also served as the reaction solvent for the aerobic DODH reactions at 150-175 °C with  $\text{Re}_2(\text{CO})_{10}$  precatalyst and TsOH co-catalyst. The authors speculate the active catalyst in these aerobic reactions is likely an oxidized rhenium species.

It was revealed by Abu-Omar and coworkers that in the catalytic reaction of MTO and glycerol a lack of an added reductant leads to the redox disproportionation of the glycol (i.e. the glycol is both substrate and reductant) [69]. The MTO/glycerol reactions were conducted at 165 °C in a distillation set up as represented in **Figure 1.5.7** allowing more volatile compounds (allyl alcohol, acrolein, and propanal; right side in

**Figure 1.5.7)** to separate from the less volatile compounds (glycerol and the reactive 1,3-dihydroxyacetone; left side in **Figure 1.5.7**). Similarly MTO with *cis*-cyclohexanediol gave cyclohexene and 1,2-cyclohexanedione. The authors determined the MTO/glycerol reaction to be first order in both MTO and glycerol.

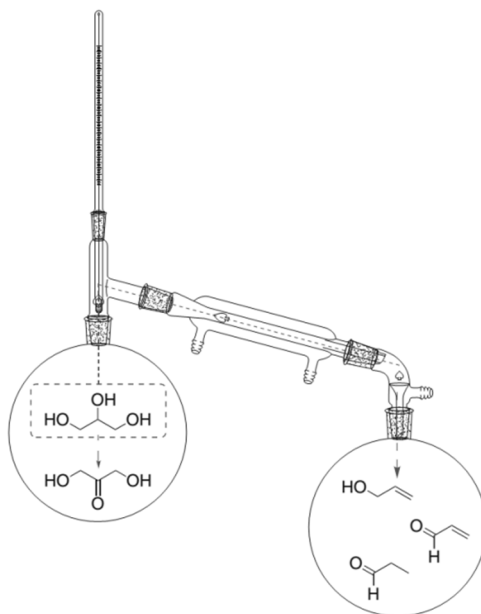


**Figure 1.5.7 Schematic representation of the MTO/glycerol distillative set up. Image from Boucher-Jacobs & Nicholas [42].**

MTO was employed with alcohol reductants by Shiramizu and Toste greatly expanding the scope of alcohol promoted DODH reactions of numerous simple and complex polyols [68]. The alcohol (e.g. 3-octanol) was typically used as solvent and reductant in the aerobic reactions with MTO at 155-200 °C with full conversion and high yield after 1-3 hours with the higher temperatures. To probe the mechanism of the MTO/glycol/alcohol reactions, 3-hexyne was added to the reaction which resulted in an isolable  $\text{MeRe}^{\text{V}}\text{O}_2(\text{alkyne})$  complex which at room temperature could react with glycol to produce a  $\text{MeRe}^{\text{V}}\text{O}(\text{glycolate})$ . The  $\text{MeRe}^{\text{V}}\text{O}_2(\text{alkyne})$  complex had similar catalytic activity to MTO supporting the authors conclusion that  $\text{MeRe}^{\text{V}}\text{O}_2$  is the likely

catalytically significant compound. This same team recently further developed the function and breadth of alcohol promoted oxorhenium DODH [57]. They demonstrated using MTO, which is reported to promote the 1,3-hydroxyl shift of allylic alcohols [70], it was possible transform a 1,4-unsaturated alcohol to a 1,3-diene with alcohol reductant/solvent (top, **Figure 1.5.8**). Additionally polyols with a carboxylic acid function were converted to the alkene esters with MTO or perrhenic acid ( $\text{HRe}^{\text{vii}}\text{O}_4$ ) and alcohol solvent/reductant (middle, **Figure 1.5.8**). A tandem one-pot, two-step DODH/Diels-Alder reaction was reported using the polyols, tartaric acid and erythritol, which after 2-methyl-1-butanol/ $\text{HReO}_4$  driven DODH formed respectively the dienophile and diene for the Diels-Alder reaction (bottom, **Figure 1.5.8**). Additionally, they reported the compatibility of two metal catalysts in a two-step, one-pot  $\text{HReO}_4$ /1-butanol DODH of a sugar diacid followed by  $\text{Pd/C/H}_2$  hydrogenation to the saturated diester. A second example of a one-pot, two-metal-catalyst DODH/hydrogenation was recently reported by Zhang and co-workers [58]. In this example a sugar diacid again was used in 3-pentaol solvent/reductant with MTO/ $\text{TsOH}$  (co-catalyst) for DODH and  $\text{Pt/C/H}_2$  for hydrogenation to the saturated esterified product, the two-step/one-pot proved to be slightly more effective as compared to the one-step reaction.

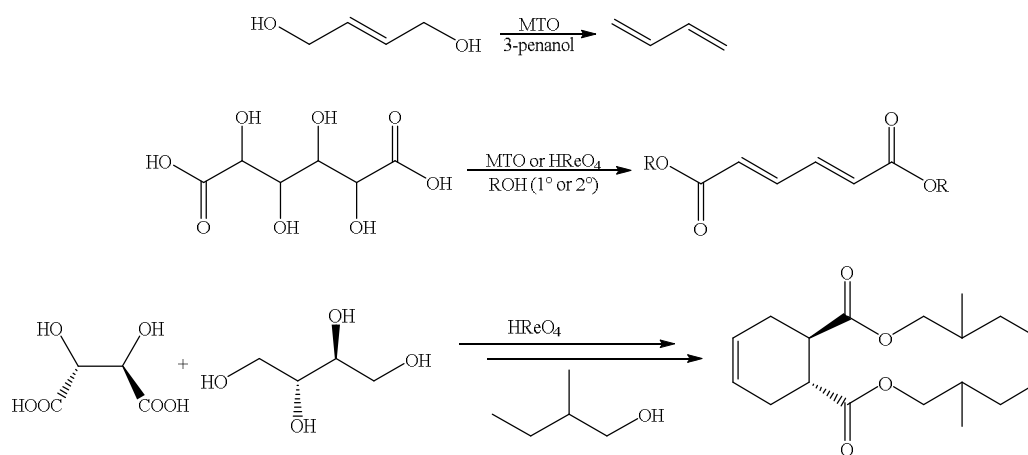


**Figure 1.5.8 Alcohol driven DODH and tandem reactions as reported by Toste and Shiramizu [57].**

The activated primary alcohol, benzyl alcohol (BnOH), was demonstrated by Boucher-Jacobs and Nicholas to be an effective reductant in ammonium perrhenate (APR) catalyzed DODH of polyols [71]. The BnOH/APR system was very effective with numerous glycols and polyols at 150 °C in non-polar solvents. It was noted that in these non-polar solvents APR is insoluble at room temperature. The recovery and reuse of the APR catalyst was demonstrated with diethyl tartrate (DET) and BnOH; the reaction was conducted then cooled to room temperature and centrifuged to separate the soluble reaction components from the solid APR (left side, **Figure 1.5.9**). The soluble reaction mixture was further treated with sodium bisulfite to precipitate the oxidized reductant, benzaldehyde, leaving the diethyl fumarate (DEF) alkene product (right side, **Figure 1.5.9**).

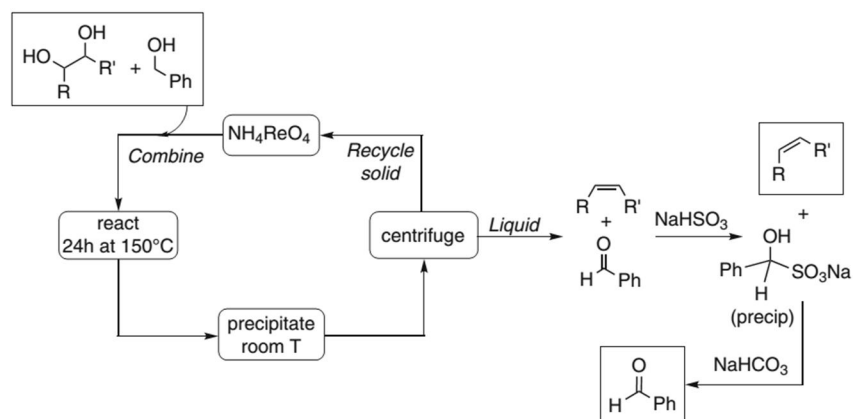


**Figure 1.5.9 Benzyl alcohol driven DODH with APR/DET recovery and reuse schematic. Image from Boucher-Jacobs & Nicholas [42].**

An MTO-catalyzed/alcohol driven DODH mechanistic study of hydrobenzoin was reported by Abu-Omar and coworkers [59]. The MTO catalyzed conversion of hydrobenzoin to *trans*-stilbene was run in 3-octanol solvent/reductant at 140 °C. The authors report an induction period, zeroth-order glycol dependence, and half order dependence for MTO. A monomer-dimer equilibrium of rhenium complexes is suggested by the half order dependence in MTO. Stoichiometric experiments indicated the formation of a MeRe<sup>V</sup>O(glycolate) species that is continuously detected during the reaction, as such the conversion from this species to product is likely rate-limiting. The authors suggest a Re<sup>iii</sup>-diolate species precedes the extrusion of the product alkene. The authors report from kinetic isotope effect studies with 3-D-octanol that the reduction of the rhenium<sup>V</sup>-diolate is rate limiting.

A computational study of alcohol driven MTO DODH of glycols was reported by Wang and coworkers [60]. They explored the pathways suggested by Toste [68] (path A **Figure 1.5.10**) and Abu-Omar [69] (path B **Figure 1.5.10**) as well as a third potential pathway (path C **Figure 1.5.10**) correcting for temperature and solvent in the

DFT calculations. Path A and C both begin with reduction of the MTO to an oxorhenium(V) species,  $\text{MeO}_2\text{Re}^{\text{V}}$  and  $\text{MeO}(\text{OH})_2\text{Re}^{\text{V}}$  respectively; while path B starts with glycol condensation to  $\text{MeO}_2\text{Re}^{\text{VII}}$ (glycolate). All three paths converge to  $\text{MeORe}^{\text{V}}$ (glycolate), paths A and C by glycol condensation and path B by reduction of the  $\text{Re}^{\text{VII}}$ -glycolate species. Path B was calculated to have the highest energy barrier, while path C was calculated as the lowest energy pathway.

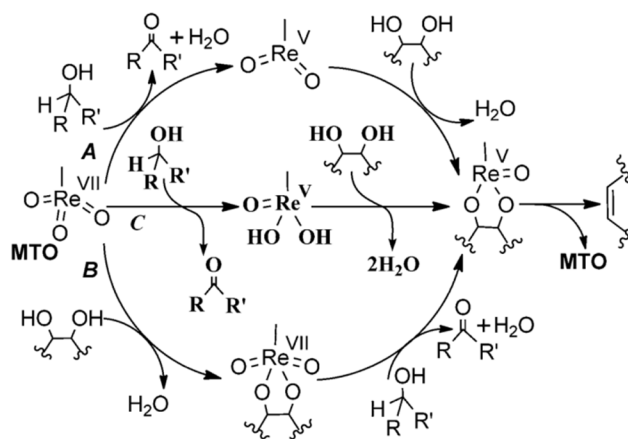


**Figure 1.5.10 Computationally evaluated potential alcohol driven MTO DODH of glycols pathways. Image from Wang et. al [60].**

The first heterogeneous oxorhenium material with catalytic DODH activity was disclosed by Nicholas, Jentoft, and co-workers [72]. In this report, activated carbon was treated with aqueous APR followed by drying giving typical Re content of 3-4 mass%. The  $\text{ReO}_x/\text{C}$  material was competent for the DODH of glycols at 150-175 °C with 6-12 atm  $\text{H}_2$  as reductant. Over reduction was not observed with their typical conditions, selectively yielding olefin. Recovery of the catalyst by filtration showed partial loss of activity for the  $\text{ReO}_x/\text{C}$  material upon subsequent use, indicating the possibility of homogeneous and heterogeneous catalysis. Hot filtration of the reaction solution exhibited a catalytically active species leached from the  $\text{ReO}_x/\text{C}$  material which

is re-adsorbed upon cooling to room temperature. Additionally the  $\text{ReO}_x/\text{C}$  material was capable of utilization of other reductants including 3-hexanol, benzyl alcohol, and tetralin.

Reports of molybdenum catalyzed DODH have emerged recently [38, 39][73]. These oxomolybdenum DODH reactions yield 10-55% alkene from glycol which cannot yet compare to the effectiveness of oxorhenium based DODH. Oxovanadium DODH was also recently reported by Chapman and Nicholas [37]. These oxovanadium DODH reactions showed to be highly efficient at alkene production from glycols, using  $\text{Bu}_4\text{N}(\text{dipic})\text{VO}_2$  with  $\text{Na}_2\text{SO}_3$  or TPP (**Figure 1.5.11**). One of these oxovanadium complexes was utilized by Krische and co-workers in a step for diol to olefin transformation in their multistep benzannulation protocol [74].

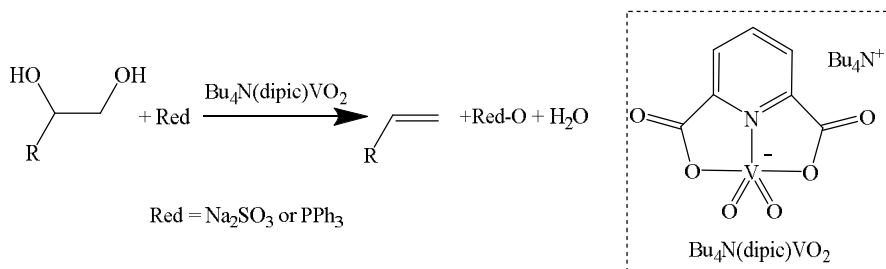


**Figure 1.5.11 Highly efficient DODH with  $\text{Bu}_4\text{N}(\text{dipic})\text{VO}_2$  employing  $\text{Na}_2\text{SO}_3$  or TPP [37].**

The heterogenation of DODH reaction components has to date been limited to sulfite/sulfate [54, 55] for reductant/oxidized reductant and that of the  $\text{ReO}_x/\text{C}$  [72] material as precatalyst. To this extent, expanding the scope of heterogeneous components for DODH is desirable if the process is to be scaled up. Ideally these heterogeneous DODH components would be inexpensive and environmentally benign.

Therefore, we explore several cheap heterogeneous reductants that are environmentally benign.

Additionally the use of oxorhenium(VII) catalysts with little to no ligand variability has thus far predominated the rhenium catalyzed DODH literature. The majority of reports speculate a  $\text{Re}^{\text{vii}} \leftrightarrow \text{Re}^{\text{v}}$  redox cycle is involved in Re-DODH but there has been a lack of stable oxorhenium(V) complexes reported. We investigate stable, ligated oxorhenium(V) compounds which are suitable for ligand variation. This ability to make analogs of these compounds can allow for investigation and understanding of catalyst structure/activity properties and mechanism in DODH.

## **Chapter 2**

### **Elemental Reductants in the Deoxydehydration of Polyols**

## 2.1 Background and Introduction

Typically for the scale up of chemical processes, cost is a major factor. Separation of reaction materials is often significant, adding to the total. This is especially true when reaction components are valuable like precious metal catalysts. The more time and effort required to separate the desired product from the reaction mixture adds to the cost. A frequent strategy is to heterogenize one or more components of the reaction. Also using cheap and abundant materials can help keep the total expense of a reaction lower. The same can be said about processes using environmentally safe reactants and, ideally, by-products as well.

In the DODH literature, phosphines have been used extensively as the reductant [31, 33, 37, 38, 49]. Phosphines are not relatively inexpensive nor are they environmentally safe. Additionally phosphines are toxic and sensitive to oxidation with exposure to air. The phosphine-oxides that are produced have little use and are generally very difficult to separate from reaction mixtures. For large scale purposes, it would not seem that phosphines are an economical choice as the reductant for DODH.

The range of viable reductants has grown from the originally reported phosphines to include the more economical and benign molecular hydrogen [35, 72]. One of the major drawbacks to hydrogen is safety as it is a flammable gas. Additionally, hydrogen has not found wide use in DODH as a reductant potentially due to its reactivity and/or its gaseous nature makes it more challenging to work with.

The Nicholas group introduced sulfite as a DODH reducing agent [37, 54, 55], additionally Krische showed the utility of this reductant for DODH in the multistep synthesis of acenes[75]. Sulfites are also more economical and benign than phosphines.

In reactions conducted in non-polar solvents, the sulfite remains largely insoluble; this is also true for the oxidized product, sulfate.

Secondary alcohols and even the polyols themselves have been shown as effective reductants [34, 54, 68, 76]. The oxidized alcohol/polyol, which potentially could be a mixture of more than one product, can be challenging to separate from the alkene for these DODH reactions. Benzylic alcohols have been utilized successfully as DODH reductant by Boucher-Jacobs and Nicholas [71]. Typically the benzylic alcohols form only the oxidized benzaldehyde product which still needs to be separated from the homogeneous reaction mixture and was demonstrated by treating the mixture with sodium bisulfite to precipitate the bisulfite adduct, which can regenerate the aldehyde upon base treatment. Precipitation of the bisulfite adduct does constitute another step in purification but it does provide a simple means to remove reaction byproducts.

The oxometal catalyst itself is another component which must be separated from the reaction mixture and preferably recovered in the case of precious metal catalysts. This has been accomplished to an extent using APR as catalyst, which in the system was sparingly soluble at room temperature [71]. Furthermore, Boucher-Jacobs and Nicholas showed in this same system the catalyst could be recovered and reused numerous times with little to no loss of activity. Denning, Jentoft and Nicholas heterogenized the catalyst, using APR on carbon [72]. With this heterogeneous catalyst, which employed H<sub>2</sub> as reductant, there was reported loss of activity over several reaction cycles.

Separation of the alkene product from the reaction mixture, which includes the oxidized reductant and oxometal catalyst, is a practical issue that needs to be addressed for large scale application of DODH reactions. The search for new, economical, and recyclable reagents with variable reduction potentials has led us to investigate zero valent elements as reductants, which would produce insoluble or volatile element-oxides. Elemental metals, such as zinc, have been reported to reduce common oxometallates, such as  $\text{MnO}_4^-$  and  $\text{ReO}_4^-$ , typically in aqueous acidic solutions.[77-82] Similarly, elemental carbon has been employed in the reduction of  $\text{MnO}_4^-$  [83] and  $\text{Re}_2\text{O}_7$ [84]. Carbon has found extensive use as a reducing agent in the history of mankind through metallurgy, one of the earliest indicated uses was that of charcoal in the smelting of copper ores in the sixth millennium BC [85-87]. To the best of our knowledge, however, elemental reagents have not been reported as terminal reductants in reactions catalyzed by oxo-metal species.

## 2.2 Exploratory Reactions with the Activated Substrate DET

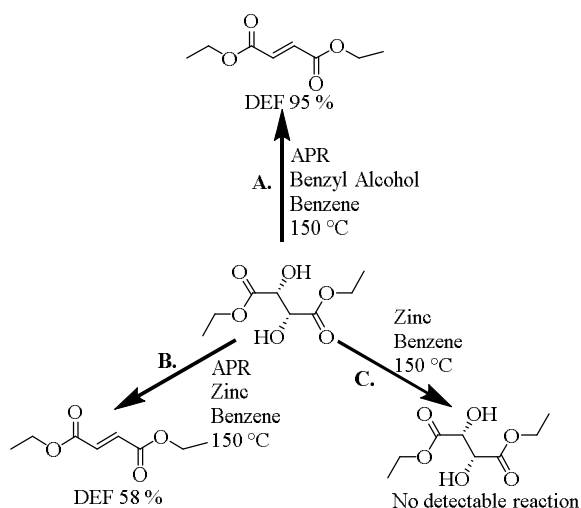


**Figure 2.2.1 Schematic depiction of pilot reaction with elemental zinc: A. Benchmark reaction using APR/DET with benzyl alcohol as reductant, 24 hours[71]; B. Exploratory reaction using APR/DET with elemental zinc, 16 hours; C. Control reaction with DET and elemental zinc with no APR added, 16 hours.**

To test the viability of elemental zinc as a reductant for the DODH of glycols, an exploratory reaction was carried out combining (+)-diethyl L-tartrate (DET), Zn (2 equiv) and ammonium perrhenate (APR, 16 mol%) in benzene (**Figure 2.2.1**). Noting that the  $\Delta H_{\text{rxn}}$  for the DODH of ethylene glycol by Zn is calculated to be -29 kcal/mole[88], This substrate with benzyl alcohol as reductant [71] gives diethyl fumarate (DEF), nearly quantitatively. After heating a nitrogen-flushed reactor tube containing these components overnight at 150 °C, analysis of the reaction solution by  $^1\text{H-NMR}$  and GC-FID showed the formation of the *trans*-alkene, diethyl fumarate (DEF, 58 %), with some remaining diol, DET (42 %). Metallic zinc clearly remains after the reaction, indicating all two equivalents of zinc were not used up. The absence of other significantly detectable organic products, especially ones derived from reduction of the carboxy group of the substrate/products is noteworthy. A control reaction conducted under the same conditions without APR, showed only the starting DET by GC and NMR.

### 2.3 Aliphatic Glycols

With this encouraging result in hand we turned to aliphatic substrates, which typically are less reactive, but are closer models for carbohydrate-derived polyols. Choosing 1,2-decanediol as the substrate (0.1 M in benzene) under similar conditions used for the DET/APR/Zn reaction, a moderate yield of 1-decene (56%) and high conversion (99%) was obtained with 11 mol% APR and 1.1 equivalents of Zn at 150 °C after 24 hr (**Table 2.3.1, Entry 2.3-1**). A partner reaction (**Table 2.3.1, Entry 2.3-2**) under an air atmosphere showed a much lower yield (8%) of 1-decene with incomplete

conversion (76%) of the diol under otherwise identical conditions. This is likely the result of molecular oxygen competitively oxidizing the Zn. The yield from the nitrogen-flushed reaction was further improved (68% yield) when two equivalents of zinc were used in a 0.2 M benzene solution of 1,2-decanediol (**Table 2.3.1, Entry 2.3-3**). The remainder of the diol is largely converted into unidentified side products having long GC retention times and low intensity peaks in the  $^1\text{H-NMR}$  spectra near the starting diol. These long retention peaks are not seen in control reactions where APR is not present.

**Table 2.3.1 1,2-Decanediol/APR/elemental reductant reactions in benzene.**

$\text{C}_8\text{H}_{17}(\text{HO})_2 + \text{El} \xrightarrow[\text{Benzene}]{\text{APR}, 150^\circ\text{C}} \text{C}_8\text{H}_{17}(\text{=}) + \text{El-O} + \text{H}_2\text{O}$			
El (Eq) Entry	APR (mol%)	Glycol Conversion (%)	Yield 1-Decene (%)
Zn (1.1) <b>2.3-1</b>	11	99	56
Zn (1.1) <b>2.3-2</b>	11	76	8 (Air atmosphere)
Zn (2) <b>2.3-3</b>	10	$\geq 99$	68
Fe (2) <b>2.3-4</b>	10	$\geq 99$	68
Mn (2) <b>2.3-5</b>	10	$\geq 99$	64
C (2) <b>2.3-6</b>	11	$\geq 99$	69

These conditions were then used with other abundant metals, namely iron and manganese (**Table 2.3.1, Entries 2.3-4 and 2.3-5** respectively), which achieved similar yields and conversions. Interestingly, elemental carbon (Darco G-60) also proved to be an effective reductant giving a 69% yield of 1-decene with very high conversion.

(**Table 2.3.1, Entry 2.3-6**), note the  $\Delta H_{\text{rxn}}$  for the DODH of ethylene glycol with C is calculated to be +28 kcal/mole [89]. The favorable entropy change (two reactants going to three products) and the formation of gaseous CO presumably improve the conversion. When the reactor tube was cooled to room temperature and opened, a gas pressure buildup was noted. This gas was collected and tested positive for carbon monoxide [90], but negative for carbon dioxide by the lime water test for carbon dioxide.

## 2.4 Reflux Reactions

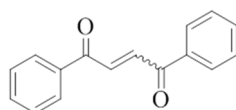
For operational convenience, reactions that could be conducted at atmospheric pressure under reflux were desired. Experiments using refluxing benzene (at 78 °C) and toluene (at 110 °C) with DET/Zn/APR showed alkene formation in low yield and conversion after two to four days. Employing higher boiling anisole (PhOMe, b.p. 154 °C) as the reaction solvent with 1,2-decanediol as substrate (**Table 2.4.1, Entry 2.4-1**) with APR as catalyst for 21 hours yielded 64% of 1-decene and nearly complete conversion of the diol with a rate of alkene formation of 0.014 M/hr and a rate of diol disappearance nearly twice that of the formation of alkene at 0.034 M/hr. The long GC-FID retention products were also noted with an increasing integration over time. When the loading of APR was lowered to 1 mol% with 2 M 1,2-decanediol in anisole (zinc reductant) a lower conversion and an alkene yield of 34% resulted (**Table 2.4.1, Entry 2.4-2**).

**Table 2.4.1 DODH of 1,2-decanediol to 1-decene using APR catalyst and elemental reductants in anisole.**

$\text{C}_8\text{H}_{17}(\text{HO})_2 + \text{El} \xrightarrow[\text{Anisole}]{150\text{ }^\circ\text{C, APR}} \text{C}_8\text{H}_{17}\text{CH}=\text{CH}_2 + \text{El-O} + \text{H}_2\text{O}$			
El (Eq) Entry	APR	Glycol Conversion (%)	Yield 1-Decene (%)
Zn (2) <b>2.4-1</b>	11 mol%	$\geq 99$	64
Zn (2) <b>2.4-2</b>	1.1 mol%	69	34

### 2.5 Electronically Different Substrates

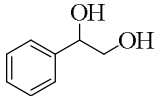
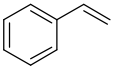
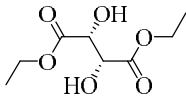
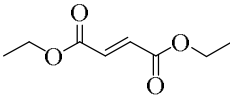
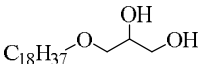
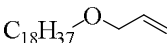
To further assess the substrate scope of the DODH reactions we tested the effectiveness of the elemental reductants on diols with different electronic properties. The activated and acid-sensitive substrate 1-phenyl-1,2-ethanediol (styrene glycol) was selected for evaluation [31, 49]. Under the standard reaction conditions with Zn/APR, styrene glycol gave a moderate yield of styrene at high conversion (**Table 2.5.1, Entry 2.5-1**) within 12 hr, accompanied by the formation of a side product with a long GC retention (ca. 15.5 min) and a mass (by GCMS) that corresponds to a condensed, unsaturated dimer of the diol, tentatively assigned as the  $\alpha,\beta$ -unsaturated-1,4-diketone (**Figure 2.5.1**) based on comparison of MS and H-NMR data (ca. 7.3-8.1 ppm) with those of an authentic sample [91]. Styrene glycol readily undergoes dehydration to acetophenone[92] and oxidation to phenylglyoxal[93, 94] the condensation of acetophenone and phenylglyoxal could then give side product (**Figure 2.5.1**).



**Figure 2.5.1 Side product in styrene glycol reactions.**

Under similar conditions used for the aliphatic diols with zinc as reductant and 10 mol% APR catalyst, polyfunctional diethyl tartrate (DET) yielded 85% of (*trans*) DEF (**Table 2.5.1, Entry 2.5-2**). Similarly, with iron as the reductant a good yield (68%) of DEF was obtained after 24 h with very high conversion (**Table 2.5.1, Entry 2.5-3**). The yields of alkene in the iron driven reactions may suffer from magnetic agglomeration of this reductant to the stir bar, limiting contact with substrate and catalyst. Since DET and its DODH product, DEF, are both high boiling liquids (280 °C and 218 °C respectively), solventless reactions were conducted at 150 °C for 16 h combining DET, carbon and APR under nitrogen. A 60% yield of DEF was obtained using these solventless conditions (**Table 2.5.1, Entry 2.5-4**). A scaled up experiment with DET (3.9 mmol)/Zn/APR was conducted and provided an 84% isolated yield of DEF after 24 hours simply by triturating the heterogeneous post-reaction residue with benzene and ethyl acetate (**Table 2.5.1, Entry 2.5-5**). The glycerol derivative batyl alcohol gave a 47% yield of the corresponding olefin in 24 h at 150 °C (**Table 2.5.1, Entry 2.5-6**).

**Table 2.5.1 DODH of non-aliphatic glycols with APR.**

$\begin{array}{c} \text{HO} \quad \text{OH} \\   \quad   \\ \text{R} \quad \text{R}' \end{array} + \text{El} \xrightarrow[24 \text{ Hrs}]{150 \text{ }^\circ\text{C}, \text{ ca. } 10 \text{ mol\% APR}} \begin{array}{c} \text{R}' \\   \\ \text{R} \end{array} + \text{El-O} + \text{H}_2\text{O}$				
El (eq) Entry	Substrate	Product	Conversion (%)	Yield (%)
Zn (2.1) <b>2.5-1</b>			≥99	46 (12 hours)
Zn (1.1) <b>2.5-2</b>			≥99	85
Fe (1.1) <b>2.5-3</b>			≥95	68
C (3) <b>2.5-4</b>			≥99	60 (Solventless)
Zn (2) <b>2.5-5</b>			≥90	84 (Isolated)
Zn (2) <b>2.5-6</b>				

## 2.6 Mass Balance for High Conversion/Moderate Yield Reactions

The reactions typically showed nearly quantitative conversion but in some cases the yield of alkene product fails to account for a significant mass of the converted starting diol. As example **Entry 2.3-1** from **Table 2.3.1**(APR/Zn/1,2-decanediol) shows a 99% conversion with a yield of 56% 1-decene. As seen in **Figure 2.6.1**, significantly noticeable products are seen at ca. 14-17 min. Additional peaks that do not correspond to the starting diol or product alkene are seen in the <sup>1</sup>H-NMR of reaction mixtures, **Figure 2.6.2** shows an example of this with the reaction mixture of **Entry 2.3-1** from **Table 2.3.1**(APR/Zn/1,2-decanediol). These are most likely combinations of species derived from side reactions such as dehydration and oxidation of the glycol reacting further to form higher molecular weight compounds.

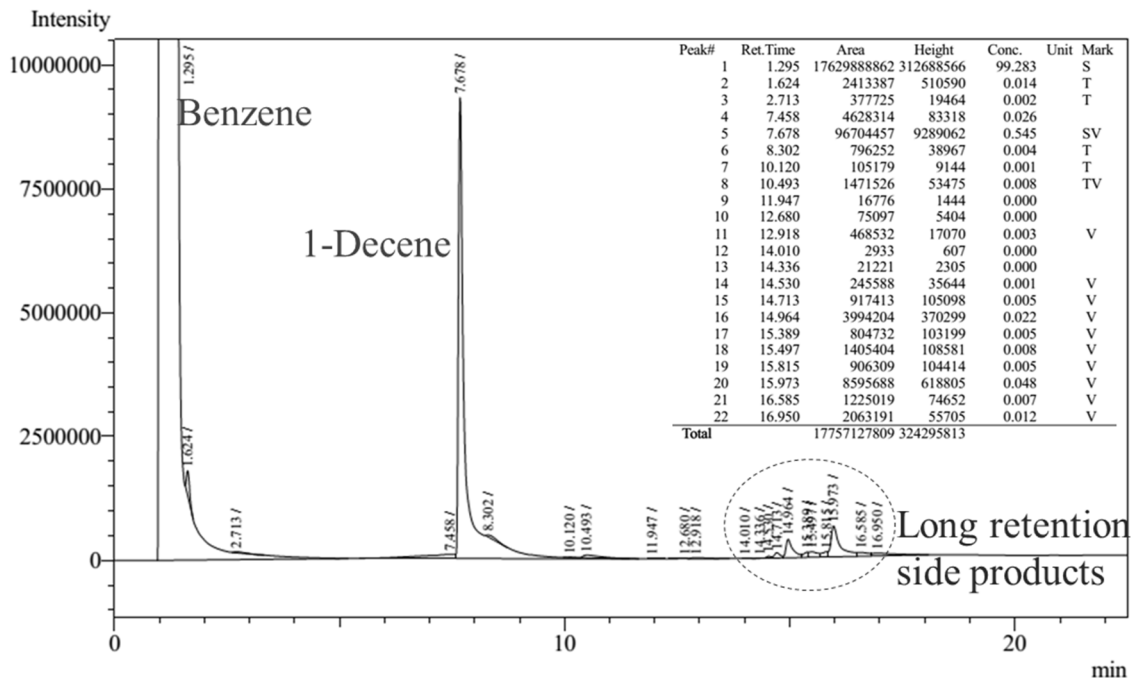
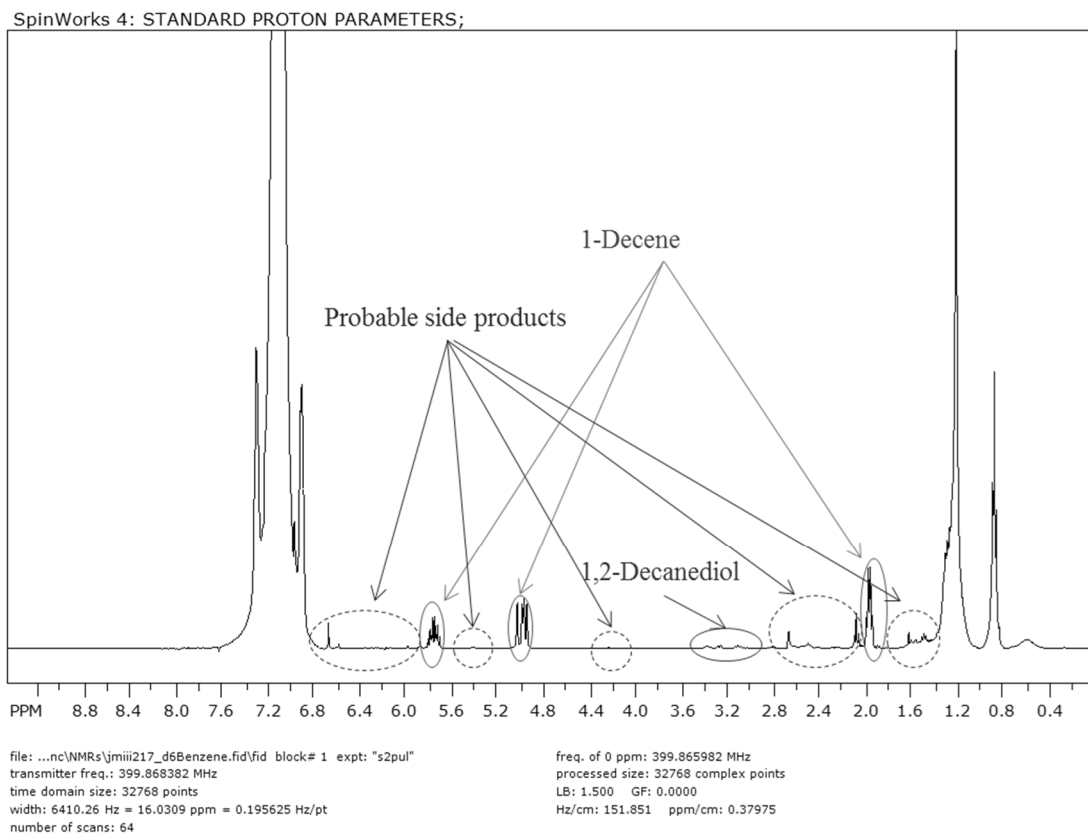
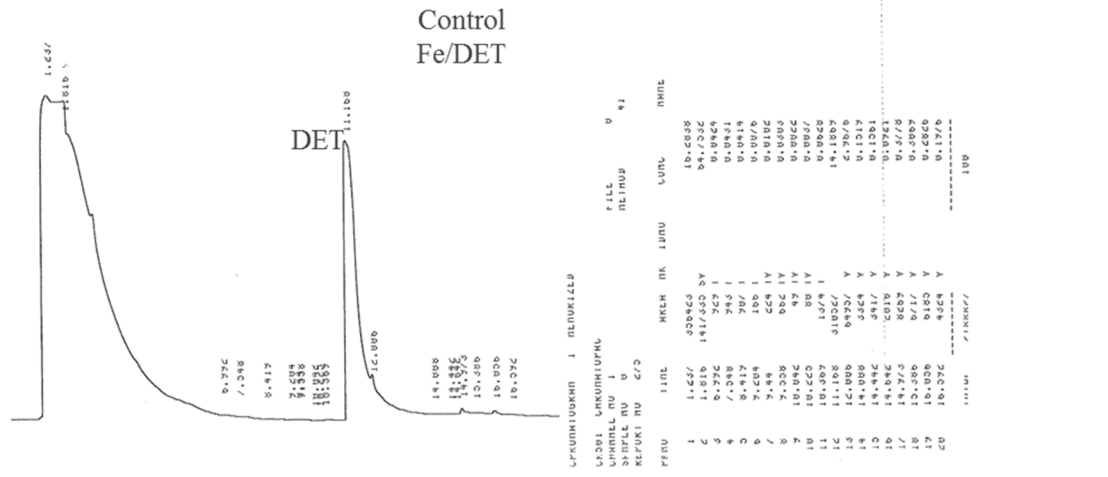
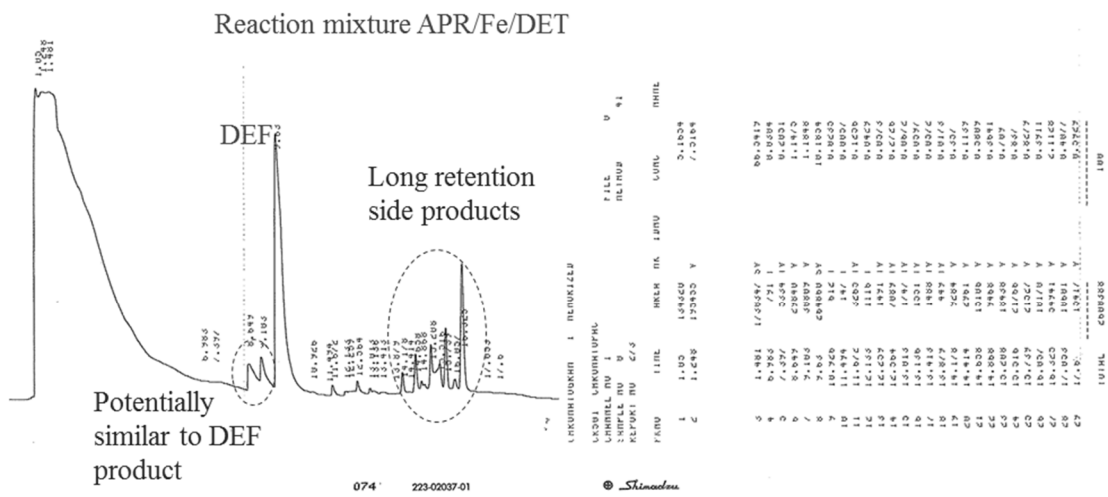


Figure 2.6.1 GC-FID of reaction mixture for Entry 2.3-1 from Table 2.3.1(APR/Zn/1,2-decanediol).



**Figure 2.6.2**  $^1\text{H-NMR}$  of reaction mixture for **Entry 2.3-1** from **Table 2.3.1 (APR/Zn/1,2-decanediol)**.

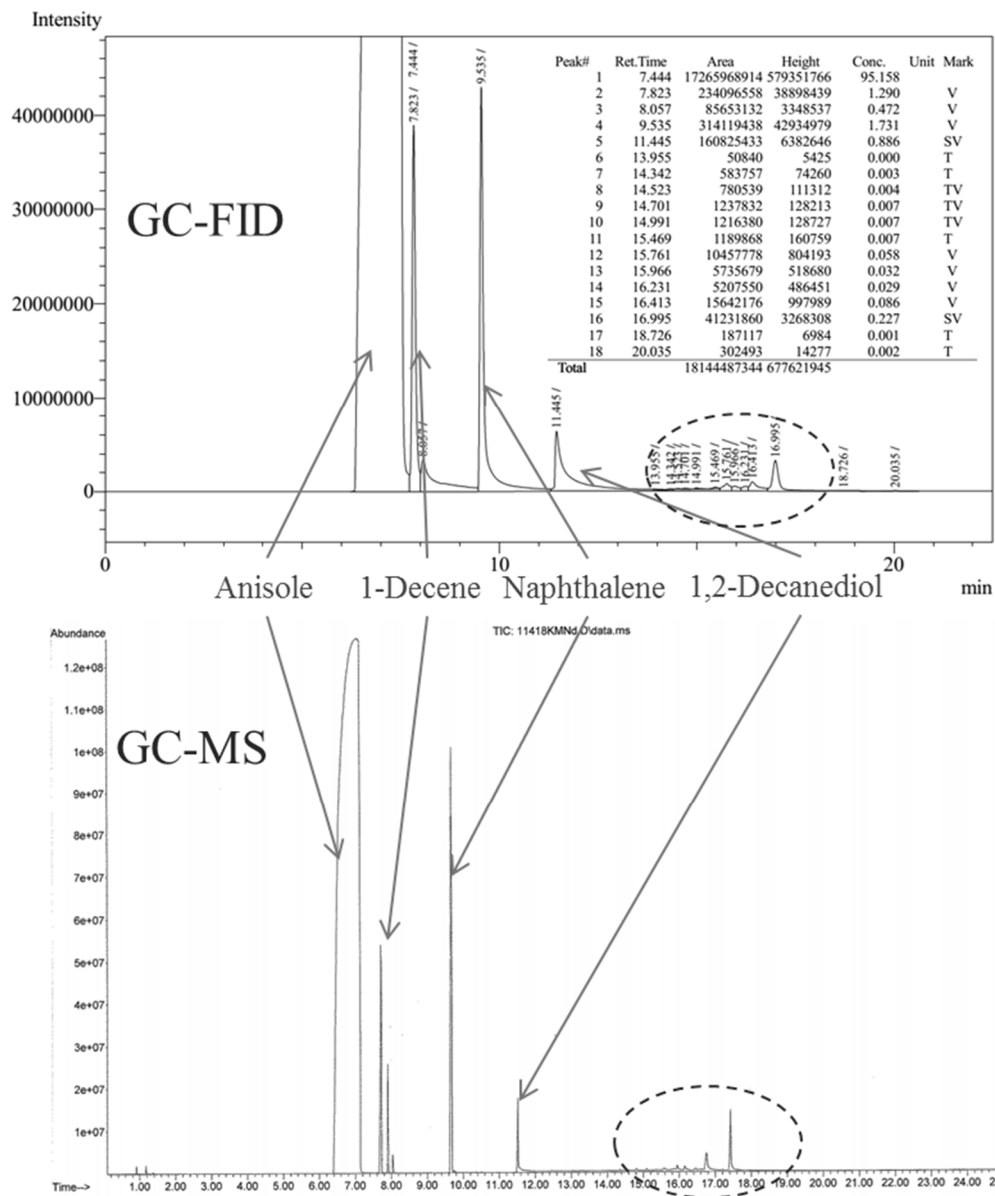
Another example can be seen by looking at the chromatograms for **Entry 2.5-3**, **Table 2.5.1 APR/Fe/DET** (**Figure 2.6.3** top) and its control partner Fe/DET (**Figure 2.6.3** bottom). It is conceivable that the two peaks (**Figure 2.6.3** top) at ca. 6.9 min before the product DEF peak could be similar to the alkene product, as we have noticed hydrolysis of one or both ester groups in other DODH reactions using DET. The long retention products appear to be substantial by their response with the FID. These extra peaks likely represent the mass accounting for  $\geq 95\%$  conversion with an alkene yield of 68%.



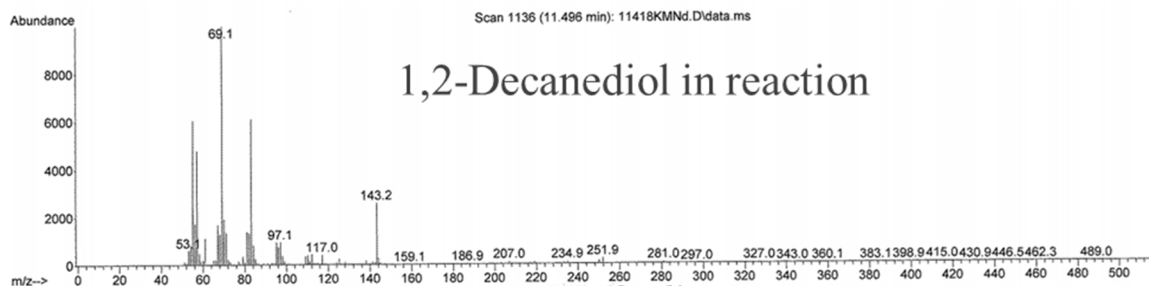
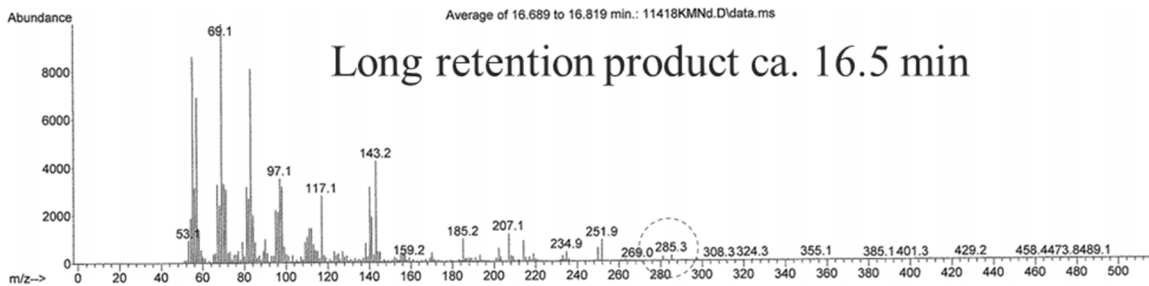
**Figure 2.6.3 GC-FID of reaction mixture for Entry 2.5-3, Table 2.5.1 APR/Fe/DET (top), GC-FID of control reaction Fe/DET (bottom).**

In the reaction for **Entry 2.4-2** from **Table 2.4.1** (1 mol% APR, 2 eq Zn, 2 M 1,2-decanediol in anisole), the long retention products were noted by GC-FID and the reaction mixture was subsequently analyzed by GC-MS (**Figure 2.6.4**). The two small peaks immediately following 1-decene are impurities in the anisole and have been identified by GC-MS and <sup>1</sup>H-NMR as two isomers of methylmethoxybenzene. The peak ca. 16.5 min has a molecular ion peak of 285 m/z which could correspond to a

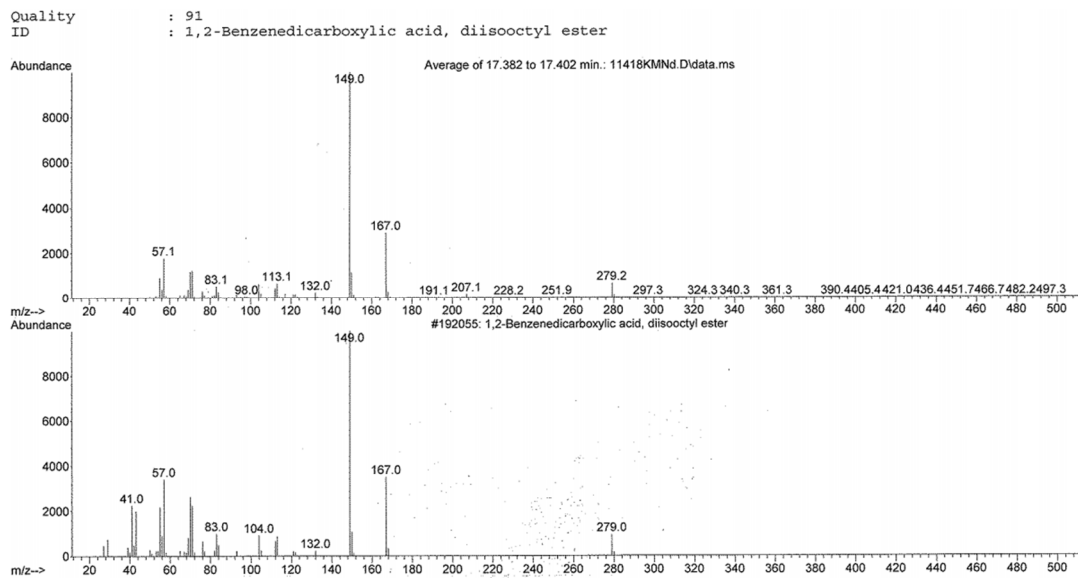
formula of  $C_{18}H_{28}O_2$  and a fragmentation pattern that is similar to the fragmentation pattern seen in 1,2-decanediol (**Figure 2.6.5**) and is likely a combination derived from 1,2-decanediol originally. The appearance of this peak ca. 16.5 min is likely one of the products that account for the remainder of the mass for the reaction. The longest retention major peak in the GC-MS (ca. 17.5 min GC-MS) is identified as 1,2-benzenedicarboxylic acid, diisooctyl ester (**Figure 2.6.6**) and is likely plasticizer contamination.



**Figure 2.6.4 GC-FID (top) and GC-MS (bottom) of reaction mixture Entry 2.4-2 from Table 2.4.1.**



**Figure 2.6.5** Fragmentation patterns for the long retention product at ca. 16.5 min and that of the remaining 1,2-decanediol in the reaction of Entry 2.4-2 from Table 2.4.1.

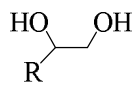
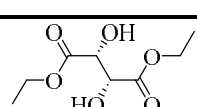
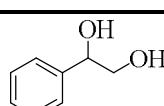
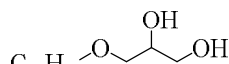


**Figure 2.6.6** Peak ca. 17.5 min in GC-MS for Entry 2.4-2 of Table 2.4.1, likely plasticizer contamination.

## 2.7 Discussion

The effectiveness of EI/APR glycol DODH with respect to the other reported Red/APR systems - Na<sub>2</sub>SO<sub>3</sub>/APR[54] and BnOH/APR[71] DODH is seen in **Table 2.7.1**. A marked improvement in alkene yield for aliphatic diol DODH utilizing EI/APR (60-69%) is seen in comparison to Na<sub>2</sub>SO<sub>3</sub>/APR (37%, [54]) and BnOH/APR (50%, [71]). Other diols such as DET yielded alkene approaching that of BnOH/APR (85-90% [71]) with EI/APR (60-85%). While the yield of styrene from styrene glycol DODH is improved to some extent with EI/APR (46%) as to that of Na<sub>2</sub>SO<sub>3</sub>/APR (34% [54]). The glycerol derivative batyl alcohol achieved an abated alkene yield with EI/APR (51%) with regard to BnOH/APR (83% [71]).

**Table 2.7.1 Comparison of APR/EI DODH to other APR/Red DODH systems.**

$\begin{array}{c} \text{HO} \quad \text{OH} \\   \quad   \\ \text{R}_1 - \text{C} - \text{C} - \text{R}_2 \\   \quad   \\ \text{H} \quad \text{H} \end{array} + \text{Red} \xrightarrow[150\text{ }^\circ\text{C}]{\text{APR}} \begin{array}{c} \text{R}_1 \quad \text{R}_2 \\ \backslash \quad / \\ \text{C} = \text{C} \end{array} + \text{RedO} + \text{H}_2\text{O}$				
Glycol	Red	Time (hr)	Conversion (%)	Yield (%) [ref]
 (R = Aliphatic chain)	Zn, Fe, Mn, C	24	100	60-69
	Na <sub>2</sub> SO <sub>3</sub>	26	100	37 [54]
	BnOH	24	100	50 [71]
	Zn, Fe, C	24	90-100	60-85
	BnOH	24	100	85-95 [71]
	Zn	12	100	46
	Na <sub>2</sub> SO <sub>3</sub>	12	100	34 [54]
	Zn	42	66	51
	BnOH	24	100	83 [71]

The mechanism for APR/EI/diol DODH could potentially parallel that of another heterogeneous-reductant system, MTO/Na<sub>2</sub>SO<sub>3</sub>/diol which was the subject of a rigorous computational investigation by Nicholas and Liu [56]. Starting from perrhenate reduction by EI could lead to an EI-O/EI stabilized rhenium(V) species that would undergo glycol condensation followed by alkene extrusion with concomitant reoxidation to perrhenate and release from EI-O/EI (**Figure 2.7.1**).

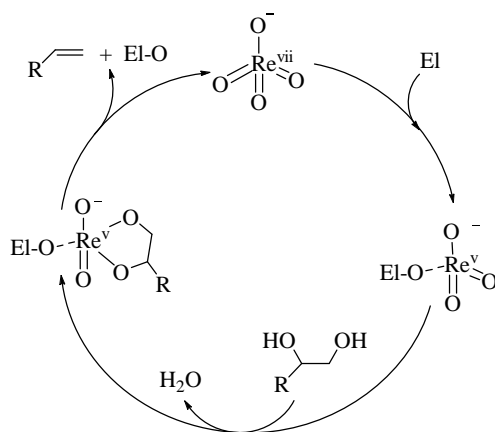


**Figure 2.7.1 Potential pathway for APR/EI/glycol DODH.**

## 2.8 Conclusion

We have reported the use of elemental zinc, iron, manganese and carbon as efficient reducing agents for the APR catalyzed DODH of polyols. These materials offer a simple, cheap, and convenient solid reagent for the conversion of polyols to olefins, allowing easy product separation from the oxidized elements. These oxidized elements have the potential to be utilized or recycled. Especially in the case of carbon the oxidized product, carbon monoxide, is a synthetically useful compound. Furthermore, these DODH reactions were shown to not require elevated pressure by running at atmospheric pressure in the high boiling solvent anisole.

## 2.9 Experimental

### 2.9.1 Reagents

Unless otherwise noted, reaction solvents (benzene, anisole, and toluene) were ACS grade and used as received from Sigma Aldrich and Alfa Aesar. Ammonium perrhenate (APR) was used as received from Alfa Aesar and stored in a dry desiccator or under vacuum. (+)-Diethyl-L-tartrate (DET) was used as received from Alfa Aesar. 1,2-Decanediol was used as received from TCI-America and Sigma Aldrich. 1-Phenyl-1,2-ethanediol (styrene glycol) was used as received from Sigma Aldrich. Elemental zinc 100-mesh and 325-mesh were from Sigma Aldrich and 30-mesh was from EM Scientific. Elemental iron 40-mesh and 100-mesh were from Fisher Scientific and 325-mesh was from Sigma Aldrich. Elemental manganese 325-mesh was from Alfa Aesar. See discussion *vide infra* concerning elemental metals used in reactions. Elemental carbon Darco G-60 100-mesh was used as received from Sigma Aldrich.

### 2.9.2 Typical Reaction Conditions

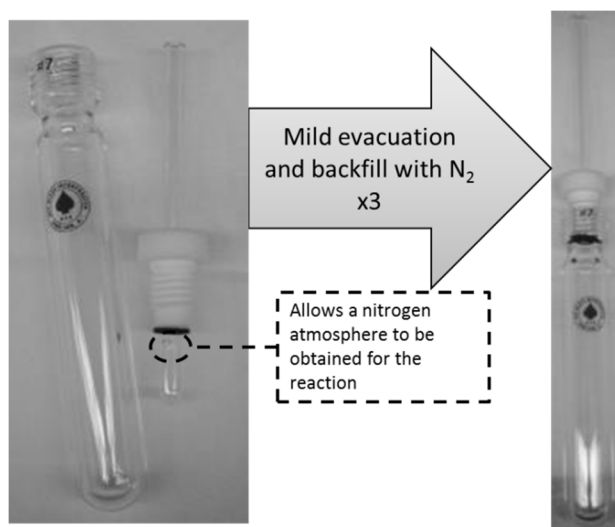


**Figure 2.9.1** Typical reaction setup for reactions carried out in pressure tubes.

Unless stated otherwise, reactions carried out in benzene (1-3 mL) using a sealed pressure tube, such as in **Figure 2.9.1**, (AceGlass and/or ChemGlass) equipped with a magnetic stir bar were 0.1-0.2 M diol with approximately 10 mol% APR catalyst, 1-3 equivalents of elemental reductant, degassed three times at room temperature with mild vacuum (ca. 60 mmHg) and backfilled with N<sub>2</sub> then heated at 150 °C for 24 h using a preheated oil bath. The reaction was cooled to room temperature and quantified by <sup>1</sup>H-NMR or GC-FID with the addition of an internal standard.

### 2.9.3 *Notes on Elemental Metals*

It was found that mild grinding of the elemental metals prior to reaction with an agate mortar and pestle gave consistent results, conceivably by exposing fresh, unoxidized surface. Alternatively, metals that were used directly out of a new bottle would show reproducible results, but after several uses from the same bottle the yield of the reactions would decrease. Cleaning the surface of the zinc by literature procedures [95] showed results similar to using from a new bottle of reagent and the same decrease in yield over time after the bottle was opened repeatedly was observed. A brisk stirring speed was found to aid in the reaction this is likely due to mass-transport effects given the heterogeneous nature of the reductants. The iron proved more difficult due to its magnetic properties with the use of magnetic stir bars, it was found a larger diameter reactor tube equipped with a large surface area stir bar partially surmounted the magnetism issue when used in similar volume reactions as the standard conditions. The effect of mesh size was found to play a role in reaction effectiveness with larger mesh reactions (30 mesh) requiring a more rapid stirring speed than the finer mesh reactions (100 & 325 mesh).

#### 2.9.4 Instrumentation

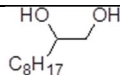
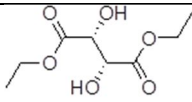
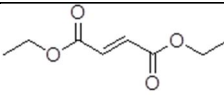
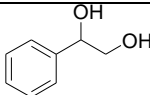
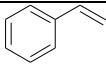
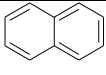
$^1\text{H}$  and  $^{13}\text{C}$  NMRs were collected on either on a Varian Mercury VX-300 MHz, Varian VNMRS-400 MHz or Varian VNMRS-500 MHz. All of the NMR data was processed using SpinWorks [96]. Gas chromatograms were collected on a Shimadzu GC-14A or a Shimadzu GC-2014 equipped with an AOC-20i+s autosampler, both with 3% SE-54 packed column, FID and thermal program 40 °C for 5 min; 20 deg/min to 250 °C; then 7 min at 250 °C or in decanediol reactions using heptadecane as standard 40 °C for 3min; 6 deg/min to 65 °C; 2 min at 65 °C; 20 deg/min to 100 °C; 2 min at 100 °C; 15 deg/min to 250 °C; 3 min at 250 °C. GC-MS analyses were performed on a Thermo-Finnigan instrument using the same thermal program as the former *vide supra* and a comparable stationary phase in a capillary column.

#### 2.9.5 Quantification Procedures

As stated, after reactions were cooled to room temperature and an internal standard was added for quantification. A known amount of naphthalene was added as a standard post reaction for reactions with 1,2-decanediol and 1-phenyl-1,2-ethanediol and quantified via GC-FID using multiple point internal standard calibration curve data obtained from authentic, weighed concentrations of diol/alkene/naphthalene. A known amount of naphthalene could also be used via  $^1\text{H}$ -NMR for quantification using the naphthalene proton signal ca. 7.6 ppm and the unique signals of the diols/alkenes for 1,2-decanediol, 1-phenyl-1,2-ethanediol and DET reactions (**Table 2.9.1**). Alternatively, known amounts of other standards possessing isolated  $^1\text{H}$ -NMR signals (DMF, DMSO, triphenylmethane, or isopropenyl acetate) could be used with certain diol/alkene reactions provided there were isolated unique peaks (diol/alkene/standard)

for quantification. The choice of deuterated solvent, typically  $\text{CDCl}_3$  or  $\text{C}_6\text{D}_6$ , and amount could be used to separate peaks in the  $^1\text{H}$ -NMR for quantification. An example is with the DET/DEF system in benzene, if  $\text{CDCl}_3$  was used as NMR solvent the characteristic DEF peaks would be adequately separated from the reaction solvent (benzene) but in  $\text{C}_6\text{D}_6$  there was not satisfactory resolution of peaks for DEF/reaction benzene. A semi-quantitative GC-FID analysis could be used in the DET/DEF systems, since naphthalene overlaps with DEF (both 9.5min), using multiple point external standard calibration curve data obtained from authentic weighed amounts of DET/DEF in the molarity range of the typical experiments (0.2M and below).

**Table 2.9.1 Compounds and approximate identifiers.**

Compound	GC Retention Time	<sup>1</sup> H-NMR Unique Signals
 C <sub>8</sub> H <sub>17</sub> 1,2-decanediol	11.5 min	CH, 3.9ppm CH <sub>2</sub> , 4.1ppm
 C <sub>8</sub> H <sub>17</sub> 1-decene	7.8 min	CH, 5.8ppm CH <sub>2</sub> , 5.0ppm CH <sub>2</sub> , 2.0ppm
 (+)-diethyl L-tartrate DET	10.9 min	2xCH, 4.5ppm
 diethyl fumarate DEF	9.5 min	2xCH, 6.8ppm
 1-phenyl-1,2-ethanediol	11.5 min	CH, 4.7ppm
 styrene	5.6 min	CH, 5.6ppm CH, 5.0ppm
 naphthalene	9.5 min	4xCH, 7.6ppm

### 2.9.6 Standard Reaction

As an example **Entry 2.3-3** from **Table 2.3.1**, in a glass pressure tube (**Figure 2.9.1**) equipped with a magnetic stir bar, 0.0429 mmol NH<sub>4</sub>ReO<sub>4</sub> was added followed by 0.421 mmol 1,2-decanediol, 0.869 mmol 325 mesh Zn (freshly ground) and 2 mL benzene. The tube was sealed with a Teflon, front-seal plunger valve and evacuated (ca. 60 mmHg) and backfilled with nitrogen (to atmospheric pressure) three times at room temperature and then the plunger valve was closed at room temperature leaving an

atmosphere of nitrogen in the tube at atmospheric pressure. The closed tube was then placed in a preheated oil bath at 150 °C for 24 hours. The tube was removed from the oil bath and allowed to cool to room temperature. A sample was removed and checked by <sup>1</sup>H-NMR in D<sub>6</sub>-benzene for completeness, showing the presence of 1-decene and very little 1,2-decanediol or any other detectable species the sample was returned to the original reaction mixture. Naphthalene (0.341 mmol) was added for quantification via GC-FID which showed a 68% yield based on multiple-point internal standard calibration curve data.

### 2.9.7 Procedure testing for CO and CO<sub>2</sub>

The buildup of a gas was noted during experiments using elemental carbon as reductant. To determine the composition of this gas was collected by connecting a hose to the purge tube of the reactor and the other end to an evacuated, sealed Schlenk tube. The purge tube was pushed back in to the reaction and the evacuated Schlenk tube was opened, transferring a gas sample to the Schlenk tube which was then closed again. A gas sample was removed from the sealed Schlenk tube and injected through a solution of barium hydroxide (lime water test) to look for the formation of carbonates of which none were observed. Next, approximately 1 mL of a dark brown beta naphthol-cuprous sulfate-sulfuric acid reagent (prepared from grinding 0.2 g cuprous oxide, 0.25 g beta naphthol in a cooled mixture of 0.25 mL water and 2 mL sulfuric acid) [97] was injected in to the Schlenk tube containing the gas sample. The beta naphthol-cuprous sulfate-sulfuric acid reagent is reported to absorb carbon monoxide slowly and completely until saturation and is useful for low concentration samples. The brown solution turned blue over a period of several hours, indicating the presence of carbon

monoxide. Controls using air and carbon dioxide both remained dark brown suspensions. A second test for carbon dioxide was performed using a reflux reaction in anisole using carbon as reductant, the reaction was sealed except for a tube that would allow gas to escape and bubble through a barium hydroxide solution. Again there were no observations of carbonate formation from the gas generated during the reaction.

## **Chapter 3 Oxorhenium(V) Catalyzed DODH**

### 3.1 Background and Introduction

The research effort on oxorhenium catalyzed DODH of polyols has primarily been dominated by Re(VII) compounds; **Figure 3.1.1** contains some of these rhenium(VII) compounds used as pre-catalysts to date with example references: **A** Cp\*ReO<sub>3</sub>, **B** MTO, **C** Tp\*ReO<sub>3</sub>, **D** ZReO<sub>4</sub>, and **E** Cp'ReO<sub>3</sub>. Fully oxidized rhenium (Re<sup>vii</sup>) is a very stable oxidation state [98-100], therefore it is not surprising the majority of the DODH oxorhenium catalysts enter the reaction as Re(VII). One exception is seen in the use of Re<sub>2</sub>(CO)<sub>10</sub> which was active as a DODH pre-catalyst only in the presence of air and is likely being oxidized to an oxorhenium(VII) species in the reaction[34]. Many investigators of the oxorhenium catalyzed DODH of polyols believe the rhenium most likely cycles between Re<sup>vii</sup> and Re<sup>v</sup> during the reaction [31, 42, 54, 101]. Rhenium(V) species require appropriate stabilizing ligands otherwise they will typically disproportionate to rhenium IV and VI species [59, 98]. With this information in mind, we set out to find a stable oxorhenium(V) compound that could potentially cycle between Re<sup>v</sup>↔Re<sup>vii</sup> and examine its potential for the DODH of polyols.

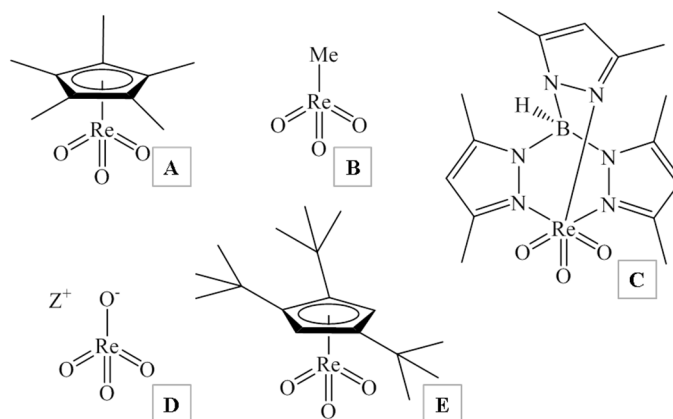
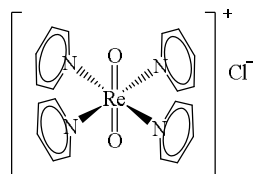


**Figure 3.1.1 Examples of oxorhenium(VII) compounds used for the DODH of polyols.** A – Cp\*ReO<sub>3</sub> [31], B – MTO [35, 55, 68], C – Tp\*ReO<sub>3</sub> [49], D – ZReO<sub>4</sub> (Z<sup>+</sup> = H<sup>+</sup>, NH<sub>4</sub><sup>+</sup>, TBA<sup>+</sup>) [54, 57, 71], E – Cp'ReO<sub>3</sub> [33].

While searching the literature we noticed the report on the reduction of perchlorate to chloride utilizing oxorhenium compounds as part of the catalytic system by Shapley and coworkers[102]. They note the likely rhenium catalytic cycle involves a  $\text{Re}^{\text{v}} \leftrightarrow \text{Re}^{\text{vii}}$  redox. In their report they use the cationic oxorhenium(V) species *trans*-dioxotetrapyridinerhenium ( $[\text{Re}^{\text{v}}\text{O}_2\text{py}_4]^+$ ) as pre-catalyst for these reactions, which peaked our interests. Upon further literature exploration, we noted numerous synthetic pathways to the air stable  $[\text{Re}^{\text{v}}\text{O}_2\text{py}_4]^+$  which were simple and tolerant of bench-top conditions (air/water presence)[103-106]. Therefore, we decided to investigate the capability of stable oxorhenium(V) compounds, particularly  $[\text{ReO}_2\text{py}_4]^+$ , for the catalytic DODH of polyols.

### 3.2 Synthesis of *Trans*-[ReO<sub>2</sub>py<sub>4</sub>]Cl (**1a**)



**1a**

**Figure 3.2.1** Structural representation of *trans*-dioxotetrapyridinerhenium chloride ([ReO<sub>2</sub>py<sub>4</sub>]Cl, **1a**).

The yellow/orange rhenium (V) complex, *trans*-[ReO<sub>2</sub>py<sub>4</sub>]Cl (**1a**), can be synthesized by multiple routes beginning with a perrhenate compound (ZReO<sub>4</sub>, Z = H<sup>+</sup>, NH<sub>4</sub><sup>+</sup>, K<sup>+</sup>, etc.) forming intermediate rhenium compounds, K<sub>2</sub>[ReOCl<sub>5</sub>] (**Route A Figure 3.2.2**), K<sub>2</sub>[ReCl<sub>6</sub>] (**Route B Figure 3.2.2**), or *trans*-[ReOCl<sub>3</sub>(TPP)<sub>2</sub>] (**Route C Figure 3.2.2**)[103, 107-109]. For our initial approach we started by using commercially available ammonium perrhenate to synthesize *trans*-[ReOCl<sub>3</sub>(TPP)<sub>2</sub>] (**Route C Figure 3.2.2**) because of its ease of synthesis. From the green *trans*-[ReOCl<sub>3</sub>(TPP)<sub>2</sub>], **1a** is readily synthesized in an aqueous acetone/pyridine solution by refluxing followed by cooling to precipitate the yellow/orange complex. This same route (**route C Figure 3.2.2**) is also reported to be effective with substituted, electron-rich pyridines.

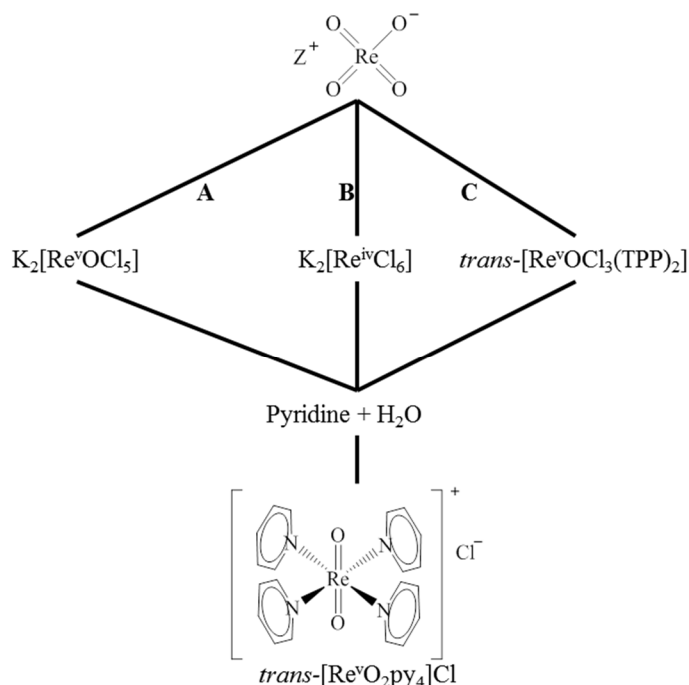


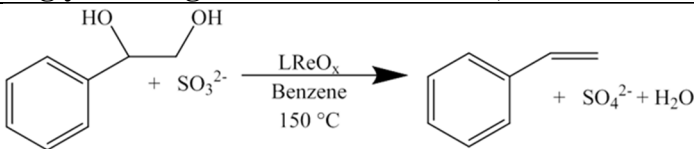
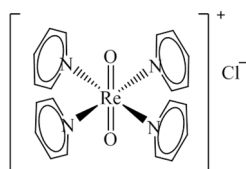
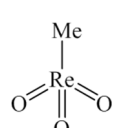
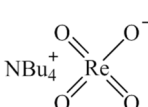
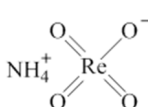
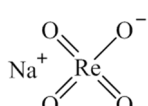
**Figure 3.2.2** Synthesis of *trans*-[ReO<sub>2</sub>py<sub>4</sub>]Cl (**1a**) by various intermediates with aqueous pyridine all starting from ZReO<sub>4</sub> (Z = H<sup>+</sup>, NH<sub>4</sub><sup>+</sup>, K<sup>+</sup>, Na<sup>+</sup>). Route A. K<sub>2</sub>[ReOCl<sub>5</sub>] [107], B. K<sub>2</sub>[ReCl<sub>6</sub>] [103], C. *trans*-[ReOCl<sub>3</sub>(TPP)<sub>2</sub>] [108, 109].

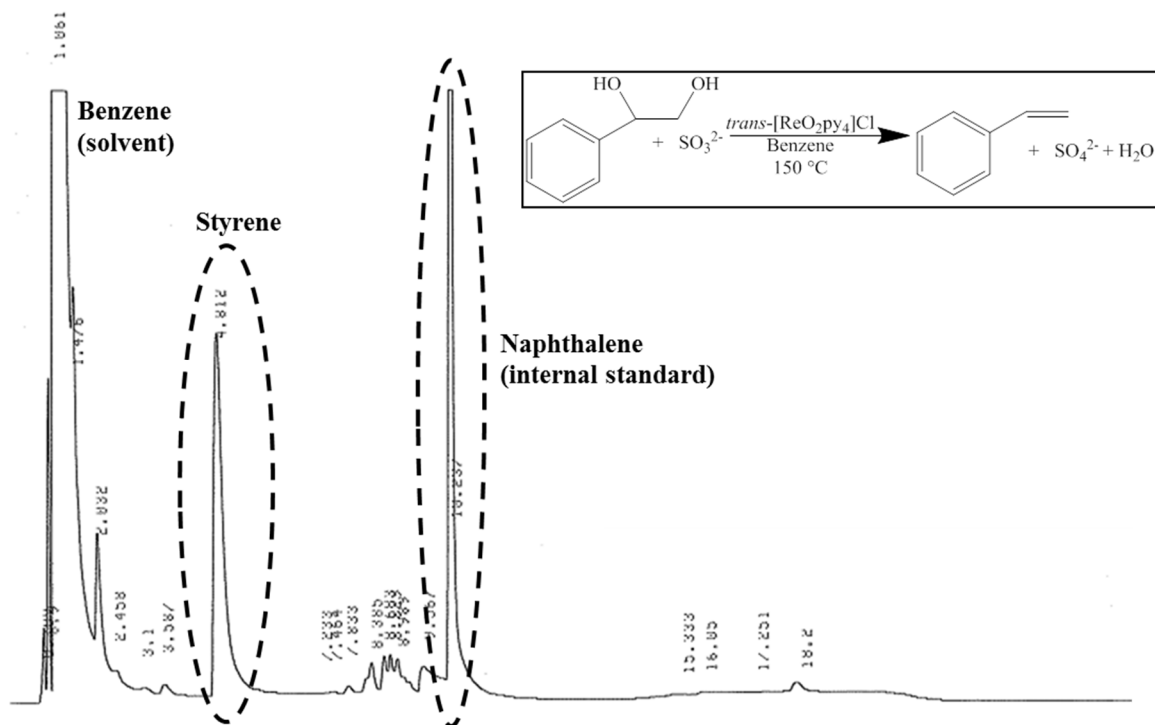
### 3.3 Establishing Catalytic Activity of [ReO<sub>2</sub>py<sub>4</sub>]Cl (**1a**) for DODH with Glycols and Sodium Sulfite

To gauge the viability of rhenium(V) complexes to be used in catalytic DODH reactions of glycols, the catalytic activity of [ReO<sub>2</sub>py<sub>4</sub>]Cl (**1a**) with styrene glycol was compared to that of more readily commercially available oxorhenium (VII) complexes employed in our lab utilizing relatively inexpensive sodium sulfite as reductant (**Table 3.3.1**). Under the conditions tested, sodium sulfite is insoluble in benzene as well as the oxidized product sodium sulfate. MTO, which has become synonymous with DODH of glycols [31, 42], under these conditions was reported to give a 59% yield of styrene and 100% conversion of the styrene glycol in four hours (**Entry 3.3-2, Table 3.3.1**). The noticeably more soluble tetrabutylammonium perrhenate was reported to impressively

yield 71% styrene in 59 hours with full conversion of the glycol (**Entry 3.3-3, Table 3.3.1**). The less soluble ammonium (**Entry 3.3-4, Table 3.3.1**) and sodium perrhenate (**Entry 3.3-5, Table 3.3.1**) were reported to both give full glycol conversion accompanied with 34% yield in 12 hours and 53% yield in 40 hours of styrene respectively. Rhenium oxide ( $\text{Re}_2\text{O}_7$ ) was noted to give a 23% yield of styrene in 63 hours with 80% glycol conversion (**Entry 3.3-6, Table 3.3.1**). Following these reports from our lab [54, 55], ca. 10 mol% *trans*- $[\text{ReO}_2\text{py}_4]\text{Cl}$  (**1a**) was combined with styrene glycol and sodium sulfite in benzene (**Entry 3.3-1, Table 3.3.1**). This reaction was conducted in a sealed, glass pressure tube at 150 °C for a day. This reaction mixture by GC-FID (**Figure 3.3.1**) was analyzed and showed a high conversion of styrene glycol and a 52% yield of styrene. As can be seen in the GC-FID in **Figure 3.3.1**, there are multiple unidentified organic compounds ca. 7-10 minutes that are likely glycol derived. Comparatively, **1a** appeared to be competent of the DODH of styrene glycol with sodium sulfite with respect to results our lab reported (**Table 3.3.1**). Although the styrene yield was not as high as the tetrabutylammonium perrhenate at 71% in 40 hours (**Entry 3.3-3, Table 3.3.1**), **1a** did comparably to the other oxorhenium compounds in 24 hours versus typically longer reaction times reported for the other compounds.

**Table 3.3.1 Comparison of 1a with other published oxorhenium compounds for DODH of styrene glycol using sulfite in benzene [54, 55].**

			
<b>LReO<sub>x</sub></b> <b>(Entry)</b>	<b>Time (hr)</b>	<b>Diol</b> <b>Conversion</b>	<b>Yield Styrene</b> <b>(%) [ref]</b>
 <b>3.3-1</b>	24	100	52
 <b>3.3-2</b>	4	100	59 [54, 55]
 <b>3.3-3</b>	59	100	71 [54, 55]
 <b>3.3-4</b>	12	100	34 [54, 55]
 <b>3.3-5</b>	40	100	53 [54, 55]
<b>Re<sub>2</sub>O<sub>7</sub></b> <b>3.3-6</b>	63	80	23 [54, 55]

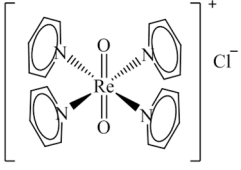
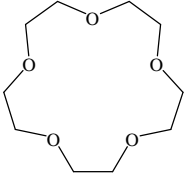


**Figure 3.3.1** GC-FID of reaction of styrene glycol with sodium sulfite catalyzed by **1a** in benzene with naphthalene internal standard.

Generally, the less activated aliphatic glycols such as 1,2-octanediol, are more challenging substrates for DODH. After 40 hours, MTO yielded 45% 1-octene and full conversion of the diol (**Entry 3.3-8, Table 3.3.2**). In an effort to make the sodium sulfite more soluble by chelating the sodium cation, 15-crown-5 was used in combination with MTO to give full conversion of the glycol and 98% yield 1-octene with a shorter reaction time of 21 hours (**Entry 3.3-9, Table 3.3.2**). Sodium perrhenate alone in the conditions shown in **Table 3.3.2** yielded 4% 1-octene after 88 hours, converting 8% of the starting diol (**Entry 3.3-10, Table 3.3.2**). The reaction using sodium perrhenate was also improved with the addition of 15-crown-5; after 100 hours full diol conversion and a 30% yield of 1-octene were achieved (**Entry 3.3-11, Table 3.3.2**). The addition of anhydrous sodium sulfate to the reaction using NaReO<sub>4</sub> and 15-

crown-5 increased the yield of 1-octene to 38% in 42 hours with nearly complete conversion of the 1,2-octanediol (**Entry 3.3-12, Table 3.3.2**). These results demonstrate that 1,2-octanediol is a less active substrate compared to styrene glycol for DODH. With this in mind, **1a** was screened (**Table 3.3.2**) with respect to results reported from our lab for oxorhenium compounds on 1,2-octanediol with sulfite as the reductant in chlorobenzene (**Entry 3.3-7, Table 3.3.2**)[54, 55]. A 49% yield of 1-octene was observed when **1a** was employed as the oxorhenium complex; the GC-FID of this reaction mixture is seen in **Figure 3.3.2**. This modest result was achieved with a full conversion of the starting 1,2-octanediol in 24 hours, **Figure 3.3.2** shows unidentified long retention organic products past ca. 14 minutes that are most likely octanediol derived. This reaction, which starts out with nearly insoluble, orange **1a** gives an extremely faint orange tint to the chlorobenzene, turns blue/green after the first five minutes at 150 °C, turning to green/brown after two hours then remaining various shades of brown till the reaction was removed from the oil bath. Looking at the reactions with oxorhenium compounds MTO and NaReO<sub>4</sub> that were conducted in the same solvent/temperature/reductant conditions as **1a**, it would appear the oxorhenium (V) compound has DODH reactivity even with this typically less active substrate making **1a** an attractive oxorhenium compound for mechanistic DODH studies

**Table 3.3.2 Comparison of **1a** with reported oxorhenium compounds in the DODH of 1,2-octanediol with sulfite in chlorobenzene reactions[54, 55].**

$\text{C}_6\text{H}_{13}\text{CH(OH)CH}_2\text{OH} + \text{SO}_3^{2-} \xrightarrow[\text{150 } ^\circ\text{C}]{\text{LReO}_x, \text{Chlorobenzene}} \text{C}_6\text{H}_{13}\text{CH=CH}_2 + \text{SO}_4^{2-} + \text{H}_2\text{O}$				
<b>LReO<sub>x</sub></b> <b>(Entry)</b>	<b>Additive</b>	<b>Time</b> <b>(hr)</b>	<b>Diol</b> <b>Conversion</b> <b>(%)</b>	<b>Yield</b> <b>1-Octene</b> <b>(%)</b>
 <b>3.3-7</b>	(none)	24	100	49
<b>MTO</b> <b>3.3-8</b>	(none)	40	100	45 [54, 55]
<b>MTO</b> <b>3.3-9</b>	 15-crown-5	21	98	43 [54, 55]
<b>NaReO<sub>4</sub></b> <b>3.3-10</b>	(none)	88	8	4 [54, 55]
<b>NaReO<sub>4</sub></b> <b>3.3-11</b>	15-crown-5	100	100	30 [54, 55]
<b>NaReO<sub>4</sub></b> <b>3.3-12</b>	15-crown-5, Na <sub>2</sub> SO <sub>4</sub>	42	98	38 [54, 55]

The results of these initial reactions using **1a** as the oxorhenium complex with the occasionally challenging sodium sulfite as the reductant gave moderate alkene yields (ca. 50% for both styrene and 1-octene) within 24 hour reaction time indicated that this complex was a good candidate for further DODH investigation. Given the 100% conversion of the diol for both styrene glycol (**Figure 3.3.1**) and 1,2-octanediol (**Figure 3.3.2**), as was typically seen in the reference reactions (**Table 3.3.1** and **Table**

3.3.2)[54, 55], there are diol consuming side reactions occurring. Given the lack of mass balance, both initial reactions were submitted for GC-MS and indicated the long retention products were diol-derived. In both cases there was not a single dominant side product but a significant mixture of organic compounds. It was decided to not explore the off DODH-pathway reactions forming these side products when sodium sulfite was used as reductant.

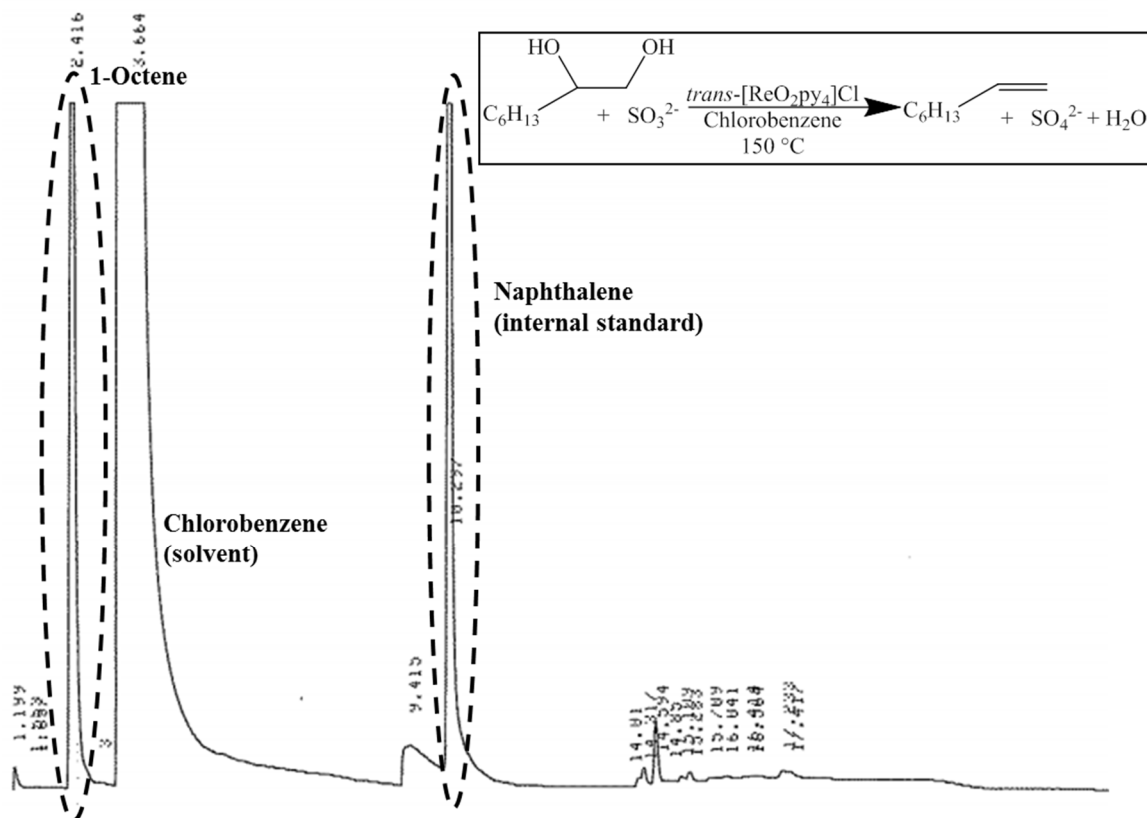


Figure 3.3.2 GC-FID of the DODH reaction of 1,2-octanediol with sodium sulfite catalyzed by **1a** in chlorobenzene with naphthalene internal standard.

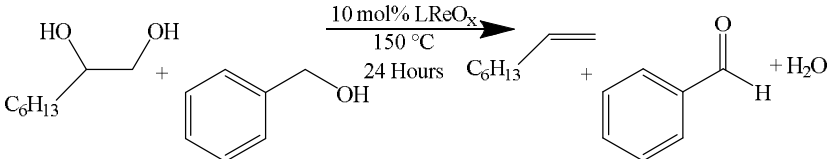
The promising initial comparative results of **1a** with reported results (Table 3.3.1 and Table 3.3.2) using sulfite as the reductant as well as color changes which would likely indicate a change in coordination and/or oxidation state of the rhenium, continued study of **1a** was merited. The 49% yield of 1-octene with 1,2-octanediol was

noteworthy since this substrate is often less reactive than styrene glycol. Further experiments did not succeed in greatly exceeding the original 49% yield of 1-octene, with a maximum of 56% yield 1-octene being reached. Given these observations it would appear that  $[\text{ReO}_2\text{py}_4]\text{Cl}$  offers improved reactivity over other oxorhenium compounds.

### 3.4 Benzyl Alcohol as Reductant

In an attempt to make the study of DODH with *trans*- $[\text{ReO}_2\text{py}_4]\text{Cl}$  (**1a**) less complicated due to appreciable side products, it was decided to try another reducing agent. Following the fruitful results of Boucher-Jacobs and Nicholas with benzyl alcohol as reductant for DODH[71], this primary alcohol was tested as reductant in DODH reactions catalyzed by **1a**. It was decided to continue with 1,2-octanediol as substrate as to allow for comparison with the sulfite results using **1a** *vide supra*. In the APR/BnOH system (**Table 3.4.1, Entry 3.4-1** [71]), a yield of 50% 1-octene was achieved in benzene in 24 hours accompanied by full conversion of the diol. It was decided for the **1a**/BnOH system to continue using chlorobenzene as previously in the sulfite system, this reaction combination remarkably yielded 80% 1-octene with full diol conversion (**Table 3.4.1, Entry 3.4-2**) under similar conditions as the benchmark APR/BnOH system.

**Table 3.4.1 Comparison of LReO<sub>x</sub> compounds using benzyl alcohol as reductant.**

			
<b>LReO<sub>x</sub> (Entry)</b>	<b>Solvent</b>	<b>Glycol Conversion (%)</b>	<b>1-Octene Yield (%) [ref]</b>
APR <b>3.4-1</b>	Benzene	100	50 [71]
<i>Trans</i> -[ReO <sub>2</sub> py <sub>4</sub> ]Cl ( <b>1a</b> ) <b>3.4-2</b>	Chlorobenzene	100	80

The <sup>1</sup>H-NMR spectrum of **Entry 3.4-2** in **Figure 3.4.1** demonstrates the convenient separation of signals for the reaction components of this reaction in chlorobenzene. The appearance of two additional signals in the vicinity of the alkene proton signal near 6 ppm can be seen in the <sup>1</sup>H-NMR spectra over the time course of the reaction conducted in chlorobenzene in **Figure 3.4.2**. A similar signal was noted by Boucher-Jacobs when using BnOH as reductant with diols in benzene. In this case she confirmed it was derived from acid catalyzed acetal formation (**Figure 3.4.3**) between the oxidized benzaldehyde DODH co-product and the substrate diol[110]. This was confirmed in my reactions in chlorobenzene – e.g. the same acetal was formed with benzaldehyde and 1,2-octanediol with a catalytic amount of *para*-toluenesulfonic acid. The appearance of two peaks of different magnitude is likely due to major and minor acetal stereoisomers being formed. Additionally it was found that at temperatures below ca. 150 °C, the acetal formation occurred faster than the DODH to the alkene in PhCl. The acetal formation is a reversible reaction (**Figure 3.4.3**) and under DODH conditions it is possible to still get full DODH conversion.

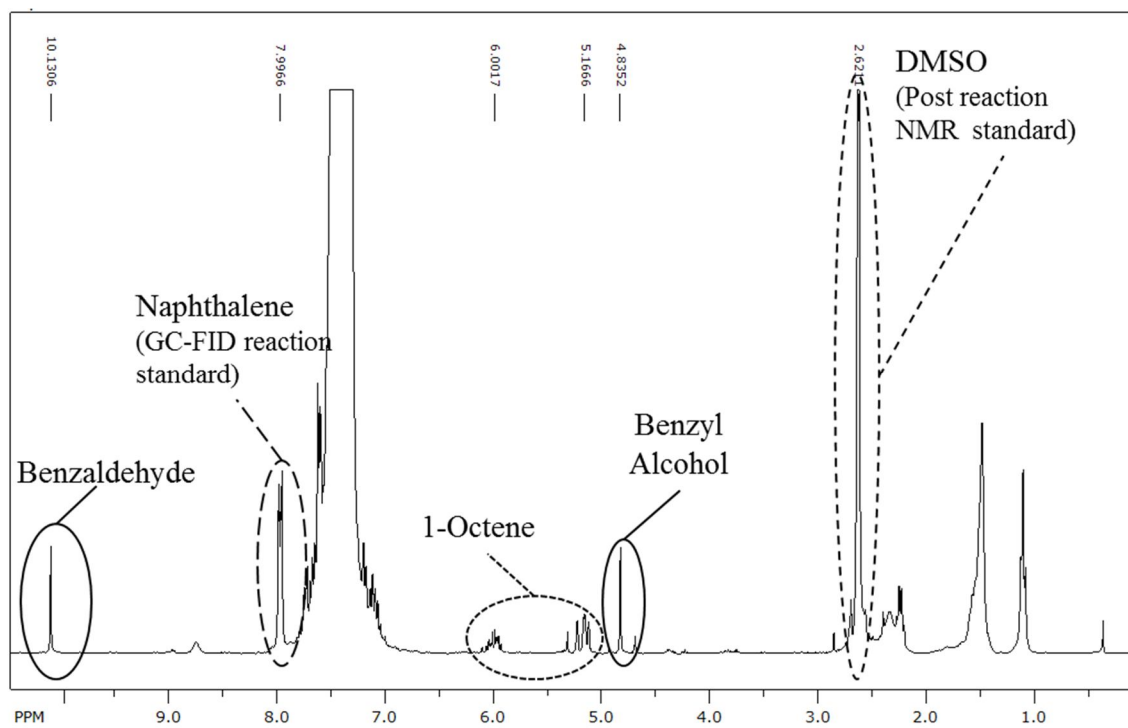


**Figure 3.4.1**  $^1\text{H-NMR}$  of the 1a/BnOH/1,2-octanediol reaction in chlorobenzene.

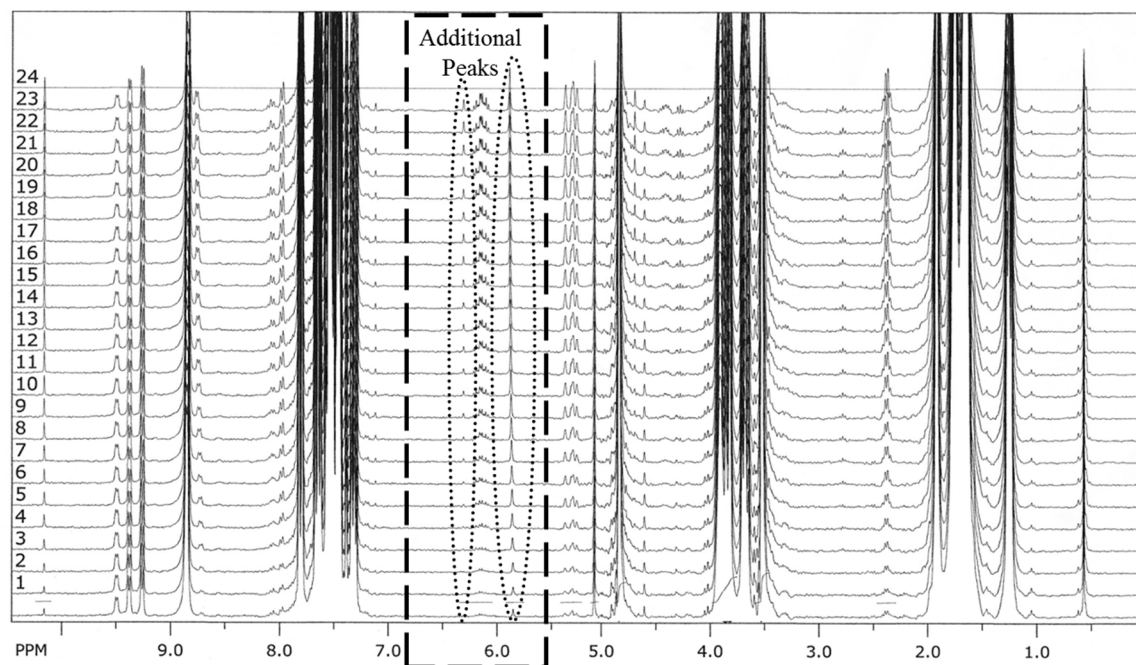


**Figure 3.4.2**  $^1\text{H-NMR}$  time course reaction of 1,2-octanediol with BnOH in chlorobenzene showing formation of additional peaks in the 6 ppm region.

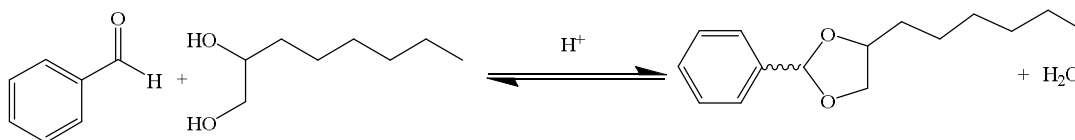


**Figure 3.4.3 Acid catalyzed acetal formation from benzaldehyde and 1,2-octanediol.**

A solution to the formation of the acetals in the APR/BnOH/diol reactions was reported using *para*-methoxybenzyl alcohol (*p*-MeOBnOH) as reductant[110]. The use of *p*-MeOBnOH as reductant with **1a** and 1,2-octanediol in chlorobenzene did suppress the formation of acetals but not completely. It was noted that the increased formation of acetals was linked to “freshness” of the chlorobenzene solvent. Reactions employing newly opened bottles or freshly distilled PhCl tended to show little to no acetal formation but subsequent use (accompanied by exposure to the air) of these solvents showed increased acetal formation. It is likely the PhCl was the source of the acid upon extended exposure to the atmosphere; therefore we tried to avoid the use of halogenated solvents when possible for DODH reactions with **1a**/BnOH, although even with the reversible acetal formation a full DODH conversion may be possible.

### 3.5 Nature of Oxorhenium Catalyst in Reaction/Post-Reaction

The nature of the oxorhenium compound that is responsible for catalysis in the high yielding DODH reaction of **1a**/BnOH/1,2-octanediol was in question. Perrhenate has been shown to catalyze DODH of diols [54, 71] and are the most likely decomposition product for high oxidation state oxorhenium compounds due to its thermodynamically stability. We set about verifying that perrhenate was not being formed appreciably in the reaction. A soluble control solution of tetrabutylammonium perrhenate solution in PhCl was diluted and analyzed by negative ESI-MS until the

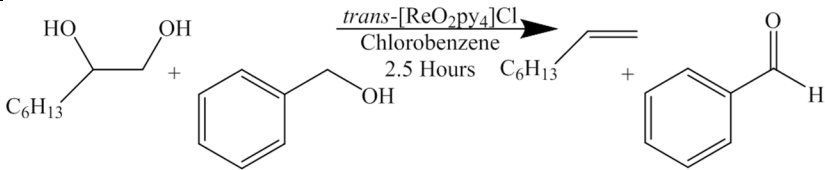
limit of detection of the instrument was reached. A DODH reaction with **1a**/BnOH/1,2-octanediol in PhCl was conducted yielding a 69% 1-octene and immediately analyzed by negative ESI MS the same as the control. The outcome showed that no more than 2.4% of the rhenium was perrhenate or in other words no more than 0.2 mol%  $\text{ReO}_4^-$ . Further support that **1a** remained intact after the reaction was seen by the crystallization of the oxorhenium complex **1a** from the post-reaction cooled solution and was confirmed by FT-IR. With this evidence combined with the comparative experiments (**Table 3.4.1**) to Boucher-Jacobs lower yielding aliphatic alkene reactions using perrhenates/BnOH and aliphatic glycols [71, 110], we believe it is likely  $[\text{ReO}_2\text{py}_4]\text{Cl}$  is responsible for the high yields of the aliphatic alkene with BnOH. Additionally, the efficient synthesis of  $[\text{ReO}_2\text{py}_4]\text{Cl}$  from perrhenate requires acidic conditions with a reductant to isolate a lower oxidation state (typically rhenium V) rhenium/oxorhenium compound [111], this is followed by a separate reaction using an excess of pyridine and water under an air atmosphere. Therefore, the visibly significant amount of **1a** that crystalized back out of solution from high alkene yielding DODH reactions would not be convincingly possible to reform post-reaction if this compound was degrading to perrhenate during the reaction.

### **3.6 Investigating the Activity of *trans*- $[\text{ReO}_2\text{py}_4]^+$ in Additional DODH Reactions**

Confident that *trans*- $[\text{ReO}_2\text{py}_4]^+$  was the origin of the observed catalytic DODH activity, we sought to further investigate the properties of this oxorhenium compound for DODH reactions. The majority of the results thus far with  $[\text{ReO}_2\text{py}_4]\text{Cl}$  for DODH have been conducted at 150 °C for 24 hours. Following multiple reports of utilizing

elevated reaction temperatures for DODH reactions for shorter periods of time [68, 71, 72], we compared the reaction using **1a**, BnOH, and 1,2-octanediol in chlorobenzene for 2.5 hours at 150 °C versus 2.5 hours at 170 °C (**Table 3.6.1**). As can be seen in **Table 3.6.1, Entry 3.6-1** at 150 °C had a lower diol conversion and alkene yield (36% and 26% respectively) compared to **Entry 3.6-2** at 170 °C (>90% and 76% respectively) in the 2.5 hour reactions. This higher alkene yielding result was not totally unexpected with the elevation in temperature. Nonetheless, there can be different reactivity or even component degradation seen at elevated temperatures, fortunately this did not appear to be happening in the case at hand.

**Table 3.6.1 Temperature effects on diol conversion and alkene yield in 2.5 hours for [ReO<sub>2</sub>py<sub>4</sub>]Cl/BnOH/1,2-octanediol reactions in chlorobenzene.**

		
Temperature (°C) (Entry)	Diol Conversion (%)	Alkene Yield (%)
150 <b>3.6-1</b>	36	26
170 <b>3.6-2</b>	>90	76

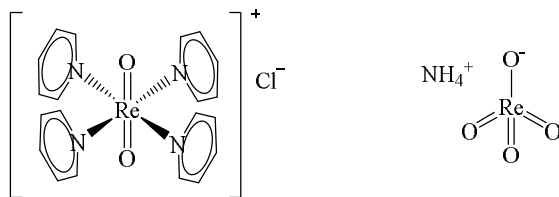


**Figure 3.6.1 Structure of the octahedral [ReO<sub>2</sub>py<sub>4</sub>]Cl compared to that of tetrahedral ammonium perrhenate.**

Given the very impressive conversion and yields of the reported APR/BnOH/DET system [71], the activity of *trans*-[ReO<sub>2</sub>py<sub>4</sub>]Cl with BnOH and DET

was of curiosity. **Table 3.6.2** illustrates the activity with respect to conversion and yield of the DET/BnOH DODH reaction catalyzed by  $[\text{ReO}_2\text{py}_4]\text{Cl}$  (**Entry 3.6-4**), 86 % and 57% respectively, compared to that of APR (**Entry 3.6-3**), 100% and 95% respectively. This result is an interesting contrast to what was observed in the 1,2-octanediol/BnOH reaction comparison (**Table 3.4.1**) where  $[\text{ReO}_2\text{py}_4]\text{Cl}$  out performed APR. This could imply the catalytically active rhenium species are not necessarily the same or similar. Looking at the two different complexes, **Figure 3.6.1**, one will notice that the rhenium species in APR starts out as a tetrahedral rhenium(VII) anion with only oxo ligands and in the case of  $[\text{ReO}_2\text{py}_4]\text{Cl}$  an octahedral rhenium(V) cation with pyridine and oxo ligands and an outer sphere chloride that could potentially coordinate.

**Table 3.6.2 Comparison of the reaction in benzene of the reported APR/BnOH/DET with that of  $[\text{ReO}_2\text{py}_4]\text{Cl}$ /BnOH/DET in 24 hours.**

<b>LReO<sub>x</sub></b> <b>(Entry)</b>	<b>DET Conversion (%)</b>	<b>DEF Yield (%)</b> <b>[ref]</b>
APR <b>3.6-3</b>	100	95 [71]
<i>Trans</i> - $[\text{ReO}_2\text{py}_4]\text{Cl}$ ( <b>1a</b> ) <b>3.6-4</b>	86	57

Since a vast number of DODH reports use triphenylphosphine (**Figure 3.6.2**) as a very active reductant[42], it was logical to try the activity of TPP with  $[\text{ReO}_2\text{py}_4]\text{Cl}$  on 1,2-octanediol. It was somewhat of a surprise that this was not the case when combined with  $[\text{ReO}_2\text{py}_4]\text{Cl}$  and 1,2-octanediol. In fact, it appears that the reaction used some of the starting diol as reductant reasoned by aldehydic signals showing up in the  $^1\text{H-NMR}$  of the reaction mixture accompanied by little sign of alkene but prominent signals of the

starting diol. Additionally, given the success with benzyl alcohol as reductant and  $[\text{ReO}_2\text{py}_4]\text{Cl}$ , it was decided to try benzhydrol as reductant which is structurally similar to benzyl alcohol except for the replacement of a proton with a phenyl group to the benzylic carbon (**Figure 3.6.2**). This larger reductant also did not appreciably yield alkene and also showed sign of oxidation of the starting diol via aldehydic protons in the  $^1\text{H-NMR}$  spectrum. These results could indicate a sterically encumbered rhenium species in the catalytic cycle.

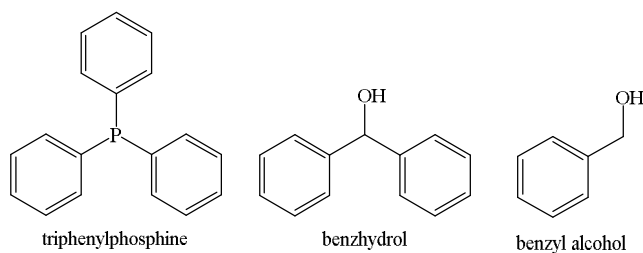


**Figure 3.6.2 Structural comparison of reductants tested in DODH.**

For operational convenience, 1,2-decanediol was tested as a substitute for 1,2-octanediol as the model diol substrate since 1,2-decanediol is a powder at room temperature and 1,2-octanediol is a waxy/near liquid substance at room temperature. Similar results were found using either of these diols with  $[\text{ReO}_2\text{py}_4]\text{Cl}$  and  $\text{BnOH}$ . Confident that 1,2-decanediol was an acceptable substrate for these studies, the effect of the counter ion was investigated, as it was noted a green color was present early in the reactions that is reminiscent of oxorhenium (V) complexes with chloride ligands and a noticeable induction period before appreciable alkene formation. This was speculated to be potentially due to a ligand substitution where chloride coordinates to the rhenium center, presumably interfering with the diol conversion to alkene. To investigate this notion identical reaction solutions of 1,2-decanediol and benzyl alcohol in benzene were

prepared, to each was added either the chloride (Cl<sup>-</sup>, **1a**) salt of [ReO<sub>2</sub>py<sub>4</sub>]<sup>+</sup> or the hexafluorophosphate (PF<sub>6</sub><sup>-</sup>, **1b**) salt of this oxorhenium compound (**Table 3.6.3**). The reactions were allowed to proceed for 30 minutes at 170 °C in benzene and the reactions were analyzed. The reaction using the chloride salt (**Table 3.6.3, Entry 3.6-5**) yielded 3% alkene and that using the hexafluorophosphate salt (**Table 3.6.3, Entry 3.6-6**) yielded 14% alkene. From this result, it would appear for DODH reactions catalyzed by [ReO<sub>2</sub>py<sub>4</sub>]<sup>+</sup> salts that the non-coordinating hexafluorophosphate salt is superior. If the reaction using **1b** as catalyst is allowed to run to full diol conversion (**Table 3.6.3, Entry 3.6-7**), a 99% yield of 1-decene was achieved in 90 minutes at 170 °C with benzyl alcohol as reductant.

**Table 3.6.3 Counter ion comparison, Cl<sup>-</sup> versus PF<sub>6</sub><sup>-</sup>, for the 30 minute DODH reaction catalyzed by [ReO<sub>2</sub>py<sub>4</sub>]<sup>+</sup> on 1,2-decanediol with BnOH.**

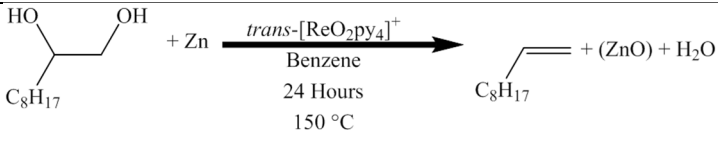
<b>Counter Ion (Entry)</b>	<b>1-Decene Yield (%)</b>
Chloride ( <b>1a</b> , Cl <sup>-</sup> ) <b>3.6-5</b>	3
Hexafluorophosphate ( <b>1b</b> , PF <sub>6</sub> <sup>-</sup> ) <b>3.6-6</b>	14
Hexafluorophosphate ( <b>1b</b> , PF <sub>6</sub> <sup>-</sup> ) <b>3.6-7</b>	99 (90 min, 100% diol conversion)

### 3.7 Elemental Reductants for *trans*-[ReO<sub>2</sub>py<sub>4</sub>]<sup>+</sup> catalyzed DODH.

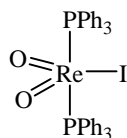
The activity of [ReO<sub>2</sub>py<sub>4</sub>]<sup>+</sup> with elemental reductants was briefly examined given their action as established in Chapter 2. The chloride salt, **1a**, catalyzed the DODH of 1,2-decanediol with zinc at 150 °C in benzene, affording a high conversion and yield (90%) of 1-decene and (**Table 3.7.1, Entry 3.7-1**) in 24 hours. The

hexafluorophosphate salt (**1b**) under the same conditions as the chloride salt (**1a**), gave a somewhat diminished yield of 1-decene (67%) and very high conversion (**Table 3.7.1, Entry 3.7-2**). It does not appear that the room temperature solubility of the oxorhenium compounds relates to their catalytic proficiency at the reaction temperature since **1a**, like APR, is practically insoluble in benzene at room temperature, while **1b** is noticeably more soluble. These results using zinc contrast what was found using BnOH as reductant in the DODH of aliphatic diols (**Table 3.6.3**), which could imply the chloride anion participates in the zinc driven DODH reaction.

**Table 3.7.1 Reaction of elemental zinc as reductant for the DODH of 1,2-decanediol using  $[\text{ReO}_2\text{py}_4]^+$  both the chloride salt (**1a**) and hexafluorophosphate salt (**1b**).**

		
Counter Ion (Entry)	Diol Conversion (%)	Alkene Yield (%)
Chloride (Cl <sup>-</sup> ) <b>3.7-1</b>	100	90
Hexafluorophosphate (PF <sub>6</sub> <sup>-</sup> ) <b>3.7-2</b>	100	67

### 3.8 $\text{ReO}_2(\text{TPP})_2\text{I}$ (**2**) as a DODH Catalyst



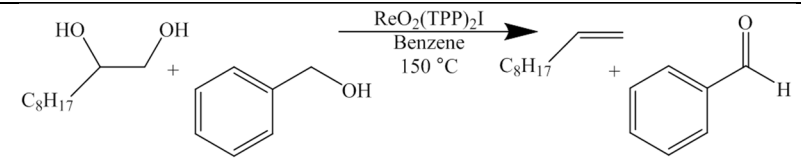
**2**

**Figure 3.8.1 Structural representation of the *cis*-dioxobis(triphenylphosphine)iodorhenium ( $\text{ReO}_2(\text{TPP})_2\text{I}$ , **2**).**

The violet oxorhenium(V) compound, dioxobis(triphenylphosphine)iodorhenium ( $\text{ReO}_2(\text{TPP})_2\text{I}$ , **2**), is interesting due to the

*cis*-dioxo ligands and pentacoordinate geometry, both of which are less common for stable oxorhenium(V) compounds[98, 104, 105, 109]. Synthesis of  $[\text{ReO}_2\text{py}_4]^+$  and related substituted pyridine dioxorhenium compounds can be readily made from  $\text{ReO}_2(\text{TPP})_2\text{I}$  in a similar fashion as with  $\text{ReOCl}_3(\text{TPP})_2$ . This oxorhenium(V) compound ( $\text{ReO}_2(\text{TPP})_2\text{I}$ , **2**) as well as  $\text{Re}^{\text{v}}\text{OCl}_3(\text{TPP})_2$  and  $\text{Re}_2^{\text{vii}}\text{O}_7$ , have been reported to catalyze the deoxygenation of activated aryl-epoxides [112]. This report also contains a brief remark on the catalytic deoxygenation of styrene glycol by these same three oxorhenium compounds giving “moderate” yields of styrene and no disclosure of the conversion of this activated glycol. There are no reported reductants added for these reductive processes, nor speculation of the origin of the reducing equivalents that would be necessary for the catalytic deoxygenation reaction. Independently of this report, we examined the potential of **2** for the DODH of 1,2-decanediol using benzyl alcohol as reductant (**Table 3.8.1**). Within 24 hours a 36% yield of 1-decene (**Entry 3.8-1**) was determined and at 39 hours the yield had increased to 52% 1-decene (**Entry 3.8-2**) with 63% of the starting diol converted. We did not continue the reaction to completion or attempt any optimization; this was a convenient opportunity to test the compatibility of another dioxorhenium(V) complex for DODH bearing different ligands than what we have studied previously. This compatibility may be useful for future attempts to combine multiple reactions in the same pot, which potentially may use multiple catalysts bearing TPP or I ligands or reagents. Reports of such tandem reactions combining the DODH of polyols with an additional reaction are already appearing in the literature [57, 58].

**Table 3.8.1  $\text{ReO}_2(\text{TPP})_2\text{I}$  (2) as catalyst for the DODH of 1,2-decanediol with benzyl alcohol in benzene at 150 °C.**

		
Reaction Time (Entry)	Diol Conversion (%)	Alkene Yield (%)
24 Hours <b>3.8-1</b>	40	39
39 Hours <b>3.8-2</b>	63	52

### 3.9 Conclusions

We have reported the deoxydehydration of polyols catalyzed primarily by the oxorhenium(V) compound  $[\text{ReO}_2\text{py}_4]^+$  ( $\text{Cl}^-$  **1a** and  $\text{PF}_6^-$  **1b**) with the reductants sodium sulfite, benzyl alcohol and elemental zinc. These dioxo tetrapyrindine complexes are readily prepared from multiple starting materials and aqueous pyridine; many of these rhenium starting materials are commercially available and/or also straightforwardly synthesized from commercial perrhenate salts. We believe this is the first report of air-stable oxorhenium(V) compounds that are capable of effectively catalyzing the DODH of polyols to their corresponding alkenes (many >75% alkene yield) with relatively uncomplicated procedures. Additionally  $\text{ReO}_2(\text{TPP})_2\text{I}$  was shown to catalyze the DODH of an aliphatic diol with benzyl alcohol as reductant. These ligated oxorhenium(V) complexes offer the opportunity to potentially change the properties of the catalyst by modifying the ligands as such would be relevant for structure/activity and mechanistic studies. These results demonstrate the versatility and compatibility of oxorhenium(V) compounds to admirably catalyze the DODH of polyols in the presence

of various chemical components, which may be useful in efforts to develop tandem catalysis reactions encompassing oxorhenium(V) DODH.

### 3.10 Experimental

#### 3.10.1 Reagents

Unless otherwise noted, reaction solvents (benzene and chlorobenzene) were ACS grade and used as received from Alfa Aesar. To attempt to keep the chlorobenzene dry and under a nitrogen atmosphere, bottles were stored over molecular sieves and purged with N<sub>2</sub> after each use. Ammonium perrhenate (APR) was used as received from Alfa Aesar and stored in a dry desiccator or under vacuum. (+)-Diethyl-L-tartrate (DET) was used as received from Alfa Aesar. 1,2-Octanediol and 1,2-decanediol were used as received from TCI-America and Sigma Aldrich, preferably storing 1,2-octanediol in the refrigerator. 1-Phenyl-1,2-ethanediol (styrene glycol) was used as received from Sigma Aldrich. Elemental zinc 100-mesh was from Sigma Aldrich, flushed with N<sub>2</sub> or Ar for storage, and ground in an agate mortar and pestle immediately prior to weighing for the reaction. Tetrabutylammonium perrhenate, sodium sulfite, triphenylphosphine, heptadecane, benzyl alcohol, benzhydrol, pyridine, *para*-toluenesulfonic acid, benzaldehyde, hydriodic acid, acetic acid, hydrochloric acid and *para*-methoxybenzyl alcohol were used as received from Sigma Aldrich.

ReOCl<sub>3</sub>(TPP)<sub>2</sub> was synthesized according to reported procedures[108, 113] from ammonium perrhenate and also several grams of ReOCl<sub>3</sub>(TPP)<sub>2</sub> were also gifted to our group from Professor Dr. Michael T. Ashby of the University of Oklahoma, for which I am extremely appreciative. [ReO<sub>2</sub>py<sub>4</sub>]Cl (**1a**) was synthesized by reported methods starting from ReOCl<sub>3</sub>(TPP)<sub>2</sub> by refluxing in acetone with pyridine and water [108].

[ReO<sub>2</sub>py<sub>4</sub>]PF<sub>6</sub> (**1b**) was synthesized from the chloride salt dissolved in water and was precipitated by the addition of aqueous potassium hexafluorophosphate. ReO<sub>2</sub>(TPP)<sub>2</sub>I (**2**) was synthesized according to reported methods from ammonium perrhenate[114].

### 3.10.2 Instrumentation and Analytical Methods

<sup>1</sup>H and <sup>13</sup>C NMR spectra were collected on either on a Varian Mercury VX-300 MHz, Varian VNMRS-400 MHz or Varian VNMRS-500 MHz. All of the NMR data was processed using SpinWorks [96]. Gas chromatograms were collected on a Shimadzu GC-14A or a Shimadzu GC-2014 equipped with an AOC-20i+s autosampler, both with 3% SE-54 packed column, FID and thermal program 40 °C for 5 min; 20 deg/min to 250 °C; then 7 min at 250 °C or in decanediol reactions using heptadecane as standard 40 °C for 3min; 6 deg/min to 65 °C; 2 min at 65 °C; 20 deg/min to 100 °C; 2 min at 100 °C; 15 deg/min to 250 °C; 3 min at 250 °C. GC-MS analyses were performed on a Thermo-Finnigan instrument using the same thermal program as the former *vide supra* and a comparable stationary phase in a capillary column. Mass spectra were recorded on a Micromass Q-TOF quadrupole time-of-flight mass spectrometer equipped with a Z-spray electrospray ionization (ESI) source. FT-IR spectra were collected on a Shimadzu IRAffinity-1 infrared spectrophotometer using KBr pellets.

### 3.10.3 Typical DODH Reaction Conditions

Unless stated otherwise, reactions were carried out in benzene (1-5 mL) using a sealed pressure tube (AceGlass and/or ChemGlass) equipped with a front seal purge tube, a magnetic stir bar with 0.1-0.2 M diol with approximately 10 mol% oxorhenium(V) catalyst, 1-2 equivalents of reductant, degassed three times at room

temperature with mild vacuum (ca. 60 mmHg) and backfilled with N<sub>2</sub> then heated at 150 °C for 24 h using a preheated oil bath. The reaction was cooled to room temperature and quantified by <sup>1</sup>H-NMR or GC-FID with an internal standard.

#### 3.10.4 Quantification

After reactions were cooled to room temperature a known amount of naphthalene was added as a standard post reaction for reactions with 1,2-octanediol, 1,2-decanediol and 1-phenyl-1,2-ethanediol and quantified via GC-FID using multiple point internal standard calibration curve data obtained from authentic, weighed concentrations of diol/alkene/naphthalene. A known amount of naphthalene could also be used via <sup>1</sup>H-NMR for quantification using the naphthalene proton signal ca. 7.6 ppm and the unique signals of the diols/alkenes for 1,2-octanediol, 1,2-decanediol, 1-phenyl-1,2-ethanediol and DET reactions, also known amounts of DMSO could be used with DET/DEF/benzene reactions with added CDCl<sub>3</sub> and nitromethane for aliphatic diols for <sup>1</sup>H-NMR quantification. Heptadecane was also used as an internal standard in some 1,2-decanediol/BnOH reactions via GC-FID using multiple point internal standard calibration curve data obtained from authentic, weighed concentrations of 1,2-decanediol/1-decene/BnOH/benzaldehyde/heptadecane.

#### 3.10.5 Standard Reaction

As an example from **Table 3.4.1, Entry 3.4-2** in a glass pressure tube equipped with a magnetic stir bar, 0.049 mmol [ReO<sub>2</sub>py<sub>4</sub>]Cl was added followed by 0.51 mmol 1,2-octanediol, 0.52 mmol benzyl alcohol and 5 mL chlorobenzene. The tube was sealed with a Teflon, front-seal plunger valve and evacuated (ca. 60 mmHg) and backfilled with nitrogen (to atmospheric pressure) three times at room temperature and

then the plunger valve was closed at room temperature leaving an atmosphere of nitrogen in the tube at atmospheric pressure. The closed tube was then placed in a preheated oil bath at 150 °C for 24 hours. The tube was removed from the oil bath and allowed to cool to room temperature. A 250 µL sample was removed and 5 µL DMSO added as standard for quantification by <sup>1</sup>H-NMR in CDCl<sub>3</sub>, showing the presence of 1-octene (80% yield) and very little to no detectable 1,2-octanediol.

#### *3.10.6 Mass Spectrometric Experiment Described in Section 3.5*

Tetrabutylammonium perrhenate, 0.0125 mmol, was dissolved in 1.3 mL chlorobenzene giving an approximately 0.01 M rhenium solution which is comparable to the typical reaction condition. This sample was consecutively diluted and analyzed by ESI negative mode, the dilutions spanned seven orders of magnitude. This dilution scale was used to analyze a [ReO<sub>2</sub>py<sub>4</sub>]Cl/BnOH/1,2-octanediol/chlorobenzene reaction which was conducted at 175 °C for one hour. One sample was taken and analyzed by <sup>1</sup>H-NMR using an added nitromethane standard to show a 69% yield of 1-octene. The rest of the reaction mixture was diluted exactly as the tetrabutylammonium perrhenate standard over seven orders of magnitude. The diluted reaction solutions were analyzed starting with the most dilute until perrhenate was detected in the ESI negative MS, which was at the fifth order of magnitude dilution of the reaction. This corresponds to there not being more than 2.4% of the original rhenium in the perrhenate form.

## **Chapter 4 Mechanistic Studies of Oxorhenium-Catalyzed DODH**

## 4.1 Background and introduction

A better understanding of a reaction's mechanism is invaluable when it comes to optimizing it such as increasing yields or decreasing by-products [115-117]. For the oxorhenium-catalyzed DODH of glycols there have been questions about the order of steps and which is turn-over limiting and is well depicted schematically (**Figure 4.1.1**) by Nicholas and coworkers[54]. There is a general agreement that the catalytic DODH has three principal stages - condensation of the glycol, reduction from  $\text{Re}^{\text{vii}} \rightarrow \text{Re}^{\text{v}}$ , and olefin extrusion with oxidation of the  $\text{Re}^{\text{v}} \rightarrow \text{Re}^{\text{vii}}$ . The two potential pathways are depicted in **Figure 4.1.1**. Glycol condensation with the oxorhenium(VII) species, moving clockwise, forms a  $\text{Re}^{\text{vii}}$ -glycolate, which can undergo reduction to the  $\text{Re}^{\text{v}}$ -glycolate then alkene extrusion and reoxidation to  $\text{Re}^{\text{vii}}$ . Alternatively, reduction of the  $\text{Re}^{\text{vii}}$  species (moving counterclockwise) to the  $\text{Re}^{\text{v}}$  species (potentially ligand stabilized, LO) continuing with condensation of the glycol to the  $\text{Re}^{\text{v}}$ -glycolate with ensuing alkene extrusion and reoxidation of the rhenium. The pathways for various DODH reactions have been examined experimentally and computationally to understand the sequence of events as discussed in **Chapter 1** and are shown to be dependent on the catalyst and reluctant used.

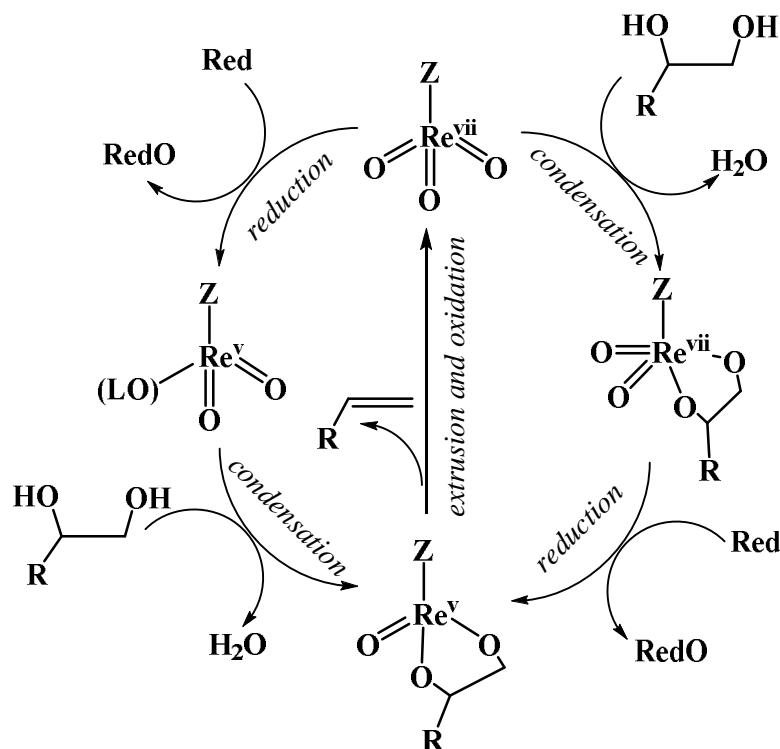


**Figure 4.1.1** Generic summary of potential pathways for oxorhenium DODH. Adapted from Nicholas [54].

There are several DODH studies that have both experimental and computational results that provide interesting insight for the potential mechanism. The DODH reaction of MTO/diol/ $H_2$  was reported by Abu-Omar and coworkers [35] with qualitative kinetic data and color change observations suggesting reduction of MTO by  $H_2$  forming a methyldioxorhenium (MDO) ligand (LO) stabilized species as depicted in the counterclockwise pathway of **Figure 4.1.1** ( $ZReO_2(LO)$ ). MDO(LO) then would undergo glycol condensation to the  $Re^V$ -glycolate and conversion to the corresponding epoxide with alkene extrusion through a metallaoxetane intermediate. This report was followed up computationally by Lin and coworkers [118] indicating that the reduction from  $Re^{vii} \rightarrow Re^v$  required significantly less energy starting from the  $Re^{vii}$ -glycolate as opposed to MTO, signifying condensation first followed by reduction was more

energetically favorable. Nicholas and coworkers reported on the potential mechanism of the DODH system MTO/diol/sulfite both experimentally and computationally [54, 56]. They found experimentally that the  $\text{Re}^{\text{vii}}$ -glycolate was readily formed at room temperature (but with  $K_{\text{eq}} < 1$ ), that its reduction by  $\text{PPh}_3$  or sulfite could also occur at room temperature, and that the alkene extrusion was rate limiting, i.e. condensation followed by reduction was energetically viable. Their computational investigation supported that alkene extrusion was rate limiting but that reduction followed by condensation was more favorable; i.e. initial  $\text{NaSO}_3^-$  attack on an oxo of MTO generates a  $\text{MeRe}^{\text{v}}\text{O}_2(\text{OSO}_3\text{Na})^-$  intermediate which the glycol subsequently coordinates. After glycol coordination, a series of H-transfer steps give the glycolate,  $\text{MeRe}^{\text{v}}(\text{glycolate})(\text{OSO}_3\text{Na})(\text{H}_2\text{O})^-$ . Concerted extrusion of alkene from this glycolate and dissociation of  $\text{NaSO}_4^-$  from the resultant  $\text{MeReO}_3(\text{OSO}_3\text{Na})$  regenerates MTO and completes the cycle. It was also shown how greatly additional coordinated species ( $\text{H}_2\text{O}$ ,  $\text{NaSO}_3^-$ , or  $\text{NaSO}_4^-$ ) at rhenium can raise the energy required for alkene extrusion from  $\text{MeRe}^{\text{v}}(\text{glycolate})(\text{OSO}_3\text{Na})(\text{H}_2\text{O})^-$ .

Secondary alcohol reductants with MTO have also been studied experimentally and computationally [60, 68, 69]. Toste and Shiramizu studying the MTO/glycol/2°-alcohol system proposed initial reduction of MTO by the alcohol to methyldioxorhenium (MDO) followed by glycol condensation, with alkene extrusion being rate limiting [68]. They proposed this from observations of reactions conducted with 3-hexyne present forming isolable  $\text{MeRe}^{\text{v}}\text{O}_2(\text{alkyne})$ , this species reacted with glycol at room temperature to form the glycolate,  $\text{MeRe}^{\text{v}}(\text{glycolate})$ . This glycolate was found to have similar catalytic DODH activity as MTO. In a related study Abu-Omar

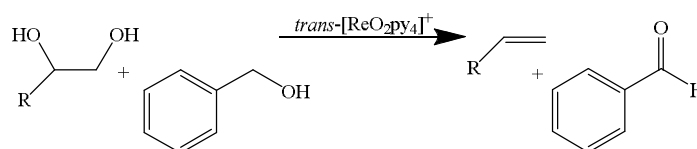
and coworkers disclosed the MTO/glycerol system, using glycerol as glycol/reductant/solvent, proposing condensation to the  $\text{Re}^{\text{vii}}$ -glycolate then reduction [69]. This was proposed on the results of MTO/glycerol DODH using glycerol-(OD)<sub>3</sub> and d<sub>5</sub>-glycerol-(OH)<sub>3</sub> kinetic isotope effect experiments. There was no KIE observed with glycerol-(OD)<sub>3</sub> but a primary KIE of 2.4 with d<sub>5</sub>-glycerol-(OH)<sub>3</sub> indicating C-H/D breakage is part of the RLS. Abu-Omar and coworkers also noted the brief heating of glycerol and MTO yields a Re-glycolate observable by <sup>1</sup>H-NMR which under further heating produced alkene. Wang and coworkers examined both of these proposed pathways computationally as well as an alternate pathway not previously considered [60]. In their lower energy pathway, MTO is coordinated by alcohol then reduced by a second alcohol forming  $\text{MeRe}^{\text{v}}\text{O}(\text{OH})_2$  species which then undergoes glycolate condensation, again demonstrating the effect of additional coordinating species in the reaction. The combination of computational studies with experimentally derived results provides interesting insight on how much an effect other components in the reaction can have on the potential lowest energy pathway.

The majority of mechanistic studies agree that rhenium is most likely cycling between the VII and the V state and the formation of a rhenium-glycolate species which extrudes alkene. There have been only a few definitive mechanistic studies and these studies do not all agree on the order of events and the turnover limiting step (TLS). It would appear that the TLS of DODH varies subject to catalyst, reductant, and other species present in the reaction (e.g. H<sub>2</sub>O, Na<sup>+</sup>/NaSO<sub>4</sub><sup>-</sup>, alcohols).

As demonstrated in **Chapter 3**,  $[\text{ReO}_2\text{py}_4]^+/\text{BnOH}$  is an effective system for DODH. Since oxorhenium(V) pre-catalysts have not previously been mechanistically

investigated,  $[\text{ReO}_2\text{py}_4]^+$  offers the unique opportunity to start from a cationic  $\text{Re}^{\text{v}}$  compound as compared to the anionic and neutral  $\text{Re}^{\text{vii}}$  of the previous studies. The ability to modify electronic properties of the previously reported  $\text{Re}^{\text{vii}}$  compounds through ligand variation has been lacking, while  $[\text{ReO}_2\text{py}_4]^+$  has been reported with various substituted pyridines[104, 109, 119]. We therefore will use this  $\text{Re}^{\text{v}}$  species to investigate the mechanism of BnOH driven DODH of aliphatic glycols.

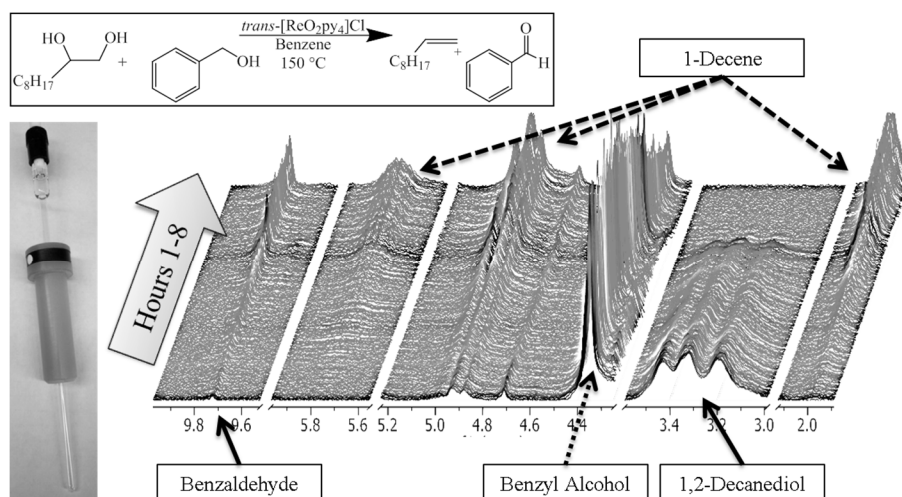
#### 4.2 Initial reaction time course experiments



**Figure 4.2.1** General reaction using  $[\text{ReO}_2\text{py}_4]^+$  and benzyl alcohol in the DODH of diols as demonstrated in Chapter 3.

As was demonstrated in **Chapter 3**,  $[\text{ReO}_2\text{py}_4]^+$  is an effective oxorhenium catalyst for the DODH of model glycols (*e.g.* 1,2-octanediol and 1,2-decanediol) with benzyl alcohol as reductant (**Figure 4.2.1**). Our earliest *in situ* endeavors tracking the progress of the DODH reaction (illustrated schematically top left, **Figure 4.2.2**) over time were conducted on a small scale in pressure-tolerant NMR tubes (bottom left, **Figure 4.2.2**) at 150 °C in the spectrometer probe, utilizing the chloride salt  $[\text{ReO}_2\text{py}_4]\text{Cl}$  (**1a**). A representative NMR plot of spectra versus reaction time is seen in **Figure 4.2.2** (bottom right), showing the reactants, BnOH and 1,2-decanediol, decreasing in intensity as the products, benzaldehyde and 1-decene, increase in intensity. At 150 °C, the reactions using  $[\text{ReO}_2\text{py}_4]\text{Cl}$  would show little alkene formation through the first hour of the reaction and take several hours for appreciable production (bottom right, **Figure 4.2.2**). The *in situ* monitoring via  $^1\text{H-NMR}$  had the

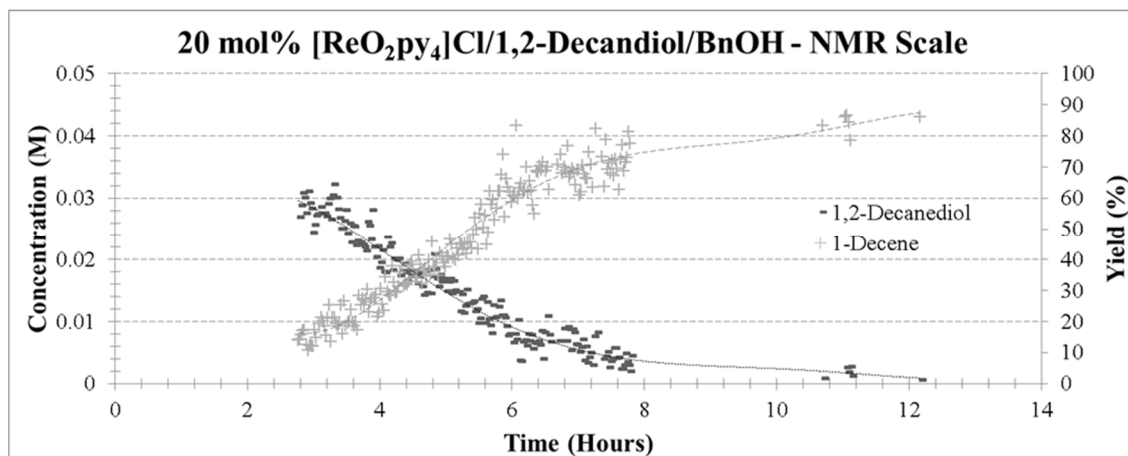
advantage of observing the reaction progress at temperature as well as providing ample data points from the massive number of spectra (often several hundred) that could be recorded over the multiple hour reaction course. A drawback was the “bumping” of the benzene solvent (benzene 80 °C b.p.) at 150 °C (reaction temperature) which frequently was accompanied the loss of the lock signal, leading to unusable spectra throughout the reaction which had to be identified and removed before further processing.



**Figure 4.2.2** Typical NMR-scale DODH reaction (top left) conducted in pressure tolerant NMR tube (bottom left) with representative reaction spectra with characteristic peaks accentuated (bottom right).

An example data set obtained from a single NMR-scale reaction is seen in **Figure 4.2.3** with data points corresponding to erroneous spectra removed. To save on valuable instrument time due to the noted induction time, this sample was first heated for the first few hours of the reaction in a temperature regulated oven before being transferred to the preheated instrument. This procedure was standard for NMR scale reactions. From the plot (**Figure 4.2.3**), one can see that in approximately the first three hours of the reaction only about 15% yield of 1-decene is obtained while in the

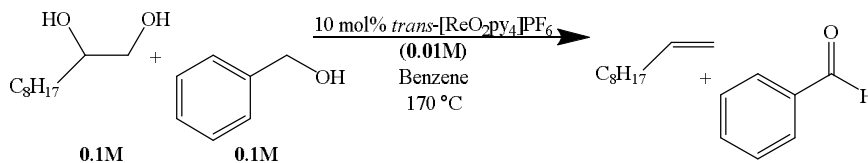
following three hours the yield increases to 60%. This behavior was typical for  $[\text{ReO}_2\text{py}_4]\text{Cl}/\text{BnOH}/1,2\text{-decanediol}$  DODH reactions.



**Figure 4.2.3** Representative data set from NMR-scale DODH reaction.

In **Chapter 3**, the effect of changing the reaction temperature from 150 to 170 °C afforded shorter reaction times for the  $[\text{ReO}_2\text{py}_4]^+/\text{BnOH}/1,2\text{-decanediol}$  systems (**Figure 4.2.1**). Likewise in **Chapter 3**, the hexafluorophosphate salt (**1b**) of  $[\text{ReO}_2\text{py}_4]^+$  was not subject to the same apparent induction period seen with the chloride salt (**1a**) for the aliphatic diol/BnOH systems. Therefore,  $[\text{ReO}_2\text{py}_4]\text{PF}_6$  (**1b**) at 170 °C was used for the majority of the 1,2-decanediol/BnOH DODH reaction studies.

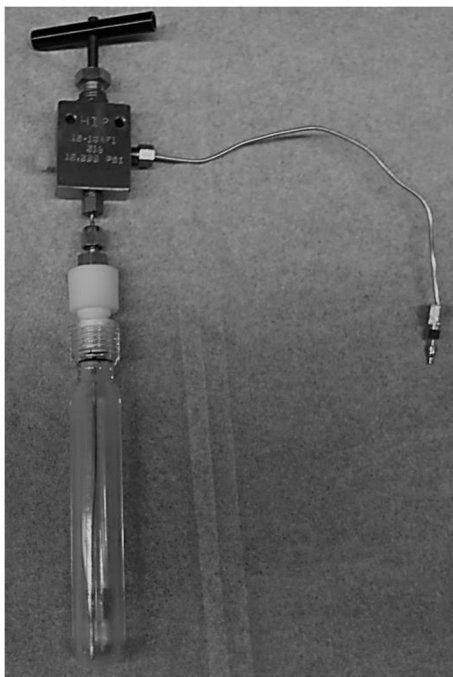
### 4.3 Establishing standard reaction conditions and stoichiometry effects



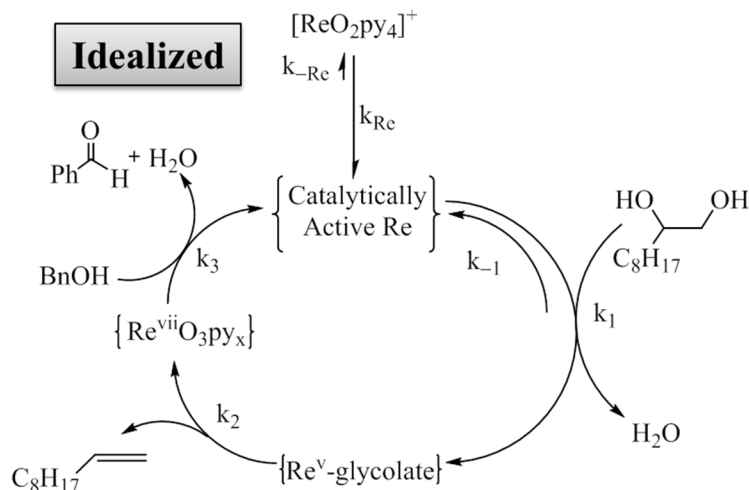
**Figure 4.3.1** Standard reaction conditions for DODH reactions for the  $[\text{ReO}_2\text{py}_4]\text{PF}_6/\text{BnOH}/1,2\text{-decanediol}$  system.

The typical reaction (**Figure 4.3.1**) for  $[\text{ReO}_2\text{py}_4]\text{PF}_6/\text{BnOH}/1,2\text{-decanediol}$  was conducted in benzene (0.01M/0.1M/0.1M respectively) at 170 °C using a glass pressure

reactor modified with a dip tube and valve for sample acquisition (see Figure 4.3.2). Under these conditions, the reaction reached maximum alkene yield and full diol conversion within 1.5-2 hours. Assuming a  $\text{Re}^{\text{v}} \leftrightarrow \text{Re}^{\text{vii}}$  cycle with the glycolate condensation as the first step in DODH (*vide infra*), an idealized pathway for this reaction is proposed in **Figure 4.3.3**. In this pathway essentially all the  $[\text{ReO}_2\text{py}_4]^+$  is converted to the catalytically active rhenium species followed by reversible glycolate condensation and irreversible alkene extrusion and reduction of the rhenium back to the catalytically active species. Observations of the actual DODH reaction (**Chapter 3**) of this system indicate that complications occur such as side reactions/off pathway reactions (e.g. acetal formation) and catalyst inhibition (e.g. induction time with  $[\text{ReO}_2\text{py}_4]\text{Cl}$ ).

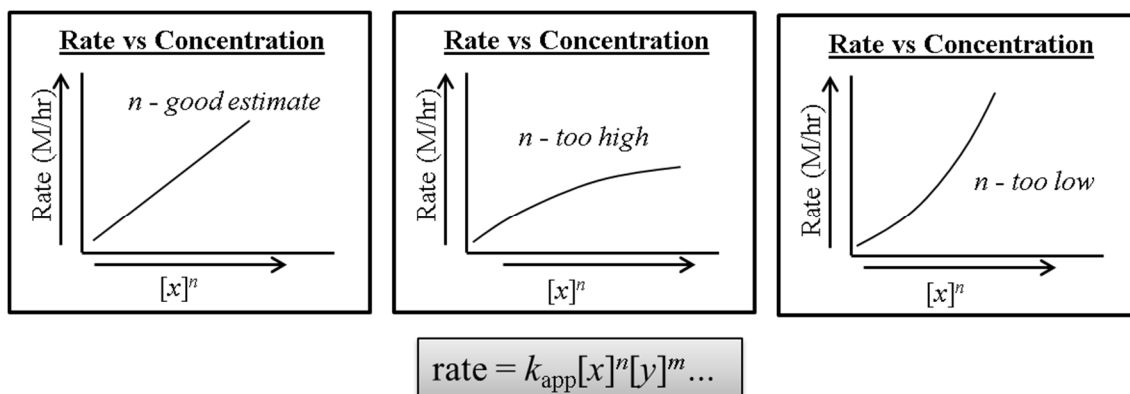


**Figure 4.3.2 Modified pressure reactor with dip tube and regulating valve for sampling.**



**Figure 4.3.3** Idealized “simple” pathway for  $[\text{ReO}_2\text{py}_4]^+/\text{1,2-decanediol}/\text{BnOH}$  DODH.

Since the DODH for  $[\text{ReO}_2\text{py}_4]\text{PF}_6/\text{BnOH}/\text{1,2-decanediol}$  does not appear to follow a simple pathway, given additional diol derived species are detected. The use of an empirical power law (**Figure 4.3.4**, bottom equation) is a good starting approximation for understanding the contribution individual components play in the overall mechanism [120]. Plotting the rate versus concentration of reaction component  $x$  raised to a power  $n$  ( $[x]^n$ ) for several reactions will give a reasonably straight line with an intercept close to zero when  $n$  is a good estimate for an empirical power law (**Figure 4.3.4**). In cases where  $n$  is not an integer (e.g.  $n \neq 1, 2, 3\dots$ ) is an indication in the actual, complex rate equation, that component appears in both the numerator and denominator.

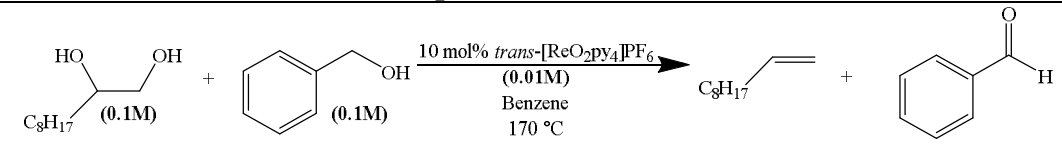
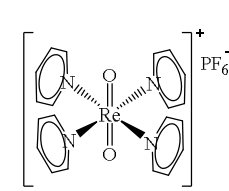
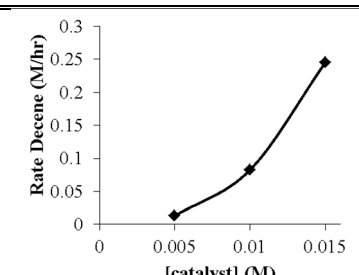
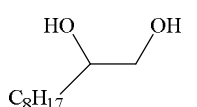
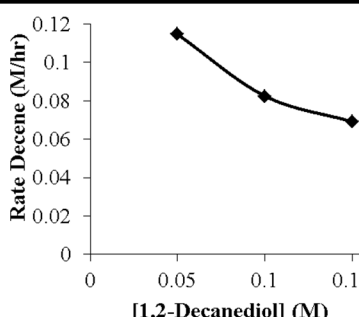
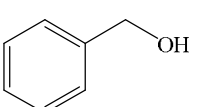
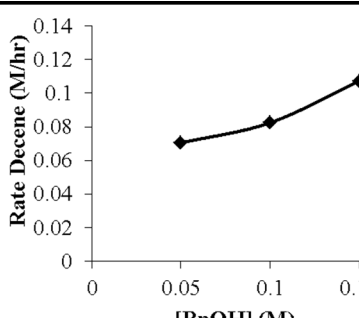


**Figure 4.3.4 Generalization for interpreting plots for an empirical power law [120].**

Systematic variation of the concentration of individual reaction components for  $[\text{ReO}_2\text{py}_4]\text{PF}_6/\text{BnOH}/1,2\text{-decanediol}$  (standard reaction) and their corresponding rates are shown in **Table 4.3.1** (standard conditions italicized, 0.0100 M/0.100 M/0.100 M respectively with a rate of M/hr). The graphical plots for these sets of reactions are shown on the right in **Table 4.3.1**. Changing the catalyst loading of  $[\text{ReO}_2\text{py}_4]\text{PF}_6$  to 0.0050 M lowered the rate to  $0.013 \pm 0.004$  M/hr while the rate increased to  $0.245 \pm 0.003$  M/hr when the catalyst concentration was raised to 0.0150 M. Looking at the plot for concentration of  $[\text{ReO}_2\text{py}_4]\text{PF}_6$  versus rate it is clear that there is not a first order rate dependency on catalyst concentration, otherwise a straight line with a near zero intercept would be observed. When the initial concentration of 1,2-decanediol is lowered to 0.050 M surprisingly the observed rate increases to  $0.115 \pm 0.003$  M/hr while an increase in molarity to 0.150 M correlates with a decrease in observed rate to  $0.07 \pm 0.01$  M/hr. These data indicate that the substrate 1,2-decanediol inhibits the reaction and will likely be a negative order in the power law estimation. Finally, when the initial concentration of BnOH is varied to 0.050 M there was a slight decrease in rate to  $0.071 \pm 0.001$  M/hr and increasing to 0.150 M was accompanied by an observed increase in

rate to  $0.11 \pm 0.01$  M/hr. Apparently the concentration of BnOH has a positive order in a power law estimation but likely less than that of  $[\text{ReO}_2\text{py}_4]\text{PF}_6$  based on the magnitude of the differences in rates for each.

**Table 4.3.1 Variations from standard reaction conditions with corresponding effect on observed rate of decene production.**

			
Reaction Component (x) Varied	Initial Concentration [x] (M)	Rate Decene Formation (M/hr)	Plot Rate vs [x]
	0.0050	$0.013 \pm 0.004$	
	0.0100	$0.08 \pm 0.01$	
	0.0150	$0.245 \pm 0.003$	
	0.0500	$0.115 \pm 0.003$	
	0.1000	$0.08 \pm 0.01$	
	0.1500	$0.07 \pm 0.01$	
	0.0500	$0.071 \pm 0.001$	
	0.1000	$0.08 \pm 0.01$	
	0.150	$0.11 \pm 0.01$	

Evaluation of the sets of reaction component variations from **Table 4.3.1** with respect to their pseudo-order by the power law estimation (rate =  $k_{app}[Re]^n[BnOH]^m[Diol]^p$  where  $[Re]=[ReO_2py_4]PF_6$ ) is a preliminary step in gaining insight to the mechanism for this DODH reaction (**Figure 4.3.5**). By varying the power ( $n, m, p$ ) by 0.5 through trial and error to obtain a reasonably straight line with a near zero intercept, the upper plots in **Figure 4.3.5** are obtained and when combined ( $[Re]^n[BnOH]^m[Diol]^p$ ) the lower plot is obtained. The order estimated for  $[ReO_2py_4]PF_6$  is  $n = 2.5$  and is not unreasonable given the magnitude in the change of rate as a function of concentration. Likewise, a value of  $m = 0.5$  for BnOH fits with the minor rate change with concentration change observed. With 1,2-decanediol a negative order would be expected as increasing the diol slowed the reaction while decreasing sped it up, so  $p = -0.5$  is realistic. Even though these values are only meant to be a starting point a wealth of insight is nonetheless gained from them. The magnitude of the pseudo-order ( $\sim 2.5$ ) for  $[ReO_2py_4]PF_6$  could indicate that the oxorhenium compound plays more than one role in the reaction and/or a bimetallic species or transition state is necessary in the RLS [121-127]. Potentially a second rhenium compound coordinates a BnOH ( $ReO(OH)BnOpy_n$  or  $ReO_2BnOHpy_n$ ) to activate it for the reduction of the oxidized Re that extruded alkene. With 1,2-decanediol showing a negative pseudo-order ( $\sim -0.5$ ) it is conceivable that the diol could be part of a catalytically inactive species such as a poly-glycol/glycolate-Re species ( $Re^vpy_n(glycoate)_2^+$ ,  $Re^{vii}Opy(glycolate)_2^+$ ). The diol is a potential bidentate chelating ligand, so it is conceivable that more than one diol on the rhenium could interfere with the DODH reaction. The pseudo half order dependency on BnOH could be caused by BnOH acting

as a competitive ligand forming Re-BnOH complexes that are not on the catalytic pathway.

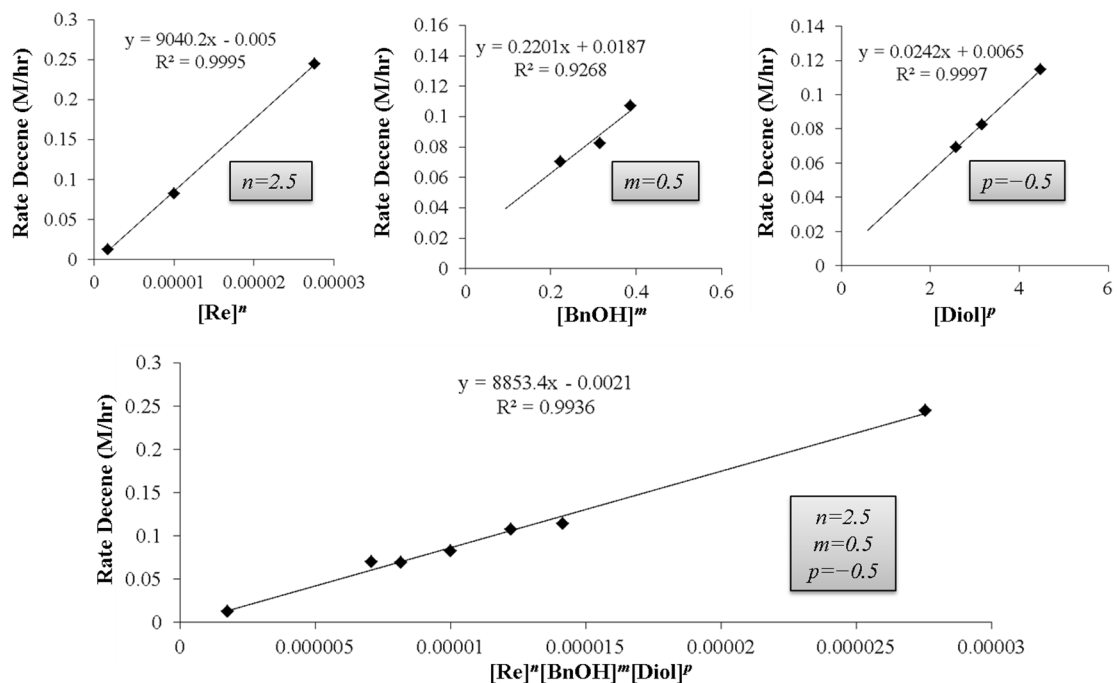


**Figure 4.3.5** Approximation of pseudo-orders graphically for the power rate law estimation for the DODH system  $[ReO_2py_4]PF_6/BnOH/1,2$ -decanediol.

#### 4.4 Substituted pyridine analogs of the type $[ReO_2(4-X-py)_4]PF_6$

The effect of changing the electronic properties of the pyridine (4 position/*para*) ligand for the starting oxorhenium compound was surveyed to examine the effects of pre-catalyst ligands on the DODH reaction. Electron donating analogs, i.e. 4-Me (4-picoline, 4-pico) and 4-NMe<sub>2</sub> (4-dimethylaminopyridine, 4-dmap), of  $[ReO_2(4-x-py)_4]^+$  are readily prepared analogously to the original  $[ReO_2py_4]^+$ ; while electron poor analogs, i.e. 4-Cl (4-chloropyridine, 4-Clpy), are notoriously more difficult to prepare [104, 105, 109]. Both  $[ReO_2(4-pico)_4]PF_6$  and  $[ReO_2(4-dmap)_4]PF_6$  were prepared first as the chloride salts, the same as  $[ReO_2py_4]Cl$  starting from  $ReOCl_3(TPP)_2$  using the 4-substituted pyridine in refluxing aqueous acetone in the preparation, followed by salt

metathesis to obtain the hexafluorophosphate salts of these compounds (see experimental for further details). An alternate synthesis was employed to prepare  $[\text{ReO}_2(4\text{-Clpy})_4]\text{PF}_6$  starting from  $\text{ReO}_2\text{I}(\text{TPP})_2$  (compound **2**, *vide supra*). Electron-withdrawing ligands, such as 4-chloropyridine, do not readily form stable  $[\text{ReO}_2\text{X}_4]^+$  complexes[104] and are also subject to competing oligomerization of the ligand at mildly elevated temperatures (ca. 90°C)[104, 128-132]. Triphenylphosphine oxide (TPPO) remained in  $[\text{ReO}_2(4\text{-Clpy})_4]\text{PF}_6$  after purification as evidenced by ESI-MS and FT-IR. The potential effect of TPPO on the reaction is examined later.

Standard DODH reaction conditions (**Figure 4.4.1**, top) for 1,2-decanediol/BnOH were employed with the substituted pyridine complexes  $[\text{ReO}_2(4\text{-X-py})_4]\text{PF}_6$  (X = 4-dmap, 4-pico, 4-Clpy; left, center, and right respectively in **Figure 4.4.1**). Under standard conditions for this system with the unsubstituted complex (i.e.  $[\text{ReO}_2\text{py}_4]\text{PF}_6$ ), a rate of  $0.08 \pm 0.01$  M/hr was observed, while the 4-X-py analogs had observed rates of  $0.014 \pm 0.001$  M/hr (X = NMe<sub>2</sub>),  $0.070 \pm 0.001$  M/hr (X = Me), and  $0.007 \pm 0.001$  M/hr (X = Cl). Taking the corresponding  $\sigma_p$  values of these substituents (-NMe<sub>2</sub> = -0.83; -Me = -0.17; -Cl = 0.23 [133]) and plotting them against  $\log \frac{k_X}{k_H}$  gives the Hammett plot at the bottom of **Figure 4.4.1**. The downward concavity of the plot potentially indicates the reactions may follow the same mechanism, but there is a change in the rate-limiting step [134]. However, with only four data points this is just one possibility; other factors that may influence the results is that the -NMe<sub>2</sub> group may coordinate to Re and the presence of TPPO in the -Cl experiment.

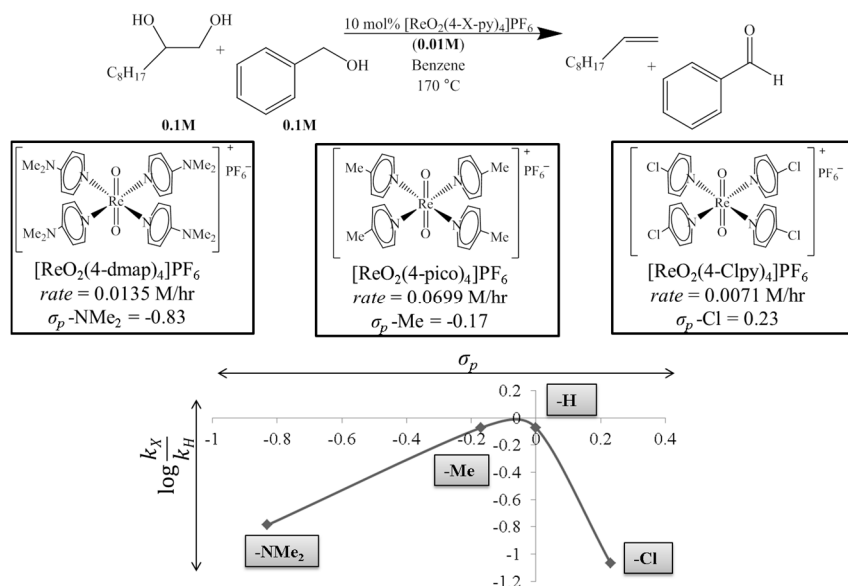


**Figure 4.4.1** Observed effect of varying electronic properties of 4-X-py in  $[\text{ReO}_2(4\text{-X-py})_4]\text{PF}_6$  (X= NMe<sub>2</sub>, Me, H, Cl) DODH of 1,2-decanediol/BnOH and consequent Hammett plot. (Values for  $\sigma_p$  from Hansch & Leo [133])

#### 4.5 Observed effect of added pyridine or triphenylphosphine oxide to the $[\text{ReO}_2\text{py}_4]\text{PF}_6/\text{BnOH}/1,2\text{-decanediol}$ DODH reaction

The observed rate of the  $\text{ReO}_2\text{py}_4]\text{PF}_6/\text{BnOH}/1,2\text{-decanediol}$  DODH reaction with the inclusion of supplementary reagents (**Table 4.5.1**) was briefly explored to examine the effect on observed rate of added reaction species. As stated above, triphenylphosphine oxide (TPPO) proved to be difficult to remove from the electron poor compound  $[\text{ReO}_2(4\text{-Clpy})_4]\text{PF}_6$ ; to gauge the potential effect of this compound, TPPO was added in one equivalent (with respect to Re) to the standard reaction (reaction scheme in **Table 4.5.1**). Interestingly with the addition of TPPO to the reaction, the observed rate increased from  $0.08 \pm 0.01\text{M/hr}$  to  $0.15 \pm 0.01\text{M/hr}$ . So the presence of TPPO in the reaction using  $[\text{ReO}_2(4\text{-Clpy})_4]\text{PF}_6$  may have led to an observed rate faster than if TPPO was not present. Additionally, the effect of added pyridine was surveyed. With the addition of one or five equivalents of Py (with respect

to Re), the measured rate increased to  $0.123 \pm 0.005$  and  $0.0978 \pm 0.0001$  M/hr respectively. The effect of added Py or TPPO correlates with an increase in rate and suggests these compounds may have a function in the turn-over limiting step. The rate increased 1.8x and 1.5x of the standard reaction when one equivalent of TPPO or Py, respectively, was added. With 5 equivalents of Py added the reaction rate increased 1.2x the standard reaction, this could also indicate these ligands play a role in activating off pathway Re-polyglycol/glycolate species. The difference between 1 and 5 equivalents of Py suggests that additional ligands can interfere with the catalytic pathway.

**Table 4.5.1 Effect of additive *L* on observed rate of the DODH for  $[\text{ReO}_2\text{py}_4]\text{PF}_6/\text{BnOH}/1,2\text{-decanediol}$ .**

<i>x</i> eq Additive <i>L</i> (with respect to Re)	Observed Rate (M/hr)
No additive	$0.08 \pm 0.01$
1 eq TPPO	$0.15 \pm 0.01$
1 eq Py	$0.123 \pm 0.005$
5 eq Py	$0.0978 \pm 0.0001$

#### 4.6 Kinetic isotope effect with singly and doubly benzylic deuterium labeled

##### BnOH

In an effort to identify the turn-over limiting step (TLS) and reaction intermediates involved, singly and doubly benzylic deuterium labeled BnOH were substituted in the standard  $[\text{ReO}_2\text{py}_4]\text{PF}_6/\text{BnOH}/1,2\text{-decanediol}$  reaction. The procedure used for probing the kinetic isotope effect (KIE) of the un-deuterated and

doubly benzylic deuterated BnOH (PhCD<sub>2</sub>OH) is shown in **Table 4.6.1**. The un-deuterated BnOH reacted at a rate of 0.08 ±0.01M/hr while PhCD<sub>2</sub>OH had an observed rate of 0.034 ±0.004 M/hr. The KIE for this experiment ( $\frac{k_H}{k_D}$ ) is calculated to be 2.4 (primary KIE) and indicates C-H/C-D bond breakage is likely involved in the TLS.

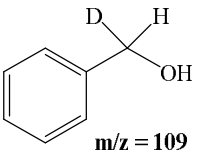
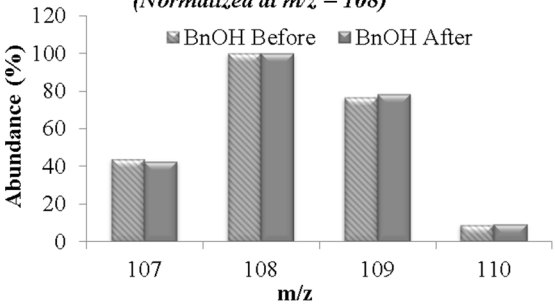
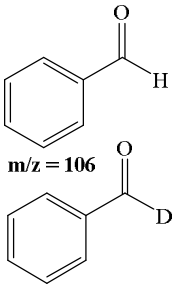
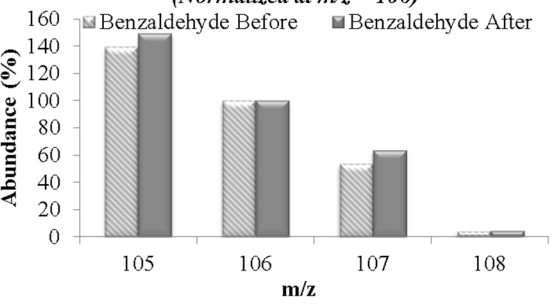
**Table 4.6.1 KIE of PhCD<sub>2</sub>OH and PhCH<sub>2</sub>OH.**

<b>BnOH Species and Initial Concentration (M)</b>	<b>Observed Rate (M/hr)</b>	<b>Kinetic Isotope Effect (<math>\frac{k_H}{k_D}</math>)</b>
	0.08 ±0.01	N/A
	0.034 ±0.004	2.4

Competition reactions, *inter*- and *intramolecular*, using deuterated and un-deuterated BnOH were also investigated to gain additional insight to the reaction and TLS. The intramolecular competition experiment employed singly labeled benzylic deuterium BnOH (PhCDHOH) with standard reaction conditions. The measured rate of this reaction was 0.17 ±0.02 M/hr which is faster than the un-deuterated BnOH (0.08 ±0.01M/hr) and substantially faster than PhCD<sub>2</sub>OH (0.034 ±0.004 M/hr). A sample of the reaction at near 50% decene yield was analyzed for BnOH and benzaldehyde by GC-MS. This was compared to a solution of the starting PhCDHOH which had a trace amount of benzaldehyde (D & H) present by GC-MS. The benzaldehyde peaks from GC-MS plots were normalized to m/z = 106 as 100% (un-deuterated benzaldehyde),

then the trace aldehyde (D/H) is subtracted from the experimental. From this data treatment a 10% excess of the deuterated benzaldehyde is observed, indicating hydrogen is preferably removed compared to deuterium. This suggests a bimolecular reaction in the TLS [135]. The mass spectrum of PhCHDOH was essentially unchanged before and during reaction (1.7% change), this would be expected unless the BnOH oxidation step was readily reversible.

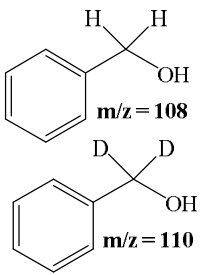
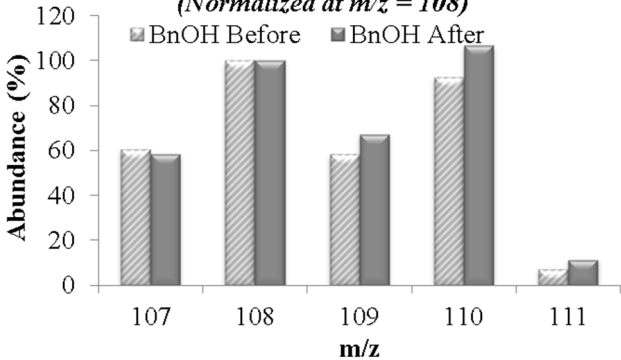
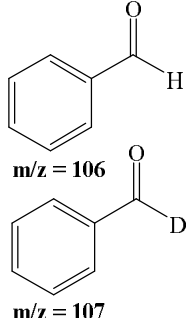
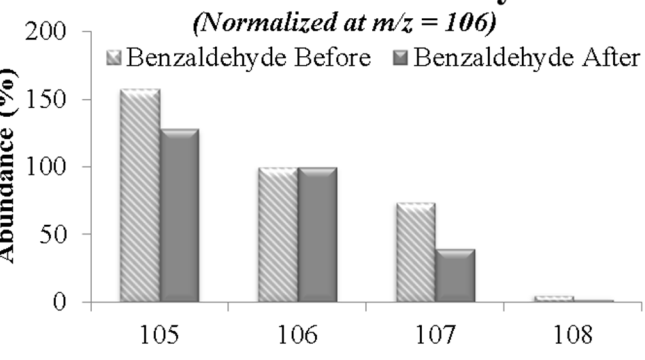
**Table 4.6.2 Analysis of PhCDHOH DODH experiment.**

Species	MS Plots (Before & After)	Difference
 <p><math>m/z = 109</math></p>	<p><b>Mass Plot BnOH</b> (Normalized at <math>m/z = 108</math>)</p> 	<p>@109 <math>m/z</math> +1.7%</p>
 <p><math>m/z = 106</math> <math>m/z = 107</math></p>	<p><b>Mass Plot Benzaldehyde</b> (Normalized at <math>m/z = 106</math>)</p> 	<p>@107 <math>m/z</math> +10%</p>

The intermolecular competition between unlabeled BnOH and PhCD<sub>2</sub>OH (50:50 mix) using standard reaction conditions was investigated to observe the preference of C-

H/D in this DODH reaction. The observed rate for this reaction was  $0.137 \pm 0.002$  M/hr which is faster than pure unlabeled BnOH ( $0.08 \pm 0.01$  M/hr). This reaction was sampled and analyzed by GC-MS at about 50% decene yield as well as the starting BnOH/PhCD<sub>2</sub>OH solution. During the reaction there is 10% more PhCD<sub>2</sub>OH than unlabeled BnOH. There is a 34% excess of the unlabeled benzaldehyde at  $m/z = 106$  from the reaction sample compared to the starting solution. These results suggest that the unlabeled BnOH is preferentially consumed versus the PhCD<sub>2</sub>OH and that there is likely a reversible Re-alkoxide species allowing kinetic selection of PhCH<sub>2</sub>OH over PhCD<sub>2</sub>OH [135].

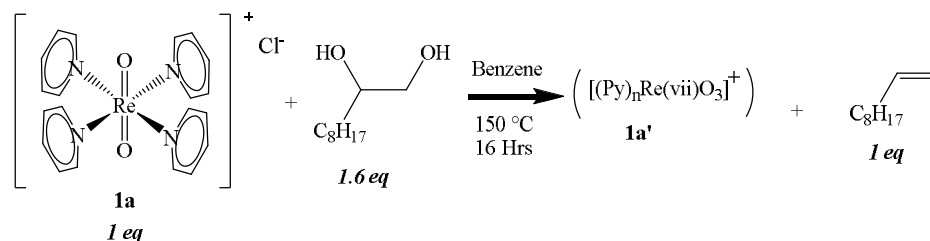
**Table 4.6.3 Analysis of 50:50 BnOH/PhCD<sub>2</sub>OH DODH experiment.**

Species	MS Plots (Before & After)	Difference
<div style="text-align: center;">  <p>m/z = 108 m/z = 110</p> </div>	<div style="text-align: center;"> <p><b>Mass Plot BnOH</b> (Normalized at m/z = 108)</p>  <p>Abundance (%)</p> <p>m/z</p> </div>	<p>@110 m/z +14%</p>
<div style="text-align: center;">  <p>m/z = 106 m/z = 107</p> </div>	<div style="text-align: center;"> <p><b>Mass Plot Benzaldehyde</b> (Normalized at m/z = 106)</p>  <p>Abundance (%)</p> <p>m/z</p> </div>	<p>@107 m/z -34%</p>

#### 4.7 Stoichiometric reactions

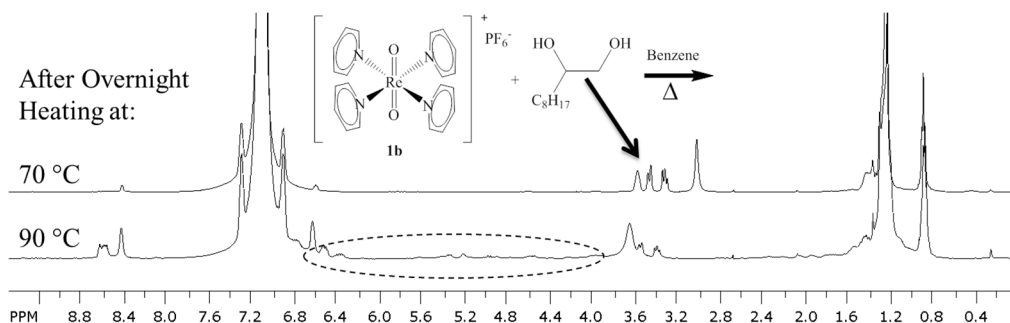
To probe the order of events in the DODH catalytic cycle the Re<sup>v</sup> complex [ReO<sub>2</sub>py<sub>4</sub>]Cl (**1a**) was mixed with 1,2-decanediol (1.0:1.6; **Figure 4.7.1**) and heated overnight at 150 °C (no added reductant). This reaction yielded 98% 1-decene with respect to Re. This finding indicates that the Re<sup>v</sup> complex **1a** is competent to efficiently turnover the glycol, presumably via condensation-dehydration to a Re<sup>v</sup>-glycolate, followed by extrusion of the olefin and formation of a ([Py]<sub>n</sub>Re<sup>vii</sup>O<sub>3</sub>)<sup>+</sup> species. In the

presence of a reductant the latter,  $\text{Re}^{\text{vii}}$ , could regenerate the  $\text{Re}^{\text{v}}$  catalyst via O-transfer reduction. If the reaction involved a  $\text{Re}^{\text{iii}} \leftrightarrow \text{Re}^{\text{v}}$  cycle, then one would expect to see oxidation products of the diol (aldehydes, ketones), but these were not observed.



**Figure 4.7.1** Stoichiometric reaction of  $[\text{ReO}_2\text{py}_4]\text{Cl}$  (**1a**) with 1,2-decanediol.

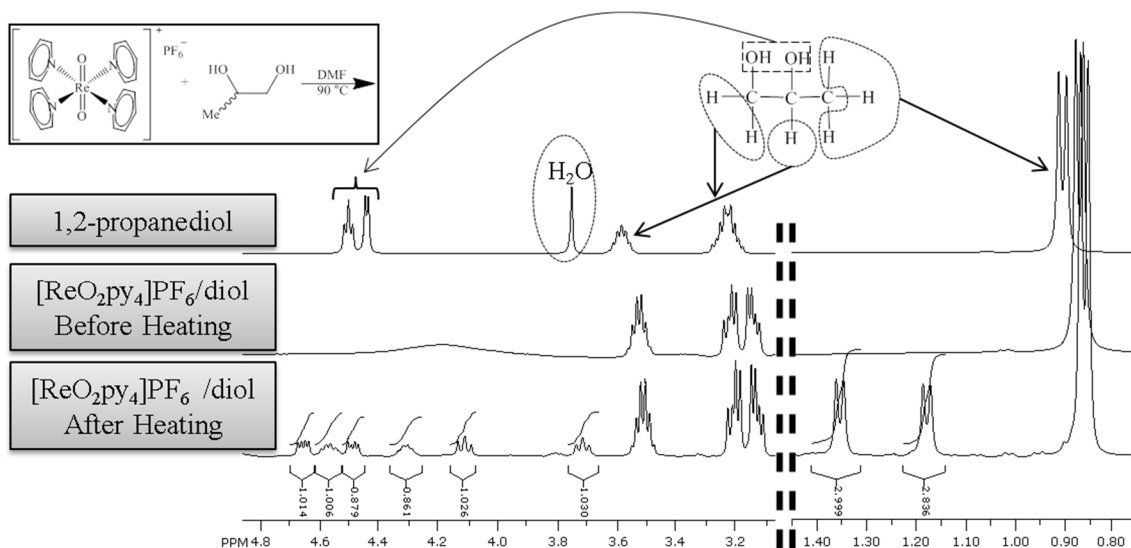
To better understand the reaction process, detection of a rhenium(V)-glycolate species was sought. Initial efforts using stoichiometric 1,2-decanediol/ $[\text{ReO}_2\text{py}_4]\text{PF}_6$  in benzene indicated no noticeable change in the NMR spectra of the reaction mixture below ca.  $90^\circ\text{C}$  (**Figure 4.7.2**). There was an evident change in the  $^1\text{H}$ -NMR spectrum of the mixture after heating at ca.  $90^\circ\text{C}$  (circled area, **Figure 4.7.2**); efforts to obtain ESI-MS data of these newly formed species were not successful. Interpretation of the NMR spectra was complicated by the long carbon chain with overlapping  $\text{CH}_2$   $^1\text{H}$ -NMR signals; therefore, simplification of the model diols was desired. To avoid any induction time interference, as noted in chapter 3,  $[\text{ReO}_2\text{py}_4]\text{PF}_6$  (**1b**) was used as the oxorhenium reactant. Additionally, due to the solubility difference between the diol and rhenium complex in benzene, solvents that could dissolve both the diol and rhenium complex were explored (e.g. DMF,  $\text{CH}_2\text{Cl}_2$ ).



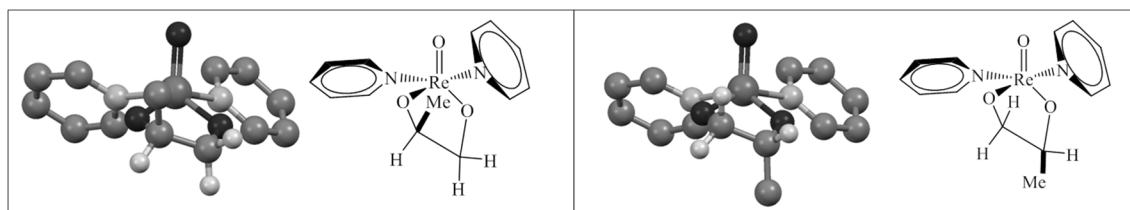
**Figure 4.7.2**  $^1\text{H-NMR}$  of  $[\text{ReO}_2\text{py}_4]\text{PF}_6$ /1,2-decanediol reaction mixture in benzene after mild heating. Characteristic diol peaks are indicated with an arrow, new area of interest circled.

To simplify the interpretation of the glycol-Re interaction spectra, 1,2-propanediol was chosen because it has unique and separated glycol-C-H  $^1\text{H-NMR}$  signals (1,2-propanediol/DMF top spectrum, **Figure 4.7.3**). When 1,2-propanediol was combined with  $[\text{ReO}_2\text{py}_4]\text{PF}_6$ , a noticeable splitting of the  $-\text{CH}_2-$  protons (ca. 3.1-3.2 ppm) is observed before heating as well as the signals for  $-\text{OH}$  protons (middle spectrum, **Figure 4.7.3**). After heating this same sample at 90 °C overnight new peaks are detected near the original glycol peaks (bottom spectrum, **Figure 4.7.3**). The very noticeable doublet for the  $-\text{CH}_3$  protons is shifted from 0.7 ppm to 1.17 ppm and 1.35 ppm with equal integrations, this would indicate two new species in equal concentration. This is could be due to the two potential modes of binding leading to two Re-glycolate isomers after condensation as depicted in **Figure 4.7.4**. Three pairs of signals are seen between 3.7-4.7 ppm (t 3.7 & 4.1 ppm;  $m_a$  4.3 & 4.55 ppm;  $m_b$  4.5 & 4.65 ppm) with a combined integration of six protons, this accounts for the remainder of the protons (C-H) for two Re-glycolates which fall in the range of other reported Re-glycolates as can be seen in **Table 4.7.1**[54, 136-138]. Gable reported a  $\text{Re}^{\text{V}}$ -glycolate using 1,2-propanediol and  $\text{Cp}^*\text{ReO}_3$  forms  $\text{Cp}^*\text{ReO}$ -glycolate and is also reported as a

mixture of 1:1 isomers by  $^1\text{H-NMR}$  ( $\text{C}_6\text{D}_6$ : 1.46 & 1.51 ppm, d, 3H each; 3.06 ppm dd 1H; 3.78 ppm, m, 3H; 4.08 ppm, dd, 1H; 4.42 ppm, ddq, 1H) [138]. Additionally the  $^{13}\text{C-NMR}$  spectrum after heating shows new peaks near 91 ppm also indicating glycolate formation.

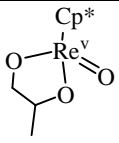
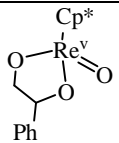
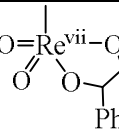
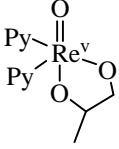


**Figure 4.7.3**  $^1\text{H-NMR}$  spectra in DMF of 1,2-propanediol (top),  $[\text{ReO}_2\text{py}_4]\text{PF}_6/\text{diol}$  before heating (middle),  $[\text{ReO}_2\text{py}_4]\text{PF}_6/\text{diol}$  after heating at  $90^\circ\text{C}$  overnight (bottom).



**Figure 4.7.4** Two proposed different binding modes for 1,2-propanediol Re-glycolate. Protons removed for clarity except glycolate protons.

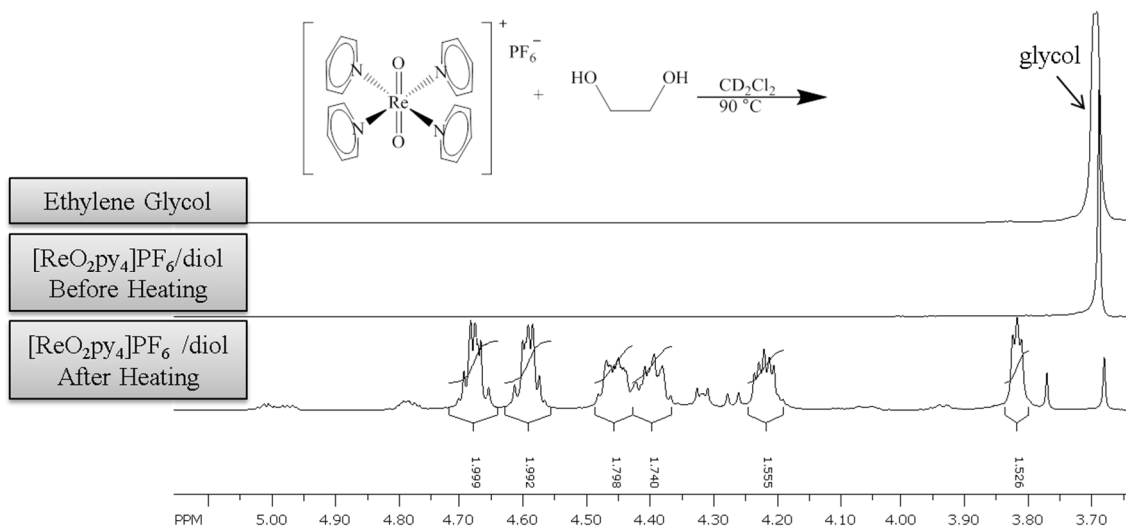
**Table 4.7.1 Rhenium-glycolate NMR signals.**

Re-Glycolate	<sup>1</sup> H-NMR Glycolate (ppm)	<sup>13</sup> C-NMR Glycolate (ppm)	[ref]
 (2 isomers 1:1)	(CH <sub>3</sub> ) 1.46 d:3H; 1.51d:3H 3.06, dd:1H; 3.78, m:3H 4.08 dd:1H, 4.42 ddq:1H	86.0; 86.1; 86.3; 86.8	[138]
 (2 isomers 5:4)	3.39, dd:1H; 4.12, m:2H 4.29, dd:1H; 4.50, dd:1H 5.3, dd:1H	87.4; 92.9; 93.3	[138]
 (2 isomers 5:4)	4.12, 4.50, 5.35:3H	N/A	[54]
 (2 isomers 1:1)	(CH <sub>3</sub> ) 1.17, d:3H; 1.35, d:3H 3.71, t:1H; 4.11 t:1H 4.30, m <sub>a</sub> :1H; 4.50, m <sub>b</sub> :1H 4.65, m <sub>b</sub> :1H, 5.55, m <sub>a</sub> :1H	89.3; 90.4; 90.7; 91.6	This work

Attempting to simplify the model glycol further, the combination of ethylene glycol and [ReO<sub>2</sub>py<sub>4</sub>]PF<sub>6</sub> in CD<sub>2</sub>Cl<sub>2</sub> was examined by NMR before heating and subsequently after heating at 90 °C overnight (see **Figure 4.7.5**). There are four major groups of peaks in the glycol/glycolate region (ca. 3.6-4.8 ppm) that develop after heating and a decrease in the ethylene glycol peak. The pair at 4.65 and 4.6 ppm appear to be mirror images (multiplet) of one another with equal integrations. The next apparent pair at 4.45 and 4.4 ppm are not well resolved but also appear to be very similar multiplets with equal integrations. The other two major peaks appear to be a pentet near 4.2 ppm and a triplet near 3.8 ppm, these two peaks also have roughly equal

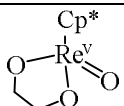
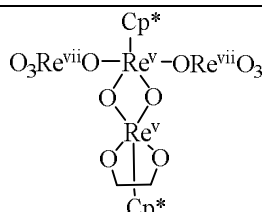
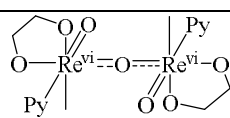
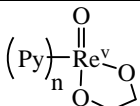
integrations. The  $^{13}\text{C}$ -NMR spectrum shows only one clear carbon signal for a glycolate carbon at 86 ppm that by gHSQCAD correlates to the multiplet at 4.65 ppm in the  $^1\text{H}$ -NMR spectrum. It would appear from the NMR data that there are one to two new glycol/glycolate species formed besides the  $\text{Re}^{\text{V}}\text{O}(\text{glycolate})\text{py}_2$ . Herrmann and coworkers using ethylene glycol reported the  $\text{Re}^{\text{V}}$ -glycolate  $\text{Cp}^*\text{ReO}(\text{O}_2\text{C}_2\text{H}_4)$ , describing the  $^1\text{H}$ -NMR of the ethylene glycolate as two sets of doublet of doublet of doublets (ddd) consisting of 2H each at 3.54 and 3.90 ppm and the  $^{13}\text{C}$ -NMR glycolate as a single peak at 80.63 ppm[136]. These assignments were also confirmed by Gable [138]. These observations are comparable with that of other rhenium-glycolates of ethylene glycol as seen in **Table 4.7.2** [136-138]. A sample of this reaction mixture was analyzed by high resolution ESI-MS; at  $m/z$  421.0557 a cluster of peaks is seen with the characteristic Re pattern and can be formulated as  $[\text{Re}^{\text{V}}\text{O}(\text{glycolate})\text{py}_2]^+$  (calc.  $m/z$  421.0562) (**Figure 4.7.6**). The calculated structure for  $[\text{Re}^{\text{V}}\text{O}(\text{glycolate})\text{py}_2]^+$  (B3LYP/LANL2DZ) is shown in **Figure 4.7.6**. Treating this structure as having an upper and lower face relative to the oxo ligand, one pair of Hs in the upper face is closer to the oxo ligand and a pair in the lower face further away from the oxo ligand. Ring flipping of the puckered Re-glycolate in **Figure 4.7.6** is likely and would not change the facial orientation of the glycolate protons and supports two sets of proton signals observed. The Re-glycolate identified by MS combined with Herrmann's description of another Re-glycolate support the likelihood that the two well resolved mirror image multiplets at 4.65 and 4.6 ppm are the  $[\text{ReO}(\text{glycolate})\text{py}_2]^+$  species. The Re-glycolate at  $m/z = 421.0557$  is the only set of MS peaks that clearly correspond to a Re-(mono)glycolate by accurate mass but other rhenium species are present in the MS at

higher  $m/z$ . It is conceivable the other multiplets represent Re-(poly)glycol/glycolate species with an unidentified accurate mass formulation in the MS. A poly-glycol/glycolate bidentate species would likely be catalytically inactive and would support the apparent negative order in glycol *vide supra*. This same MS data set also revealed a rhenium species at  $m/z$  313.9819 which fits the formulation of  $[\text{Re}^{\text{vii}}\text{O}_3\text{py}]^+$  (calc.  $m/z$  313.9827) and could be the oxidized form of the rhenium catalyst. Addition of a stoichiometric amount of BnOH to this reaction mixture followed by heating at 90 °C overnight showed no change in the signals from **Figure 4.7.5**. It should be noted that a partner reaction where  $[\text{ReO}_2\text{py}_4]\text{PF}_6$  and BnOH were first initially heated together followed by addition of ethylene glycol and heating produces the same spectrum. This would seem to indicate glycolate condensation is a relatively low energy step.



**Figure 4.7.5**  $^1\text{H-NMR}$  spectra in  $\text{CD}_2\text{Cl}_2$  of ethylene glycol (top),  $[\text{ReO}_2\text{py}_4]\text{PF}_6/\text{diol}$  before heating (middle),  $[\text{ReO}_2\text{py}_4]\text{PF}_6/\text{diol}$  after heating at 90 °C overnight (bottom).

**Table 4.7.2 Rhenium-ethylene glycolates NMR signals.**

Re-Glycolate	<sup>1</sup> H-NMR Glycolate (ppm)	<sup>13</sup> C-NMR Glycolate (ppm)	[ref]
	3.54, ddd:2H 3.90; ddd:2H	80.6	[136, 138]
	3.92, ddd:2H 4.40, ddd:2H	N/A	[136]
	3.67, s:4H	N/A	[137]
	4.60, m:2H 4.65, m:2H	86.0	This work

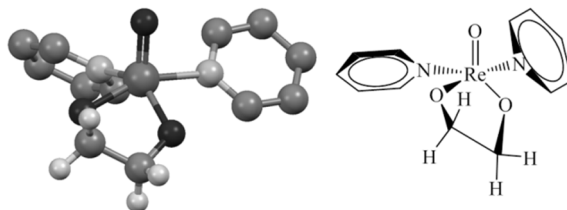


**Figure 4.7.6 Computed structure of  $[\text{Re}^{\text{V}}\text{O}(\text{glycolate})\text{py}_2]^+$  (B3LYP/LANL2DZ). Protons removed for clarity except for those on ethylene glycolate.**

## 4.8 Conclusions

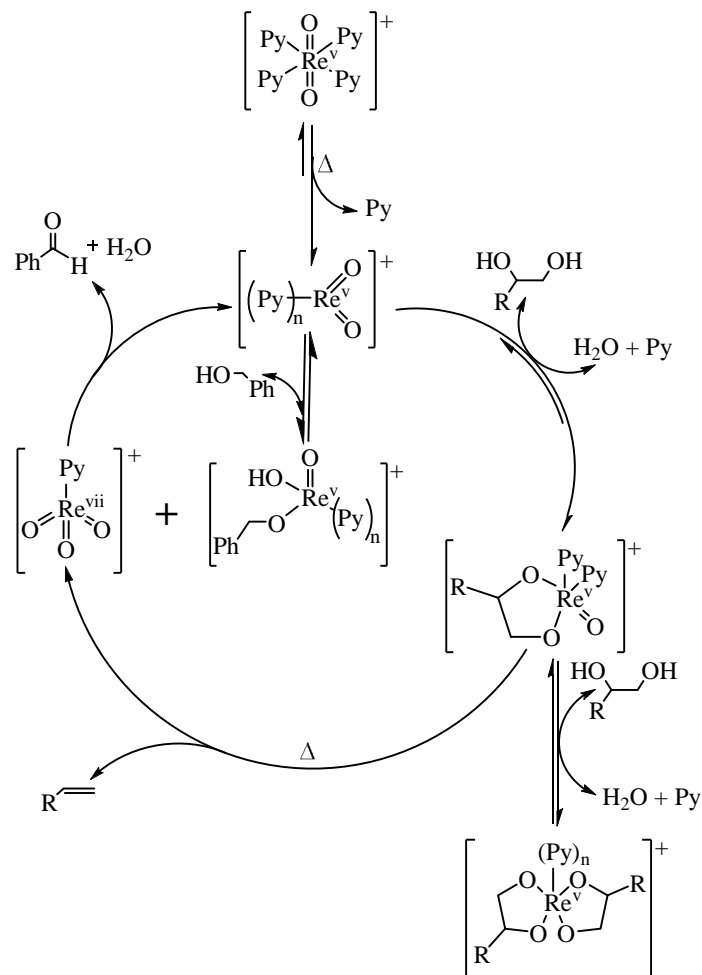


**Figure 4.8.1** Proposed pathway of BnOH driven,  $[\text{ReO}_2\text{py}_4]^+$  catalyzed DODH.

The pathway in **Figure 4.8.1** is proposed for the BnOH driven,  $[\text{ReO}_2\text{py}_4]^+$  catalyzed DODH of aliphatic glycols. The results *vide supra* indicate that glycolate condensation likely occurs first to a  $\text{Re}^{\text{v}}$ -glycolate species with a minimum temperature requirement of ca. 90 °C. This temperature requirement is likely due to ligand dissociation at the rhenium center to allow coordination/condensation of the glycol[139]. This is conceivably the point where inhibition takes place with additional glycol coordination thus giving an observed negative order in the glycol. Therefore, the

concentration of free ligand like pyridine or TPPO would play a role in the reverse reaction of glycol inhibition/coordination accounting the rate increase observed with these ligands. The extrusion of alkene is shown to occur thermally in the absence of a reductant with only one turnover of the rhenium compound indicating a  $\text{Re}^{\text{V}} \rightarrow \text{Re}^{\text{vii}}$  oxidation from glycol DODH. The rhenium(V) glycolate observed by NMR and by MS fit the formulation  $\text{ReO}(\text{glycolate})\text{py}_2^+$ . The apparent second order dependency on  $[\text{ReO}_2\text{py}_4]^+$  implies this compound plays more than one role in the catalytic cycle. This may be due to the activation of BnOH as a  $[\text{Re}^{\text{V}}\text{O}(\text{py})_n(\text{OH})(\text{OBn})]^+$  (**Figure 4.8.2**) complex involved in a bimolecular TLS, given that  $[\text{Re}^{\text{V}}\text{OL}_n(\text{OH})(\text{OR})]^+$  complexes form between ROH and  $[\text{Re}^{\text{V}}\text{O}_2\text{L}_n]^+$  [111, 140]. After glycol extrusion, the oxidized  $\text{PyRe}^{\text{vii}}\text{O}_3^+$  could be reduced by the  $[\text{Re}^{\text{V}}\text{O}(\text{py})_n(\text{OH})(\text{OBn})]^+$  in a bimolecular step completing the catalytic cycle. Changing ligands from pyridine to the derivatives 4-NMe<sub>2</sub>, 4-Me, or 4-Cl –pyridine yielded a concave down Hammett plot which suggests the same mechanism but a change in the RLS. The two end points of this plot, 4-NMe<sub>2</sub> and 4-Cl, represent a very strong and a very weak Lewis base (ligand) respectively. If pyridine (free or ligated) is involved in the RLS, then these two derivatives might suffer from potentially low dissociation for 4-NMe<sub>2</sub> and poor ligation/interaction for 4-Cl. The similarity in apparent rate with 4-Me and pyridine would then be expected since 4-Me is just slightly more electron donating than pyridine. The substantially slower reaction using PhCD<sub>2</sub>OH gave a KIE of 2.4, signifying C-H(D) bond breaking is part of the TLS. Inter- and intramolecular deuterium labeled BnOH experiments support C-H bond breakage is preferred over C-D and support a bimolecular species in the TLS. The breakage of the C-H bond in BnOH would correspond to the reduction of a  $\text{Re}^{\text{vii}}$  species

back to a  $\text{Re}^{\text{v}}$  species which can undergo subsequent glycol condensation. The ease of the  $\text{Re}^{\text{vii}} \rightarrow \text{Re}^{\text{v}}$  reduction is very likely influenced by additional species bound at this point to the rhenium center [56, 60] and therefore the concentration and electronic nature of these species would be relevant to the rate.

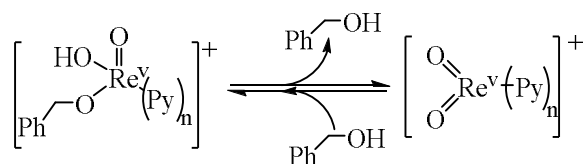


**Figure 4.8.2 Rapid interconversion of  $[\text{Re}^{\text{v}}\text{O}_2(\text{py})_n]^+$  +  $\text{BnOH}$  and  $[\text{Re}^{\text{v}}\text{O}(\text{py})_n(\text{OH})(\text{OBn})]^+$ .**

## 4.9 Experimental

### 4.9.1 Reagents

Unless otherwise noted, reaction solvents were ACS grade and used as received from Alfa Aesar. Ammonium perrhenate (APR) was used as received from Alfa Aesar and stored in a dry desiccator or under vacuum. 1,2-Octanediol and 1,2-decanediol were used as received from TCI-America and Sigma Aldrich, preferably storing 1,2-octanediol in the refrigerator. Triphenylphosphine, triphenylphosphine oxide, ethylene glycol, 1,2-propanediol, heptadecane, benzyl alcohol, pyridine, hydriodic acid, acetic acid, and hydrochloric acid were used as received from Sigma Aldrich.

$\text{ReOCl}_3(\text{TPP})_2$  was synthesized according to reported procedures[108, 113] from ammonium perrhenate and also several grams of  $\text{ReOCl}_3(\text{TPP})_2$  were gifted to our group from Professor Dr. Michael T. Ashby of the University of Oklahoma, for which I am extremely appreciative.  $[\text{ReO}_2\text{py}_4]\text{Cl}$  (**1a**) was prepared by reported methods starting from  $\text{ReOCl}_3(\text{TPP})_2$  by refluxing in acetone with pyridine and water [108].  $[\text{ReO}_2\text{py}_4]\text{PF}_6$  (**1b**) was synthesized from the chloride salt dissolved in water and was

precipitated by the addition of aqueous potassium hexafluorophosphate.  $\text{ReO}_2(\text{TPP})_2\text{I}$  (**2**) was synthesized according to reported methods from ammonium perrhenate[114]. The previously reported [102] electron donating substituted pyridine  $[\text{ReO}_2\text{py}_4]^+$  analogs  $[\text{ReO}_2(4\text{-dmap})_4]^+$  and  $[\text{ReO}_2(4\text{-pico})_4]^+$  were synthesized the same as **1a** where pyridine was replaced by either 4-dimethylaminopyridine or 4-picoline respectively and refluxed in water/acetone mixture of  $\text{ReOCl}_3(\text{TPP})_2$ . The chloride salts were isolated then treated with aqueous potassium hexafluorophosphate to give  $[\text{ReO}_2(4\text{-X})_4]\text{PF}_6$  compounds (4-X = 4-dmap or 4-pico).

The synthesis of  $[\text{ReO}_2(4\text{-Clpy})_4]\text{PF}_6$  (817.35 g/mol) was modified from the procedure for the mixed  $[\text{ReO}_2(\text{py})_2(4\text{-Clpy})_2]^+$  reported by Ram and Hupp [104]. The pyridine derivative comes commercially as the 4-chloropyridine hydrochloride salt (4-Clpy·HCl), 5.74 mmol (0.8610 g) 4-Clpy·HCl was dissolved in 10 mL acetone to which 5.466 mmol (0.4592 g) sodium bicarbonate ( $\text{NaHCO}_3$ ) was added and allowed to stir overnight. The resultant green turbid mixture was separated by filtering on filter paper and washing with 15 mL acetone giving a clear solution free of the green precipitate. To this 4-Clpy/acetone solution was added 1 mL  $\text{H}_2\text{O}$  and 0.1506 mmol  $\text{ReO}_2\text{I}(\text{TPP})_2$  and stirred at room temperature, the mixture turns orange within the first 5 minutes. The solution was stirred for 30 minutes at room temperature then the acetone solution was reduced by rotary evaporation. Then 20 mL water was added to the remaining acetone/water solution along with 0.76 mmol (0.14 g) potassium hexafluorophosphate to precipitate out the orange compound. The orange compound was collected on a sintered glass frit, washed 3 times with toluene (10 mL) and 3 times with diethylether (10 mL). The presence of triphenylphosphine oxide was detected by NMR, FT-IR

(Figure 4.9.1), and ESI-MS (Figure 4.9.2). Subsequent washes could not remove all of the triphenylphosphine oxide, likely due to competitive coordination to Re compared to 4-Clpy.

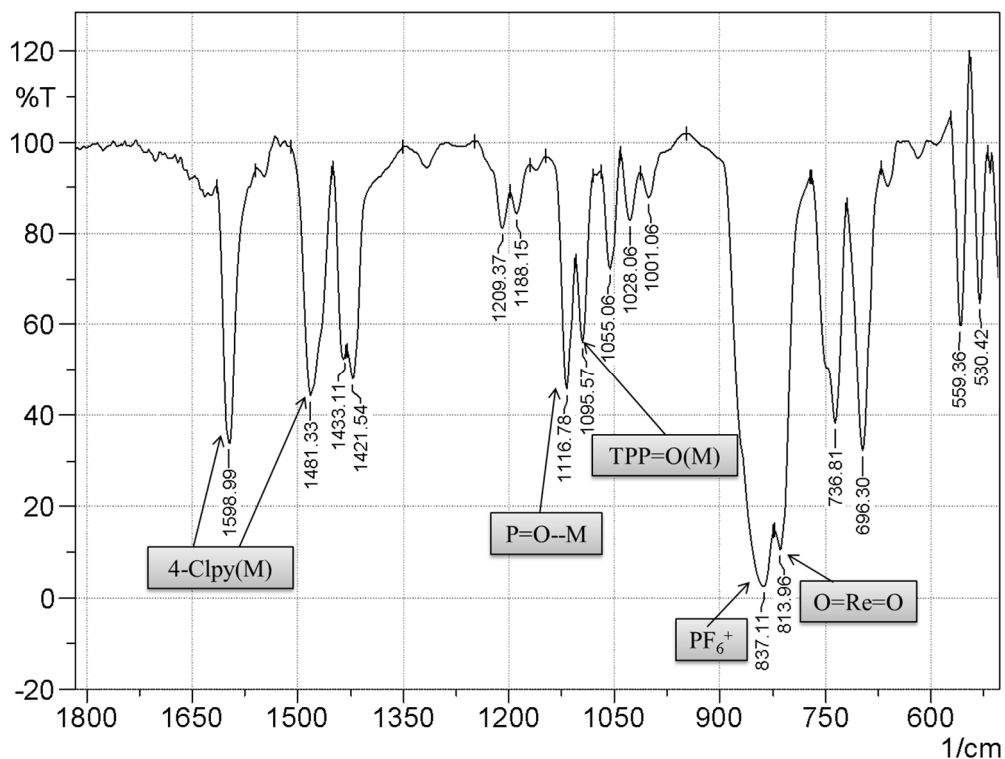


**Figure 4.9.1** KBr FT-IR of  $[\text{ReO}_2(4\text{-Clpy})_4]\text{PF}_6$  also showing presence of triphenylphosphine oxide.

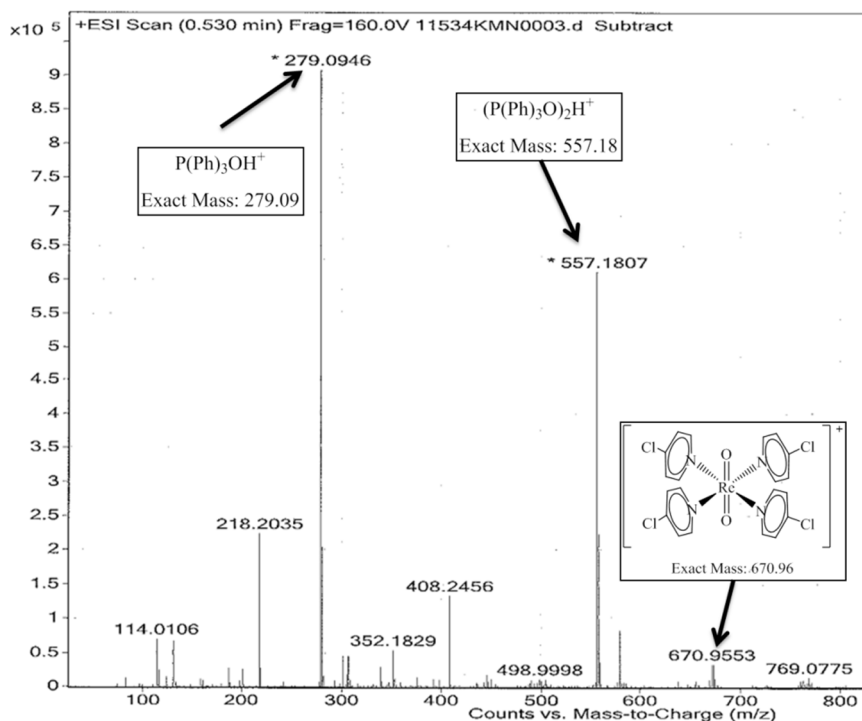


**Figure 4.9.2 High resolution ESI-MS of [ReO<sub>2</sub>(4-Clpy)<sub>4</sub>]PF<sub>6</sub> also showing the presence of triphenylphosphine oxide.**

The deuterated BnOH compounds PhCDHOH and PhCD<sub>2</sub>OH prepared by literature procedures. PhCDHOH was synthesized from benzaldehyde and LiAlD<sub>4</sub> in THF [141]. PhCD<sub>2</sub>OH was synthesized from methylbenzoate and LiAlD<sub>4</sub> in THF [135].

#### 4.9.2 Instrumentation

<sup>1</sup>H and <sup>13</sup>C NMRs were collected on either on a Varian Mercury VX-300 MHz, Varian VNMRS-400 MHz, Varian VNMRS-500 MHz, or Varian VNMRS-600 MHz. All of the NMR data was processed using SpinWorks [96]. Gas chromatograms were collected on a Shimadzu GC-14A or a Shimadzu GC-2014 equipped with an AOC-20i+s autosampler, both with 3% SE-54 packed column, FID and thermal program 40 °C for 5 min; 20 deg/min to 250 °C; then 7 min at 250 °C or in decanediol reactions

using heptadecane as standard 40 °C for 3min; 6 deg/min to 65 °C; 2 min at 65 °C; 20 deg/min to 100 °C; 2 min at 100 °C; 15 deg/min to 250 °C; 3 min at 250 °C. GC-MS analyses were performed on a Thermo-Finnigan instrument using the same thermal program as the former *vide supra* and a comparable stationary phase in a capillary column. Mass spectra were recorded on a Micromass Q-TOF quadrupole time-of-flight mass spectrometer equipped with a Z-spray electrospray ionization (ESI) source. FT-IR spectra were collected on a Shimadzu IRAffinity-1 infrared spectrophotometer using KBr pellets.

#### 4.9.3 *Typical Catalytic DODH Reaction Conditions*

Unless stated otherwise, reactions were carried out in benzene with 0.0200 M heptadecane standard (ca. 5 mL) using a sealed pressure tube (AceGlass) equipped with a front seal Teflon cap normal pipe thread adapter for a dip tube with a regulating valve for sampling, a magnetic stir bar with 0.10 M diol with 10 mol% oxorhenium(V) catalyst, 1 equivalent of reductant, degassed at room temperature by bubbling N<sub>2</sub> through the reaction via the dip tube with the vessel partially open, then both the valve and vessel were closed then heated at 170 °C for ca. 2 h using a preheated oil bath. The reaction was sampled at regular intervals and the analyzed by GC-FID with an internal standard. Rates and associated error were obtained by least squares fitting of the linear portions of concentration of decene versus reaction time plots, typically corresponding to the regions of 30-100% yield decene.

#### 4.9.4 *Quantification*

Heptadecane was used as an internal standard for 1,2-decanediol/BnOH reactions via GC-FID using multiple point internal standard calibration curve data

obtained from authentic, weighed concentrations of 1,2-decanediol/1-decene/BnOH/benzaldehyde/heptadecane.

#### 4.9.5 ESI-MS of ethylene glycol/[ReO<sub>2</sub>py<sub>4</sub>]<sup>+</sup>

The high resolution ESI-MS of assignable species from the stoichiometric ethylene glycol and [ReO<sub>2</sub>py<sub>4</sub>]PF<sub>6</sub> reaction are shown below with their corresponding assignments and simulation. In **Figure 4.9.3**, the species [Re<sup>vii</sup>O<sub>3</sub>py]<sup>+</sup> is assigned with a calculated mass of m/z = 313.9827. In **Figure 4.9.4**, the species [Re<sup>v</sup>O(glycolate)py<sub>2</sub>]<sup>+</sup> is assigned with a calculated mass of m/z = 421.0562. Simulations of isotope distributions were calculated in Molecular Weight Calculator v6.48.

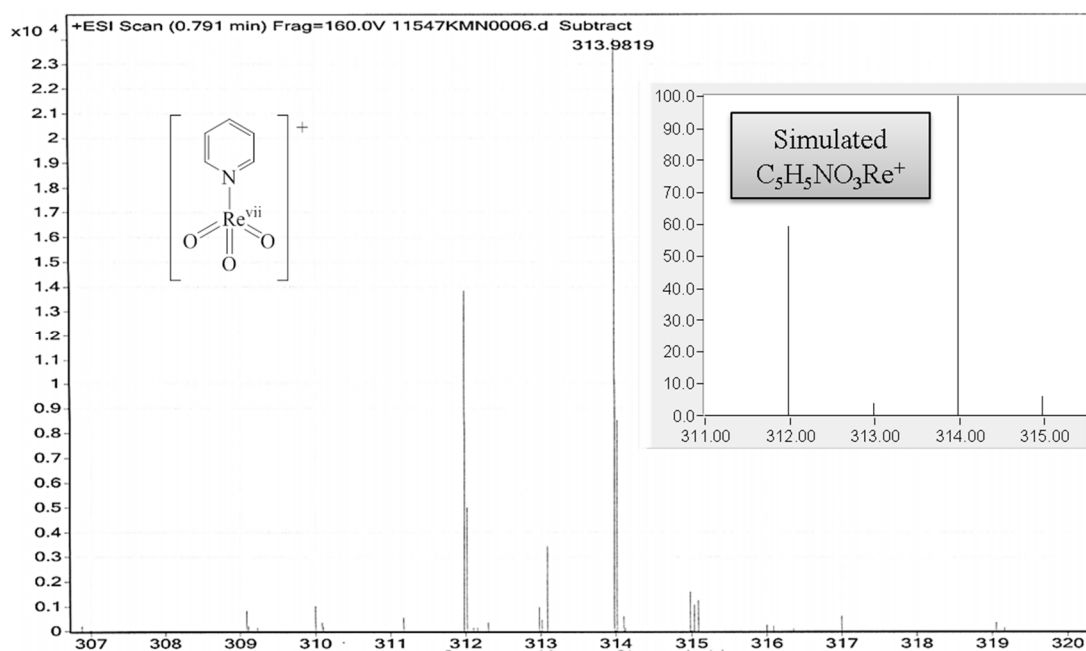


**Figure 4.9.3** ESI-MS [ReO<sub>3</sub>py]<sup>+</sup> and simulation.

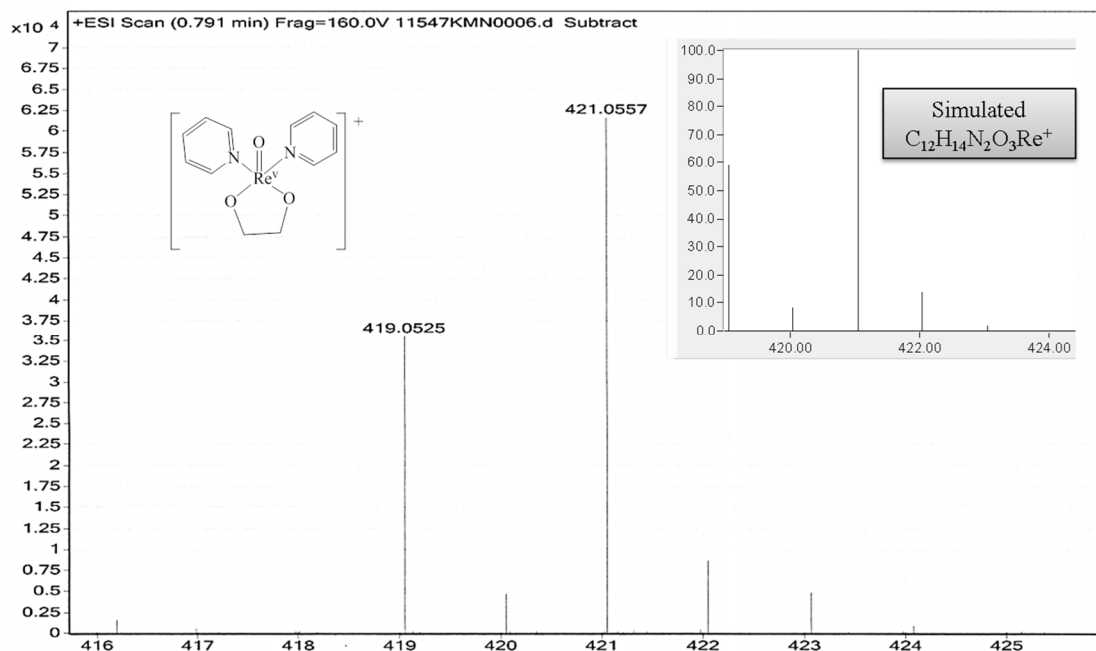


**Figure 4.9.4 ESI-MS  $[\text{ReO}(\text{glycolate})\text{py}_2]^+$  and simulation.**

#### 4.9.6 Rhenium calculations

All calculations (Opt Freq SCRF=(CPCM,Solvent=Dichloromethane)) were performed in Gaussian 09 through the WebMO interface using the B3LYP functional and the LANL2DZ basis set. Compounds were originally constructed in Spartan Student v5.0.0 and initial geometry optimization was done through an equilibrium conformer calculation via molecular mechanics MMFF. Gaussian input files were created from these initial optimized structures using Avogadro v1.1.1 - Gaussian Input extension. Resultant structures were rendered for figures in Mercury v3.3.

ReO(1,2-propanediolate)py<sub>2</sub> – Isomer 1:

```

35
Generated by WebMO
Re  0.00000000  0.00000000  0.00000000
O   -0.06330600 -0.00001200  1.70529700
O   -0.15092600 -1.73382900 -0.82861500
C   -1.44238300 -2.13283000 -1.43443000
C   -2.50733800 -1.06583100 -1.07924400

```

O	-1.75752400	0.18625000	-0.77794600
H	-3.12436400	-0.83526200	-1.95451000
C	-3.39778500	-1.43622600	0.11231400
H	-2.79928400	-1.70660300	0.99166700
H	-4.03310000	-2.29259600	-0.14684200
H	-4.04877500	-0.59520300	0.37634700
H	-1.28071500	-2.20286500	-2.51506100
H	-1.70111900	-3.11965400	-1.03689500
N	0.13033700	2.08857300	-0.36434300
C	-0.79316300	2.90306700	0.23641000
C	-0.79511700	4.28485100	0.02891400
C	0.14711800	4.85025400	-0.85203900
C	1.07290000	4.00624500	-1.49298000
C	1.04703900	2.63459700	-1.22142500
H	1.74962200	1.95709400	-1.68998300
H	1.80897800	4.39721600	-2.18591300
H	0.15549100	5.91955600	-1.03751900
H	-1.53007900	4.89777300	0.53795000
H	-1.52126000	2.42426000	0.87843800
N	2.10949100	-0.29532200	-0.21221700
C	2.62488400	-1.26190000	-1.03366300
C	4.00200700	-1.49798000	-1.11417000
C	4.88189700	-0.73962100	-0.32106200
C	4.34782900	0.24870600	0.52885000
C	2.96671400	0.45846400	0.55025700
H	2.52432500	1.21866100	1.18256700
H	4.98626600	0.85605300	1.16036900
H	5.95280600	-0.91059700	-0.36417200
H	4.36793700	-2.26888300	-1.78298100
H	1.90355600	-1.83698000	-1.59860900

ReO(1,2-propanediolate)py<sub>2</sub> – Isomer 2

35

Generated by WebMO

Re	0.00000000	0.00000000	0.00000000
O	-0.00434500	-0.21424800	-1.69299900
O	1.08302700	1.43406700	0.67407400
C	0.43770600	2.71398000	1.09830800
C	-1.01895800	2.64916800	0.58508300
O	-1.40554100	1.22287300	0.52313600
H	-1.71543000	3.15075400	1.26344700
H	-1.10954800	3.07333100	-0.42151900
H	0.99617000	3.51037000	0.59395400
C	0.56313800	2.84439700	2.61822900
H	1.61158900	2.75351600	2.92362100
H	-0.02186300	2.06791000	3.12696800
H	0.19527900	3.82553800	2.94348400
N	-1.36875000	-1.46942800	0.65468700
C	-2.62152100	-1.47328000	0.09822100
C	-3.59173400	-2.40050200	0.48706300

C	-3.29243300	-3.32477800	1.50649500
C	-2.01636600	-3.29599800	2.09958400
C	-1.07453400	-2.36796900	1.64580300
H	-0.08105000	-2.32282500	2.07256600
H	-1.74643600	-3.98157400	2.89453000
H	-4.03625700	-4.04410900	1.83394700
H	-4.56439400	-2.38377800	0.00899600
H	-2.82370900	-0.72018400	-0.65233400
N	1.69518200	-1.24371400	0.43091200
C	2.72714700	-0.81099000	1.21914500
C	3.86722900	-1.59475200	1.43099400
C	3.96917800	-2.85115700	0.80655900
C	2.90917500	-3.28986300	-0.01094500
C	1.78425400	-2.47595200	-0.16709600
H	0.94709400	-2.78827700	-0.77970200
H	2.94384700	-4.24881300	-0.51544200
H	4.84716800	-3.47226700	0.95264300
H	4.65850900	-1.21612800	2.06824400
H	2.61149100	0.17445000	1.65035200

ReO(ethyleneglycolate)py<sub>2</sub>:

32

Generated by WebMO

Re	0.00000000	0.00000000	0.00000000
O	0.11387000	-0.05040000	1.69766000
O	0.85534200	-1.35034900	-1.05206000
C	0.04890300	-2.47332000	-1.59702000
C	-1.32849700	-2.39787100	-0.91280000
O	-1.55876900	-0.96916100	-0.61014000
H	-2.13966700	-2.73602200	-1.56375000
H	-1.34729700	-2.95900100	0.02888000
H	-0.01567700	-2.32491000	-2.68035000
H	0.58426400	-3.40215900	-1.37968000
N	-1.23806200	1.65005900	-0.43249000
C	-2.51384100	1.62525800	0.07116000
C	-3.41462300	2.66760700	-0.16670000
C	-3.02269400	3.74476700	-0.98322000
C	-1.72426400	3.74970800	-1.52964000
C	-0.85417300	2.69926900	-1.22653000
H	0.15512700	2.67578000	-1.61747000
H	-1.38699500	4.55374900	-2.17453000
H	-3.71268500	4.55604600	-1.19503000
H	-4.40785300	2.62021600	0.26592000
H	-2.78923100	0.74891700	0.64348000
N	1.82451900	1.08620200	-0.35843000
C	2.79901000	0.63368300	-1.20753000
C	4.03760900	1.27796500	-1.31390000
C	4.30393800	2.40555500	-0.51648000
C	3.30469700	2.86258400	0.36541000

C	2.07793800	2.19557200	0.41132000
H	1.28815800	2.51785200	1.08033000
H	3.46848600	3.72028400	1.00888000
H	5.26234700	2.91235600	-0.57579000
H	4.77981900	0.88663500	-2.00127000
H	2.55817000	-0.26440700	-1.76174000

## **Chapter 5 Project Summary and Future Directions**

## 5.1 Project summary

We have shown that the elemental reductants Zn, Fe, Mn, and C are effective in APR catalyzed DODH of polyols. These reductants and their oxidized products are both heterogeneous in the DODH reaction mixture allowing for straightforward separation. The oxidized products of Zn, Fe, and Mn are environmentally benign while the oxidized product of C, CO is a synthetically useful commodity.

The feasibility of stable, dioxorhenium(V) complexes as DODH precatalysts was demonstrated. Particularly the cationic  $[\text{Re}^{\text{V}}\text{O}_2\text{py}_4]^+$  complex is capable of DODH of polyols with a range of reductants including  $\text{Na}_2\text{SO}_3$ , Zn, and BnOH. The generally less reactive aliphatic glycols are converted to their corresponding alkenes highly efficiently using  $[\text{Re}^{\text{V}}\text{O}_2\text{py}_4]^+/\text{BnOH}$  driven DODH. Additionally the commercially available and readily synthesized  $\text{ReO}_2(\text{TPP})_2\text{I}$  was shown to be capable of DODH on glycols with BnOH as reductant.

The reaction mechanism of aliphatic diols in  $[\text{ReO}_2\text{py}_4]^+/\text{BnOH}$  driven DODH was examined. The reaction has an apparent second order dependence on the rhenium complex and suggests the TLS involves two rhenium species. One rhenium species is the oxidized rhenium after alkene extrusion while the other appears to activate BnOH to act as the reductant leading to C-H bond breaking the TLS. There was a negative order observed for the glycol which is likely due to formation of polyglycol rhenium species which are catalytically inactive. The presence of catalytic amounts of additional ligands such as pyridine or triphenylphosphine oxide appears to aid in reactivation of the inactive polyglycol rhenium species. Alkene extrusion is observed in the absence of

reducing agent which further supports reduction of the oxorhenium(VII) species is turn over limiting.

## 5.2 Future directions

The continued exploration of the mechanism for glycol DODH using  $[\text{ReO}_2\text{py}_4]^+/\text{BnOH}$  is warranted. The identification of catalytically inactive polyglycol rhenium species can lead to efforts to reduce this effect. Variation of BnOH is likely to provide a wealth of information since its apparent involvement the TLS. The electronic properties of BnOH using 4-substituted analogs will aid in understanding their effect on the overall DODH reaction. The effects of added species and how they can accelerate or slow the reaction is intriguing for improving reaction times, yields, and selectivity. A further investigation of where and how these added species act in the catalytic cycle could allow for lower catalyst loading and/or improving other oxometal DODH catalysts. Developing a reactor system where the diol and reductant can be continuously fed in at favorable concentrations (low concentration for diol, higher concentration for BnOH) could decrease reaction times. An alkene-distillative continuous flow reactor could conceivably be developed with the controlled feed of glycol and reductant using a higher boiling solvent such as  $\text{C}_{>10}$ -alkanes; this would also allow for assessment of the lifetime of the  $[\text{ReO}_2\text{py}_4]^+$  precatalyst which has not been examined yet.

## References

1. *International Energy Outlook*, 2013. DOE/EIA-0484, U.S. Department of Energy, 2013.
2. Serrano-Ruiz, J.C., Pineda, A., Balu, A.M, Rafael Luque, Campelo, J.M, Romero, A.A., and Ramos-Fernández, J.M., *Ch. 7 Catalytic Transformations of Biomass-Derived Acids into Advanced Biofuels*, in *Advances in Biofuel Production*. Editor Gikonyo, B. 2013, Apple Academic Press. p. 213-232.
3. *Bioenergy Technologies Office Multi-Year Program Plan May 2013*, DOE/EE-0915, U. S. Department of Energy, 2013.
4. Ragauskas, A.J., Williams, C.K., Davison, B.H., Britovsek, G., Cairney, J., Eckert, C.A., Frederick Jr., W.J., Hallett, J.P., Leak, D.J., Liotta, C.L., Mielenz, J.R., Murphy, R., Templer, R., and Tschaplinski, T., *The path forward for biofuels and biomaterials*. *Science* (Washington, DC, U. S.), 2006. **311**(5760): p. 484-489.
5. Serrano-Ruiz, J.C., Pineda, A., Balu, A.M, Rafael Luque, Campelo, J.M, Romero, A.A., and Ramos-Fernández, J.M., *Catalytic transformations of biomass-derived acids into advanced biofuels*. *Catalysis Today*, 2012. **195**(1): p. 162-168.
6. Lovins, A.B., *Winning the Oil Endgame: Innovation for Profits, Jobs and Security*. 2004: Rocky Mountain Institute.
7. Deluisi, B. Basics of the Carbon Cycle and the Greenhouse Effect [cited 2014; Available from: [http://www.esrl.noaa.gov/gmd/outreach/carbon\\_toolkit/images/carbon\\_cycle.jpg](http://www.esrl.noaa.gov/gmd/outreach/carbon_toolkit/images/carbon_cycle.jpg)]
8. *Communication from the Commission - an E.U. Strategy for Biofuels*, {SEC(2006) 142}, Commission of the European Communities, E. U., 2006.
9. Bozell Joseph, J., *Feedstocks for the Future: Using Technology Development as a Guide to Product Identification*, in *Feedstocks for the Future*. 2006, American Chemical Society. p. 1-12.
10. Moreau, C. *Microporous and Mesoporous Catalysts for the Transformation of Carbohydrates*, in *Catalysts for Fine Chemical Synthesis: Microporous and Mesoporous Solid Catalysts*, V. 4 (ed E. G. Derouane) 2006, John Wiley & Sons, Ltd, Chichester, UK. P 141-156
11. Chheda, J.N. and J.A. Dumesic, *An overview of dehydration, aldol-condensation and hydrogenation processes for production of liquid alkanes from biomass-derived carbohydrates*. *Catalysis Today*, 2007. **123**(1-4): p. 59-70.
12. Chheda, J.N., G.W. Huber, and J.A. Dumesic, *Liquid-phase catalytic processing of biomass-derived oxygenated hydrocarbons to fuels and chemicals*. *Angewandte Chemie-International Edition*, 2007. **46**(38): p. 7164-7183.
13. Mehdi, H., Horváth, I.T., Torkos, K., Bodor, A., Mika, L. T., and Tuba, R., *Chapter 4 Catalytic conversion of carbohydrates to oxygenates in Renewable Resources and Renewable Energy A Global Challenge*, Second Edition, Editors Graziani, M., and Fornasiero, P. 2007. CRC Press LLC.

14. Huber, G.W. and J.A. Dumesic, *An overview of aqueous-phase catalytic processes for production of hydrogen and alkanes in a biorefinery*. *Catalysis Today*, 2006. **111**(1–2): p. 119-132.
15. Haveren, J.v., E.L. Scott, and J. Sanders, *Bulk chemicals from biomass*. *Biofuels, Bioproducts and Biorefining*, 2008. **2**(1): p. 41-57.
16. U.S. Department of Energy. 2011. *U.S. Billion-Ton Update: Biomass Supply for a Bioenergy and Bioproducts Industry*. R.D. Perlack and B.J. Stokes (Leads), ORNL/TM-2011/224. Oak Ridge National Laboratory, Oak Ridge, TN. 227p.
17. Dusselier, M., M. Mascal, and B. Sels, *Top Chemical Opportunities from Carbohydrate Biomass: A Chemist's View of the Biorefinery*, in *Selective Catalysis for Renewable Feedstocks and Chemicals*, K.M. Nicholas, Editor. 2014, Springer International Publishing. p. 1-40.
18. Schwartz, T.J., O'Neill, B.J., Shanks, B.H., and Dumesic, J.A., *Bridging the Chemical and Biological Catalysis Gap: Challenges and Outlooks for Producing Sustainable Chemicals*. *ACS Catalysis*, 2014: p. 2060-2069.
19. Mettler, M.S., D.G. Vlachos, and P.J. Dauenhauer, *Top ten fundamental challenges of biomass pyrolysis for biofuels*. *Energy & Environmental Science*, 2012. **5**(7): p. 7797-7809.
20. Brown, R.C., *Introduction to Thermochemical Processing of Biomass into Fuels, Chemicals, and Power*, in *Thermochemical Processing of Biomass*. 2011, John Wiley & Sons, Ltd. p. 1-12.
21. Singh, R., Shukla, A., Tiwari, S., Srivastava, M., *A review on delignification of lignocellulosic biomass for enhancement of ethanol production potential*. *Renewable and Sustainable Energy Reviews*, 2014. **32**(0): p. 713-728.
22. Mosier, N., Wyman, C., Dale, B., Elander, R., Lee, Y.Y., Holtzapple, M., Ladisch, M., *Features of promising technologies for pretreatment of lignocellulosic biomass*. *Bioresource Technology*, 2005. **96**(6): p. 673-86.
23. Wan, C. and Y. Li, *Fungal pretreatment of lignocellulosic biomass*. *Biotechnology Advances*, 2012. **30**(6): p. 1447-1457.
24. Abdel-Hamid, A.M., J.O. Solbiati, and I.K.O. Cann, *Chapter One - Insights into Lignin Degradation and its Potential Industrial Applications*, in *Advances in Applied Microbiology*, S. Sima and M.G. Geoffrey, Editors. 2013, Academic Press. p. 1-28.
25. Kumar, R., S. Singh, and O.V. Singh, *Bioconversion of lignocellulosic biomass: biochemical and molecular perspectives*. *Journal of Industrial Microbiology & Biotechnology*, 2008. **35**(5): p. 377-391.
26. Tao, L., Aden, A., Elander, R.T., Pallapolu, V.R., Lee, Y.Y., Garlock, R.J., Balan, V., Dale, B.E., Kim, Y., Mosier, N.S., Ladisch, M.R., Falls, M., Holtzapple, M.T., Sierra, R., Shi, J., Ebrik, M.A., Redmond, T., Yang, B., Wyman, C.E., Hames, B., Thomas, S., Warner, R.E., *Process and techno-economic analysis of leading pretreatment technologies for lignocellulosic ethanol production using switchgrass*. *Bioresource Technology*, 2011. **102**(24): p. 11105-11114.
27. Lipinsky, E.S., *Chemicals from Biomass: Petrochemical Substitution Options*. *Science*, 1981. **212**(4502): p. 1465-1471.

28. *Bioenergy Technologies Office Replacing the Whole Barrel To Reduce U.S. Dependence on Oil*, DOE/EE-0920, U. S. Department of Energy, 2013.
29. Chatterjee, C., F. Pong, and A. Sen, *Chemical conversion pathways for carbohydrates*. *Green Chemistry*, 2015, **17**(1): p 40-71.
30. Mascal, M. and S. Dutta, *Chemical-Catalytic Approaches to the Production of Furfurals and Levulinates from Biomass*, in *Selective Catalysis for Renewable Feedstocks and Chemicals*, K.M. Nicholas, Editor. 2014, Springer International Publishing, p. 41-83.
31. Cook, G.K. and M.A. Andrews, *Toward Nonoxidative Routes to Oxygenated Organics: Stereospecific Deoxydehydration of Diols and Polyols to Alkenes and Allylic Alcohols Catalyzed by the Metal oxo complex (C(5)Me(5))ReO<sub>3</sub>*. *Journal of the American Chemical Society*, 1996. **118**(39): p. 9448-9449.
32. Gable, K.P., AbuBaker, A., Zientara, K., and Wainwright, A.M., *Cycloreversion of Rhenium(V) Diolates Containing the Hydridotris(3,5-dimethylpyrazolyl)borate Ancillary Ligand*. *Organometallics*, 1999. **18**(2): p. 173-179.
33. Raju, S., Jastrzebski, J.T.B.H., Lutz, M., Klein Gebbink, R.J.M., *Catalytic deoxydehydration of diols to olefins by using a bulky cyclopentadiene-based trioxorhenium catalyst*. *ChemSusChem*, 2013. **6**(9): p. 1673-1680.
34. Arceo, E., J.A. Ellman, and R.G. Bergman, *Rhenium-catalyzed didehydroxylation of vicinal diols to alkenes using a simple alcohol as a reducing agent*. *Journal of the American Chemical Society*, 2010. **132**(33): p. 11408-11409.
35. Ziegler, J.E., Zdilla, M.J., Evans, A.J., Abu-Omar, M.M., *H<sub>2</sub>-driven deoxygenation of epoxides and diols to alkenes catalyzed by methyltrioxorhenium*. *Inorganic Chemistry*, 2009. **48**(21): p. 9998-10000.
36. Chapman, G., S. Maradur, and K.M. Nicholas. *Polyol to olefin deoxydehydration catalyzed by nonprecious oxo-metal compounds*. Abstracts of Papers, 244th ACS National Meeting and Exposition, August 19 –23, 2012, Philadelphia, PA; American Chemical Society: Washington, DC, 2012; CATL-79.
37. Chapman, G. and K.M. Nicholas, *Vanadium-catalyzed deoxydehydration of glycols*. *Chemical Communications*, 2013. **49**(74): p. 8199-8201.
38. Hills, L., Moyano, R., Montilla, F., Pastor, A., Galindo, A., Álvarez, E., Marchetti, F., Pettinari, C., *Dioxomolybdenum(VI) Complexes with Acylpyrazolonate Ligands: Synthesis, Structures, and Catalytic Properties*. *European Journal of Inorganic Chemistry*, 2013. **2013**(19): p. 3352-3361.
39. Dethlefsen, J.R., Lupp, D., Oh, B.C., Fristrup, P., *Molybdenum-Catalyzed Deoxydehydration of Vicinal Diols*. *ChemSusChem*, 2014. **7**(2): p. 425-428.
40. Metzger, J.O., *Catalytic Deoxygenation of Carbohydrate Renewable Resources*. *ChemCatChem*, 2013. **5**(3): p. 680-682.
41. Dutta, S., *Deoxygenation of biomass-derived feedstocks: hurdles and opportunities*. *ChemSusChem*, 2012. **5**(11): p. 2125-2127.
42. Boucher-Jacobs, C. and K. Nicholas, *Deoxydehydration of Polyols*. 2014, Springer Berlin Heidelberg. p. 1-22.

43. Korstanje, T.J. and R.J.M.K. Gebbink, *Catalytic Oxidation and Deoxygenation of Renewables with Rhenium Complexes*. 2012. **39**: p. 129-174.
44. Crank, G. and F.W. Eastwood, *Derivatives of ortho acids. II. Preparation of olefins from 1,2-diols*. Australian Journal of Chemistry, 1964. **17**(12): p. 1392-1398.
45. Ando, M., H. Ohhara, and K. Takase, *A mild and stereospecific conversion of vicinal diols into olefins via 2-methoxy-1,3-dioxolane derivatives*. Chemical Letters, 1986(6): p. 879-882.
46. Corey, E.J. and R.A.E. Winter, *A New, Stereospecific Olefin Synthesis from 1,2-Diols*. Journal of the American Chemical Society, 1963. **85**(17): p. 2677-2678.
47. Bergman, R.G., *CONVERSION OF GLYCEROL FROM BIODIESEL PRODUCTION TO ALLYL ALCOHOL*. WO Patent, 2008.
48. Arceo, E., Marsden, P., Bergman, R.G., Ellman, J.A., *An efficient didehydroxylation method for the biomass-derived polyols glycerol and erythritol. Mechanistic studies of a formic acid-mediated deoxygenation*. Chemical Communications (Cambridge, U. K.), 2009(23): p. 3357-3359.
49. Gable Kevin, P. and B. Ross, *Improved Catalytic Deoxygenation of Vicinal Diols and Application to Alditols*, in *Feedstocks for the Future*. 2006, American Chemical Society. p. 143-155.
50. Gable, K.P. and T.N. Phan, *Extrusion of Alkenes from Rhenium(V) Diolates: Energetics and Mechanism*. Journal of the American Chemical Society, 1994. **116**(3): p. 833-839.
51. Gable, K.P. and J.J.J. Juliette, *Extrusion of Alkenes from Rhenium(V) Diolates: The Effect of Substitution and Conformation*. Journal of the American Chemical Society, 1995. **117**(3): p. 955-962.
52. Gable, K.P. and J.J.J. Juliette, *Hammett Studies on Alkene Extrusion from Rhenium(V) Diolates and an MO Description of Metal Alkoxide-Alkyl Metal Oxo Interconversion*. Journal of the American Chemical Society, 1996. **118**(11): p. 2625-2633.
53. Gable, K.P. and F.A. Zhuravlev, *Kinetic Isotope Effects in Cycloreversion of Rhenium (V) Diolates*. Journal of the American Chemical Society, 2002. **124**(15): p. 3970-3979.
54. Ahmad, I., G. Chapman, and K.M. Nicholas, *Sulfite-Driven, Oxorhenium-Catalyzed Deoxydehydration of Glycols*. Organometallics, 2011. **30**(10): p. 2810-2818.
55. Vkuturi, S., Chapman, G., Ahmad, I., Nicholas, K.M., *Rhenium-catalyzed deoxydehydration of glycols by sulfite*. Inorganic Chemistry, 2010. **49**(11): p. 4744-4746.
56. Liu, P. and K.M. Nicholas, *Mechanism of sulfite-driven, MeReO<sub>3</sub>-catalyzed deoxydehydration of glycols*. Organometallics, 2013. **32**(6): p. 1821-1831.
57. Shiramizu, M. and F.D. Toste, *Expanding the Scope of Biomass-Derived Chemicals through Tandem Reactions Based on Oxorhenium-Catalyzed Deoxydehydration*. Angewandte Chemie International Edition, 2013. **52**(49): p. 12905-12909.
58. Li, X., Wu, D., Lu, T., Yi, G., Su, H., Zhang, Y., *Highly Efficient Chemical Process To Convert Mucic Acid into Adipic Acid and DFT Studies of the*

- Mechanism of the Rhenium-Catalyzed Deoxydehydration*. *Angewandte Chemie International Edition*, 2014. **53**(16): p. 4200-4204.
59. Liu, S., Senocak, A., Smeltz, J.L., Yang, L., Wegenhart, B., Yi, J., Kenttamaa, H.I., Ison, E.A., Abu-Omar, M.M., *Mechanism of MTO-Catalyzed Deoxydehydration of Diols to Alkenes Using Sacrificial Alcohols*. *Organometallics*, 2013. **32**(11): p. 3210-3219.
  60. Qu, S., Dang, Y., Wen, M., Wang, Z.X., *Mechanism of the Methyltrioxorhenium-Catalyzed Deoxydehydration of Polyols: A New Pathway Revealed*. *Chemistry A European Journal*, 2013. **19**(12): p. 3827-3832.
  61. Davis, J. and R.S. Srivastava, *Oxorhenium-catalyzed deoxydehydration of glycols and epoxides*. *Tetrahedron Letters*, 2014. **55**(30): p. 4178-4180.
  62. Abu-Omar, M.M., E.H. Appelman, and J.H. Espenson, *Oxygen-Transfer Reactions of Methylrhenium Oxides*. *Inorganic Chemistry*, 1996. **35**(26): p. 7751-7757.
  63. Espenson, J.H. and M.M. Abu-Omar, *Reactions Catalyzed by Methylrhenium Trioxide*, S.S. Isied, Editor. 1997, American Chemical Society: Washington, DC. p. 99-134.
  64. Herrmann, W.A., Fischer, R.W., Rauch, M.U., Scherer, W., *Alkylrhenium oxides as homogeneous epoxidation catalysts: Activity, selectivity, stability, deactivation*. *Journal of Molecular Catalysis*, 1994. **86**(1-3): p. 243-266.
  65. Santos, A.M., Pedro, F.M., Yogalekar, A.A., Lucas, I.S., Romano, C.C., Kuhn, F.E., *Oxorhenium complexes as aldehyde-olefination catalysts*. *Chemistry A European Journal*, 2004. **10**(24): p. 6313-6321.
  66. Gable, K.P., *Rhenium and Technetium Oxo Complexes in the Study of Organic Oxidation Mechanisms*, in *Advances in Organometallic Chemistry*, F.G.A. Stone and W. Robert, Editors. 1997, Academic Press. p. 127-161.
  67. Owens, G.S., J. Arias, and M.M. Abu-Omar, *Rhenium oxo complexes in catalytic oxidations*. *Catalysis Today*, 2000. **55**(4): p. 317-363.
  68. Shiramizu, M. and F.D. Toste, *Deoxygenation of Biomass-Derived Feedstocks: Oxorhenium-Catalyzed Deoxydehydration of Sugars and Sugar Alcohols*. *Angewandte Chemie International Edition*, 2012. **51**(32): p. 8082-8086, S8082/1-S8082/36.
  69. Yi, J., S. Liu, and M.M. Abu-Omar, *Rhenium-Catalyzed Transfer Hydrogenation and Deoxygenation of Biomass-Derived Polyols to Small and Useful Organics*. *ChemSusChem*, 2012. **5**(8): p. 1401-1404
  70. Herrmann, A.T., Saito, T., Stivala, C.E., Tom, J., Zakarian, A., *Regio- and stereocontrol in rhenium-catalyzed transposition of allylic alcohols*. *Journal of the American Chemical Society*, 2010. **132**(17): p. 5962-5963.
  71. Boucher-Jacobs, C. and K.M. Nicholas, *Catalytic deoxydehydration of glycols with alcohol reductants*. *ChemSusChem*, 2013. **6**(4): p. 597-599.
  72. Denning, A.L., Dang, H., Liu, Z., Nicholas, K.M., Jentoft, F.C., *Deoxydehydration of Glycols Catalyzed by Carbon-Supported Perrhenate*. *ChemCatChem*, 2013. **5**(12): p. 3567-3570.
  73. Maradur S., Nicholas K.M., 2012, unpublished results.
  74. Geary, L.M., Chen, T.Y., Montgomery, T.P., Krische, M.J *Benzannulation via Ruthenium-Catalyzed Diol-Diene [4+2] Cycloaddition: One- and Two-*

- Directional Syntheses of Fluoranthenes and Acenes*. Journal of the American Chemical Society, 2014, **136**(16), 5920-5922.
75. Geary, L.M., Chen, T.Y., Montgomery, T.P., Krische, M.J., *Benzannulation via Ruthenium-Catalyzed Diol–Diene [4+2] Cycloaddition: One- and Two-Directional Syntheses of Fluoranthenes and Acenes*. Journal of the American Chemical Society, 2014. **136**(16): p. 5920-5922.
  76. Shiramizu, M. and F.D. Toste, *Expanding the Scope of Biomass-Derived Chemicals through Tandem Reactions Based on Oxorhenium-Catalyzed Deoxydehydration*. Angewandte Chemie International Edition, 2013: p 12905-12909.
  77. Briscoe, H.V.A., P.L. Robinson, and E.M. Stoddart, *XCI.—The reduction of potassium per-rhenate*. Journal of the Chemical Society (Resumed), 1931(666): p. 666-669.
  78. Young, R.C. and J.W. Irvine, *Reduction of Perrhenate*. Chemical Reviews, 1938(67): p. 187-191.
  79. Cotton, F.A. and S.J. Lippard, *Chemical and Structural Studies of Rhenium(V) Oxyhalide Complexes. II. M[ReX<sub>4</sub>O] and M[ReX<sub>4</sub>OL] Complexes from KReO<sub>4</sub>*. Inorganic Chemistry, 1966. **5**(1): p. 9-16.
  80. Tomicek, O. and F. Tomicek, *Reduction of perrhenates*. Collection of Czechoslovak Chemical Communications, 1939. **11**: p. 626-638.
  81. Ehret, W. and A. Greenstone, *Red Zinc Oxide*1. Journal of the American Chemical Society, 1943. **65**(5): p. 872-877.
  82. Norman, V.J., *The photometric determination of excess of zinc in zinc oxide*. Analyst, 1964. **89**(1057): p. 261-265.
  83. Ramat, A., *Reduction by activated charcoal of inorganic reducing agents in solution*. Bull. Soc. Chim. Fr., 1940. **7**: p. 227-229.
  84. Vodop'yanov, A.G. and G.N. Kozhevnikov, *Recovery of rhenium and osmium from sulfurous gases with solid carbon*. Russian Journal of Applied Chemistry, 2012. **85**(10): p. 1567-1569.
  85. Craddock, P.T., *From hearth to furnace : evidences for the earliest metal smelting technologies in the Eastern Mediterranean*. Paléorient, 2000: p. 151-165.
  86. Shriver, D.F., Atkins, P.W., Overton, T.L., Rourke, J.P., Weller, M.T., Armstrong, F.A., *Shriver & Atkins Inorganic Chemistry 4<sup>th</sup> edition*. 2006, New Delhi: Oxford University Press.
  87. Habashi, F., *Fire and the art of metals: a short history of pyrometallurgy*. Mineral Processing & Extractive Metallurgy: Transactions of the Institution of Mining & Metallurgy, Section C, 2005. **114**(3): p. 165-171.
  88. NIST website: <http://webbook.nist.gov/chemistry>
  89. NIST website: <http://webbook.nist.gov/chemistry>
  90. Beatty, R.L., *Methods for Detecting and Determining Carbon Monoxide Revision of Technical Paper 582*. 1955. 22.
  91. Xu, K., Fang, Y., Yan, Z., Zha, Z., Wang, Z., *A Highly Tunable Stereoselective Dimerization of Methyl Ketone: Efficient Synthesis of E- and Z-1,4-Enediones*. Organic Letters, 2013. **15**(9): p. 2148-2151.

92. Avola, S., Goettmann, F., Antonietti, M., Kunz, W., *Organic reactivity of alcohols in superheated aqueous salt solutions: an overview* New Journal of Chemistry, 2012. **36**: p. 1568-1573.
93. Liu, Z., Z.C. Chen, and Q.G. Zheng, *Mild Oxidation of Alcohols with O-Iodoxybenzoic Acid (IBX) in Ionic Liquid 1-Butyl-3-methyl-imidazolium Chloride and Water* Organic Letters, 2003. **5**: p. 3321-3323.
94. Shirini, F., M.A. Zolfigol, and M. Khaleghi, *Oxidation of Alcohols Using (NH<sub>4</sub>)<sub>2</sub>Cr<sub>2</sub>O<sub>7</sub> in the Presence of Silica Chloride/Wet SiO<sub>2</sub> in Solution and under Solvent Free Conditions* Bulletin of the Korean Chemical Society, 2003. **24**: p. 1021-1022.
95. Fennelly, J.P. and A.L. Roberts, *Reaction of 1,1,1-trichloroethane with zero-valent metals and bimetallic reductants*. Environmental Science & Technology, 1998. **32**(13): p. 1980-1988.
96. Marat, K., *SpinWorks 2013*, University of Manitoba: Winnipeg, Canada.
97. Beatty, R.L., *Methods for Detecting and determining Carbon Monoxide Revision of Technical Paper 582*. 1955: Bulletin 557.
98. Woolf, A.A., *An outline of rhenium chemistry*. Quarterly Reviews, Chemical Society, 1961. **15**(3): p. 372-391.
99. Davenport, W.H., V. Kollonitsch, and C.H. Klein, *ADVANCES IN RHENIUM CATALYSTS*. Industrial & Engineering Chemistry, 1968. **60**(11): p. 10-19.
100. Broadbent, H.S., *RHENIUM AND ITS COMPOUNDS AS HYDROGENATION CATALYSTS*. Annals of the New York Academy of Sciences, 1967. **145**(1): p. 58-71.
101. Qu, S., Dang, Y., Wen, M., Wang, Z.X., *Mechanism of the Methyltrioxorhenium-Catalyzed Deoxydehydration of Polyols: A New Pathway Revealed*. Chemistry – A European Journal, 2013. **19**(12): p. 3827-3832.
102. Hurley, K.D., Y. Zhang, and J.R. Shapley, *Ligand-enhanced reduction of perchlorate in water with heterogeneous Re-Pd/C catalysts*. Journal of the American Chemical Society, 2009. **131**(40): p. 14172-14173.
103. Chakravorty, M.C., *preparations of trans-dioxotetrakis(pyridine)-rhenium(V) chloride, [ReO<sub>2</sub>py<sub>4</sub>]Cl, and Perchlorate, [ReO<sub>2</sub>py<sub>4</sub>]ClO<sub>4</sub>*. Inorganic Syntheses, 1982: p. 116-118.
104. Ram, M.S. and J.T. Hupp, *Generalized synthesis of cis- and trans-dioxorhenium(V) (bi)pyridyl complexes*. Inorganic Chemistry, 1991. **30**(1): p. 130-133.
105. Brewer, J.C. and H.B. Gray, *Efficient syntheses of dioxorhenium (V) complexes*. Inorganic Chemistry, 1989. **28**(17): p. 3334-3336.
106. Thorp, H.H., J.V. Houten, and H.B. Gray, *Excited-state properties of dioxorhenium (V). Generation and reactivity of dioxorhenium (VI)*. Inorganic Chemistry, 1989. **7**(eq 11): p. 889-892.
107. Lebedinskii, V.V. and B.N. Ivanov-Emin, *Complex compounds of Re(V) with pyridine*. Zh. Neorg. Khim., 1959. **4**: p. 1762-1767.
108. Booyesen, I.N., *Rhenium(V)-Imido Complexes with Potentially Multidentate Ligands Containing the Amino Group*, in *Nelson Mandela Metropolitan University*. 2007, Nelson Mandela Metropolitan University.

109. Ram, M.S., Jones, L.M., Ward, H.J., Wong, Y.H., Johnson, C.S., Subramanian, P., Hupp, J.T., *Ligand Tuning Effects upon the Multielectron Reduction and Single-Electron Oxidation of (Bi)pyridyl Complexes of*. 1991. *Inorganic Chemistry*: p. 2928-2938.
110. Boucher-Jacobs, C., *Oxo-Rhenium Catalyzed Deoxydehydration of Polyols*, in *Department of Chemistry and Biochemistry*. 2012, University of Oklahoma: Norman, Oklahoma.
111. Rouschias, G., *Recent advances in the chemistry of rhenium*. *Chemical Reviews*, 1974. **74**(5): p. 531-566.
112. Sousa, S.C.A. and A.C. Fernandes, *Rhenium-catalyzed deoxygenation of epoxides without adding any reducing agent*. *Tetrahedron Letters*, 2011. **52**(51): p. 6960-6962.
113. Johnson, N.P., Lock, C.J.L., Wilkinson, G., *Complexes of Rhenium(V)*, in *Inorganic Syntheses*. 1967, John Wiley & Sons, Inc. p. 145-148.
114. Ciani, G.F., D'Alfonzo, G., Romiti, P.F., Sironi, A., Freni, M., *Rhenium(V) oxide complexes. Crystal and molecular structures of the compounds trans-ReI2O(OR)(PPh3)2 (R = Et, Me) and of their hydrolysis derivative ReIO2(PPh3)2*. *Inorganica Chimica Acta*, 1983. **72**(0): p. 29-37.
115. Roduner, E., *Understanding catalysis*. *Chemical Society Reviews*, 2014. **43**(24): p. 8226-8239.
116. Mitchell, S., N.-L. Michels, and J. Perez-Ramirez, *From powder to technical body: the undervalued science of catalyst scale up*. *Chemical Society Reviews*, 2013. **42**(14): p. 6094-6112.
117. Kedia, S.B. and M.B. Mitchell, *Reaction Progress Analysis: Powerful Tool for Understanding Suzuki–Miyaura Reaction and Control of Polychlorobiphenyl Impurity*. *Organic Process Research & Development*, 2009. **13**(3): p. 420-428.
118. Bi, S., Wang, J., Liu, L., Li, P. Lin, Z., *Mechanism of the MeReO3-Catalyzed Deoxygenation of Epoxides*. *Organometallics*, 2012. **31**(17): p. 6139-6147.
119. Ram, M.S., Johnson, C.S., Blackbourn, R.L., Hupp, J.T., *Synthesis and electrochemistry of 2,2'-bipyridyl complexes of dioxorhenium(V)*. *Inorganic Chemistry*, 1990. **29**(2): p. 238-244.
120. *Chapter 3 Experiments and their evaluation*, in *Comprehensive Chemical Kinetics*, F.G. Helfferich, Editor. 2004, Elsevier. p. 39-76.
121. Dengler, J.E., Lehenmeier, M. W., Klaus, S., Anderson, C. E., Herdtweck, E. and Rieger, B., *A One-Component Iron Catalyst for Cyclic Propylene Carbonate Synthesis*. *European Journal of Inorganic Chemistry*, **2011**(3): p. 336-343.
122. Grace, M.R. and P.A. Tregloan, *An alternative mechanism for the formation of the cobalt(III) molybdate cation, Co(NH3)5MoO4+*. *Polyhedron*, 1991. **10**(19): p. 2317-2329.
123. Schaus, S.E. and E.N. Jacobsen, *Asymmetric Ring Opening of Meso Epoxides with TMSCN Catalyzed by (pybox)lanthanide Complexes*. *Organic Letters*, 2000. **2**(7): p. 1001-1004.
124. Nakazono, T., A.R. Parent, and K. Sakai, *Cobalt porphyrins as homogeneous catalysts for water oxidation*. *Chemical Communications*, 2013. **49**(56): p. 6325-6327.

125. Marchaj, A., A. Bakac, and J.H. Espenson, *Sixth-order kinetics in a catalyzed autoxidation of a macrocyclic cobalt(II) complex*. Inorganic Chemistry, 1992. **31**(23): p. 4860-4863.
126. Adler, B. Beger, J., Duschek, C., Gericke, C., Pritzkow, W., Schmidt, H., *Dienoligomerisierung. XII. 3-Vinylcycloalkene durch Nickelkomplekxkatalysierte Codimerisierung von Cycloalkadienen-(1,3) mit Äthylen*. Journal für Praktische Chemie, 1974. **316**(3): p. 449-462.
127. Martín, C. and A.W. Kleij, *Comparing kinetic profiles between bifunctional and binary type of Zn(salen)-based catalysts for organic carbonate formation*. Beilstein Journal of Organic Chemistry, 2014. **10**: p. 1817-1825.
128. Kosuge, K., Nose, K., Suzuki, Y., Kamata, K., Iyoda, T., *Controlled Polymerization of 4-Chloropyridine:  $\pi$ -Conjugated Polypyridinium Wiring toward Molecular Circuitry*. Meeting Abstracts, 2008. **MA2008-02**(16): p. 1530.
129. Berlin, A.A. and E.F. Razvodovskii, *Synthesis of polymers with charged heteroatoms in the chain by the onium polymerization method*. Journal of Polymer Science, Polymer Symposium, 1966. **No. 16**: p. 369-375.
130. Berlin, A.A. and E.F. Razvodovskii, *Synthesis of Polymers with Charged Heteroatoms in the Chain by the "Onium Polymerization" Method*. Journal of Polymer Science Part C: Polymer Symposia, 1967. **16**(1): p. 369-375.
131. Nose, K., T. Iyoda, and T. Sanji, *Terminal defined chain-growth polycondensation of 4-chloropyridine*. Polymer, 2014. **55**(16): p. 3454-3457.
132. Wibaut, J.P. and F.W. Brockman, *Pyridine derivatives. CIX. The polymerization of 4-chloropyridine*. Recl. Trav. Chim. Pays-Bas Belg., 1959. **78**: p. 593-603.
133. Hansch, C. and A. Leo, *Substituent constants for correlation analysis in chemistry and biology*. 1979, New York: Wiley.
134. Schreck, J.O., *Nonlinear Hammett relationships*. Journal of Chemical Education, 1971. **48**(2): p. 103.
135. Hoover, J.M., B.L. Ryland, and S.S. Stahl, *Mechanism of Copper(I)/TEMPO-Catalyzed Aerobic Alcohol Oxidation*. Journal of the American Chemical Society, 2013. **135**(6): p. 2357-2367.
136. Herrmann, W.A., Marz, D., Herdweck, E., Schaefer, A., Wagner, W., Kneuper, H.J., *Glycolate and Thioglycolate Complexes of Rhenium and Their Oxidative Elimination of Ethylene and of Glycol*. Angewandte Chemie International Edition in English, 1987. **26**(5): p. 462-464.
137. Herrmann, W.A., P. Watzlowik, and P. Kiprof, *MULTIPLE BONDS BETWEEN MAIN GROUP ELEMENTS AND TRANSITION-METALS .90. SELECTIVE FORMATION OF ALKYLRHENIUM OXIDES FROM GLYCOLATO COMPLEXES*. Chemische Berichte, 1991. **124**(5): p. 1101-1106.
138. Gable, K.P., *Condensation of Vicinal Diols with the Oxo Complex  $\{Cp^*Re(O)\}_2(\mu-O)_2$  Giving the Corresponding Diolate Complexes*. Organometallics, 1994. **13**(6): p. 2486-2488.
139. Helm, L., Deutsch, K., Deutsch, E.A., Merchach, A.E., *Multinuclear NMR Studies of Ligand-Exchange Reactions on Analogous Technetium(V) and Rhenium(V) Complexes. Relevance to nuclear medicine*. Helvetica Chimica Acta, 1992. **75**(1): p. 210-217.

140. Fergusson, J.E., *Recent advances in the coordination chemistry of rhenium*. Coordination Chemistry Reviews, 1966. **1**(4): p. 459-503.
141. Pratt, R.C. and T.D.P. Stack, *Mechanistic Insights from Reactions between Copper(II)–Phenoxy Complexes and Substrates with Activated C–H Bonds*. Inorganic Chemistry, 2005. **44**(7): p. 2367-2375.

## Appendix 1

### Abbreviations

APR	Ammonium perrhenate
BnOH	Benzyl alcohol
C	Carbon (elemental, charcoal)
Cp*	Pentamethylcyclopentadiene
DEF	Diethyl fumarate
DET	(+)-Diethyl-L-tartrate
DODH	Deoxydehydration
Fe	Iron (elemental)
Mn	Manganese (elemental)
MTO	Methyltrioxorhenium
py	Pyridine
Zn	Zinc (elemental)
Styrene glycol	1-Phenyl-1,2-ethanediol
Btu	British thermal unit
15-Crown-5	1,4,7,10,13-Pentaoxacyclopentadecane
mol%	Mole percent
eq	Equivalents
TPP	Triphenylphosphine
ca.	Approximately
PhOMe	Anisole
PhCl	Chlorobenzene

El	Element
El-O	Oxidized element
b.p.	Boiling point
$\Delta H_{\text{rxn}}$	Change in enthalpy of the reaction
ppm	Parts per million
Cp'	1,2,4-Tri- <i>tert</i> -butyl-cyclopentadiene
Trp*	Tris-dimethylpyrazolylborate
Red	Reductant
RedO	Oxidized reductant